# The role of Slit family members and their receptor Robo-2 in the formation of stereotypic sensory maps in the mammalian olfactory system

**Jin hyung Cho**

**Department of Neurology and Neurosurgery**

**McGill University, Montreal**

**February 2011**

A thesis dissertation submitted to the faculty of Graduate and Postdoctoral Studies, McGill University, in partial fulfillment of the degree of Doctor of Philosophy

## TALBE OF CONTENTS

# ABSTRACT

To precisely distinguish all the sensorial information from our environment, many millions of neurons must make proper synaptic connections with their target areas in the central nervous system (CNS). These precise connections are hallmarks of any sensory system such as the visual system and the main olfactory system. To achieve stereotypic connections, axons are guided to their targets by patterned chemical cues during embryogenesis and these connections are refined during postnatal development. This thesis examines the role of Slit and Robo family of axon guidance molecules in the innervations of olfactory sensory neuron (OSN) axons to their relay structure called the olfactory bulb (OB). I test the hypothesis that different Slits may be expressed in the target area, the OB, to repel and to guide OSN axons which might express their receptors, Robos, to form accurate connections with the second order neuron located in the OB.

I report that *Robo-2* is expressed in a graded manner in the olfactory epithelium (OE) where OSNs reside and its ligands, *Slit-1* and *Slit-3* are expressed in the ventral region of the OB. In addition, we demonstrate that Slit-1 and Slit-2 are also expressed by the OSN axons targeting the ventral region of the OB. In Chapter 2, we demonstrate that by either ablating Slit-1 or Robo-2 in the mouse, Slit-1-Robo-2 signaling is essential for the accurate segregation of zone 1 OSN axons in the dorsal to ventral axis of the OB because zone 1 OSN axons are ectopically present in the ventral region of the OB. In Chapter 3, we further examine the role of Robo-2 in the accurate innervations of two subdomains of zone 1 (DI and DII) along the dorsal to ventral region of the OB and demonstrate that OSN axons targeting the DII subdomain of the OB require Robo-2. Moreover, we illustrate that the accurate segregation of OSN axons along the dorsal to

ventral axis of the OB is essential for the processing of aversive odorants by the animals. In Chapter 4, we reveal that Slit-1 and Robo-2 are required for the accurate innervation of zones 2 and 4 OSN axons along the dorsal-ventral axis of the OB. Additionally, we show that Slit-1 and Slit-2 are expressed in the OSN. This thesis provides insights into how different Slits and Robo-2 axon guidance molecules are required for the accurate innervation of OSN axons to the OB and these observations indicate that proper segregation of OSN axons to the OB is essential to process aversive odorants by mice. Therefore, our results support the notion that the olfactory system might be hard-wired to process odorants that elicit innate behavior.

## RÉSUMÉ

Afin de distinguer précisément toutes les informations sensorielles de notre environnement, plusieurs millions de neurones doivent former correctement des connections avec leur cibles dans le système nerveux central. Ces connections hautement précises sont à la base des principaux systèmes sensoriels comme la vue ou l'odorat. Pour pouvoir former ces connections, les axones des neurones sont guidées vers leurs cibles par différentes substances chimiques durant l'embryogenèse. Ces connections seront, par la suite, raffinées au cours du développement. La présente thèse examine le rôle des familles de molécules de guidage neuronale Slit et Robo lors de l'innervation du bulbe olfactif (BO) par les axones des neurones sensoriel olfactives (NSO). J'ai émis l'hypothèse que les molécules de la famille Slit allaient être exprimées par le BO afin de repousser et guider les axones NSO lesquels exprimeraient les récepteurs des Slits, les Robos pour finalement mener à la formation d'une représentation précise.

J'ai montré dans le chapitre 2 que le récepteur *Robo-2* est exprimé dans l'épithélium olfactif où les NSO résident et que les ligands, *Slit-1* et *Slit-3*, sont exprimés dans la région ventrale du BO. J'ai aussi pu démontrer que Slit-1 et Slit-2 sont aussi exprimés par les axones NSO qui se dirigent vers le BO. Je vais aussi démontrer que la cascade mécanistique résultant de l'interaction Slit-1-Robo-2 est essentielle pour la ségrégation d'une sous-population d'axones NSO sur l'axe dorsal-ventral. Le chapitre 3 sera consacré à l'approfondissement du rôle joué par Robo-2 dans l'innervation précise de deux sous-domaines de la zone 1 du BO. De plus, je vais démontrer que le positionnement correct des axones NSO sur l'axe dorsal-ventral du BO est nécessaire à la détection d'odeurs aversives pour la souris. Finalement, le chapitre 4 traitera de

l'importance de Slit-1 et Robo-2 pour l'innervation précise du BO par les axones NSO provenant des zones 2 et 4, en plus de montrer que les axones NSO exprimant Slit-1 et Slit-2.

Dans l'ensemble, cette thèse présente de nouvelles données concernant la fonction des protéines de la famille Slit et Robo dans le guidage des axones OSN vers le BO. De plus, mes résultats indiquent que cette ségrégation est essentielle pour la reconnaissance de certaines odeurs par l'animal.

## LIST OF FIGURES

Chapter 1



Chapter 2



Chapter 3

## LIST OF TABLES

Chapter 4

## LIST OF ABBREVIATIONS

**2MB:** 2-methylbutyric acid
**β3GnTI:** β1,3-N-acetylglucosaminyltransferase I
**AOB:** Accessory olfactory bulb
**AOS:** Accessory olfactory system
**Arx:** X-linked prd-type homeogenes
**bHLH:** Basic helix-loop-helix
**BNST:** Bed nucleus of the stria terminalis
**Boc:** Biregional Cdon-binding protein
**cAMP:** Cyclic-adenosine monophosphate
**Cdon:** Cell-adhesion-molecule-related/downregulated by oncogenes
**CNGA:** Cyclic nucleotide gated channel
**CNS:** Central nervous system
**DCC:** Deleted in colorectal caner
**DHB:** dehydro-exo-brevicomin
**Dlx:** Distalless-related homeognes
**E:** Embryonic day
**ECM:** Extracellular matrix
**GL:** Glomerular layer
**GPI:** Glycosylphosphatidylinositol
**IGF:** Insulin growth factor
**IRES:** Internal ribosome entry site
**KO:** Knock-out
**LOT:** Lateral olfactory tract
**MCL:** Mitral cell layer
**MOS:** Main olfactory system
**MOR:** Murine olfactory receptor
**Npn:** Neurophilin
**NQO-1:** NADPH quinone oxidoreductase 1
**OAZ**: O/E associated zinc finger protein
**OB:** Olfactory bulb
**OCAM:** Olfactory cell adhesion molecule
**O/E:** Olf1/EBF family of repeated helix-loop-helix transcription factor
**OE:** Olfactory epithelium
**OMP:** Olfactory marker protein
**ONL:** Olfactory nerve layer
**OR:** Olfactory receptor
**OS:** Olfactory system
**OSN:** Olfactory sensory neuron
**Pcdh:** Protocadherin
**RMS:** Rostral migratory stream
**Robo:** Roundabout
**SAGE:** Serial analysis of gene expression
**SBT:** 2-sec-Butyl-dihydrothiazole

**Shh:** Sonic hedgehog
**Sema:** Semaphorin
**SVZ:** Subventricular zone
**TF:** Transcription factor
**TMT:** Trimethyl-thiazoline
**VSN:** Vomeronasal sensory neurons

**ACKNOWLEDGEMENTS**

I would like to express my sincere appreciation and gratitude to Dr. Jean-François Cloutier who gave me the chance to prove myself as a researcher. During all these years, he gave me continued support, guidance and encouragement which were tremendous for me. I would also like to thank him for providing an optimal working environment and a great degree of scientific freedom to explore and develop new ideas for the project. This journey has been a very memorable adventure with more ups than downs. I am very proud to leave a big mark on the lab by publishing the first manuscript of the lab. While hard work in the lab is a must, Dr. Cloutier always knew how to compensate us with lots of great activities which will stay in my memory forever. Although I am very happy to start a new chapter in my life, it is with heavy heart that I will leave this lab…

I also would like to thank my advisory committee members Dr. Stefano Stifani and Dr. Alyson Fournier for their countless number of reference letters and valuable insights into my project.

To all formers and current members of the lab (David, Janet, François, Vesselina, Émilie, Joseph, Manon, Pavel and all different students) I am very grateful to have known and worked with such a wonderful group of people. I am especially thankful to David, Janet, François and Joseph for sharing experiences and discussion about lab work and also about life. You guys are great scientists and friends. I am also thankful to Émilie and Vesselina to have endured me for all these years. I know I can be difficult! To all the colleagues at the MNI, you are too many to acknowledge individually here. I just want to thank all of you for making this journey a very memorable one.

I would like to thank all my very best friends who have been there with me along this journey. Thank you for supporting me through this journey! One day, I will not be a student anymore...

Finally, I take this opportunity to express my profound gratitude to my parents, brother and my sister in law for their continued and unconditional support in all my undertakings throughout my years of study.

To my wife, Dong-Young, being a wonderful person that you are, you stuck with me through thick and thin. You are my biggest supporter and my biggest critic. Because of you, I am a stronger person. Thank you Dong-Young, you bring me happiness, strength, love and laughs!

## AUTHOR CONTRIBUTIONS

**Chapter 1: Literature review:** A large part of this chapter comes from a review article I co-wrote entitled**:** *Axon guidance events in the wiring of the mammalian olfactory system*

- **Jin hyung Cho:** Co-wrote parts on: axonal projections in antero-posterior axis of the OB and axon-axon interactions in the formation of glomeruli and edited manuscript.
- **Janet E.A. Prince:** wrote the part on: compartmentalization of axons in the olfactory bulb by glycans and edited manuscript.
- **Jean-François Cloutier:** Drew all the figures and co-wrote manuscript.

**Chapter 2:** *Requirement for Slit-1 and Robo-2 in zonal segregation of olfactory sensory neuron axons in the main olfactory bulb*

- **Jin hyung Cho**: Developed rationales, performed all experiments, assembled all figures and edited manuscript.
- **Manon Lépine:** Characterized Robo-2 antibodies used in this manuscript.
- **William Andrews:** Provided the floxed Robo-2 mouse line.
- **John Parnavelas:** Provided the floxed Robo-2 mouse line.
- **Jean-François Cloutier:** Developed rationales, edited all figures and wrote manuscript.

**Chapter 3:** *The pattern of glomerular map formation defines responsiveness to aversive odorants in mice*

- **Jin hyung Cho**: Developed rationales, performed all experiments, assembled all figures and co-wrote manuscript.
- **Janet E.A. Prince:** Performed immunohistochemistry (Figure S1).
- **Tyler Cutforth:** Provided the OMP-Cre, MOR13-tauLacZ and MOR174-9-tauGFP mouse lines.
- **Jean-François Cloutier:** Developed rationales, edited all figures and co-wrote manuscript.

**Chapter 4:** *Slit-1 and Robo-2 control the targeting of subsets of OSN axons in the ventral region of the OB*

- **Jin hyung Cho:** Developed rationales, performed all experiments, assembled all figures and co-wrote manuscript.
- **Jean-François Cloutier:** Developed rationales, edited all figures and co-wrote manuscript.

# CHAPTER 1

# LITERATURE REVIEW

## GENERAL INTRODUCTION

To accurately perceive all the sensorial information coming from our environment, many millions of neurons must form precise synapses with specific target areas in the central nervous system (CNS). These connections are formed during embryogenesis and refined during postnatal development. During development, neurons will extend their axon across a relatively large distance in order to terminate in their target areas. During this process, the axons will bypass millions of potential but inappropriate synaptic targets and ultimately recognize their appropriate synaptic partners. During the 20$^{th}$ century, several models were put forth to explain the general mechanism of axon guidance. In the late 19$^{th}$ century, the great pioneering neuroanatomist Ramon y Cajal suggested that the tip of the axon, which he termed growth cone, might be attracted to its appropriate target by detecting chemical cues secreted by the target (Ramón y Cajal, 1892). In contrast, Paul Weiss' studies of dissociated neurons in vitro suggested that mechanical information directs nerve growth. He noticed that neurites followed differently oriented fibrils present in collagen gels (Weiss, 1934). Based on this finding, Paul Weiss put forth a stereotropic model where by axons only respond to relatively non-specific physical cues to reach their appropriate target area. His resonance principle stated that axons only receive general directives to grow randomly and that only appropriate connections are maintained when the electrical activity of the axon matches activity of the neurons in the target area (Weiss, 1941). Ironically, it was a student of Weiss, Roger Sperry in the early 1940s who demonstrated

that axonal out growth is not a random event and that chemical cues are involved in the targeting of axons to their target. Using the regenerative properties of the optic nerve in Xenopus, Sperry performed a simple yet groundbreaking experiment that demonstrated the mechanism by which retinotectal projections are formed. He severed the optic nerve and rotated the eye by $180^0$ before allowing the nerve to regenerate. The frog exhibited normal but dysfunctional behavior such that when a fly was presented above its head, the frog struck downward. Furthermore, the frog never learned and never corrected its mistakes (Sperry, 1943). From this experiment, he concluded that axons rely on chemical cues to find their targets rather than forming random connections. This lead to a paradigm shift and the chemospecificity hypothesis was born. This new hypothesis inspired researchers, using a variety of organisms and approaches, to discover molecular cues influencing the growth of axons to their targets during development.

A fundamental organizational principle of the nervous system is the use of space to encode external information. Neural maps are used in all sensory modalities and also in motor control. There are two qualitatively different kinds of neural maps present in the nervous system: continuous and discrete maps. The retinotopic map in the visual system is a great example of a continuous map where nearby neurons in the input field connect with nearby neurons in the target field to preserve spatial order. This is important for the function of the visual system where a two-dimensional image on the retina is recast in higher visual processing areas of the brain. In discrete neural maps, the spatial organization of the one field reflects discrete qualities and not the spatial organization like the visual system. One of the most studied discrete neural maps is the olfactory system where olfactory sensory neurons (OSN) expressing the same olfactory receptor

(OR) project their axons to the same glomeruli in the brain forming a glomerular map which creates a spatial map of discrete information to the brain.

What are the molecular cues that mediate the formation of these sensory maps? The molecular cues influencing the growth of axons to their target are called axon guidance molecules. Axon guidance cues can act both as attractants and repellents and these cues could either have their effect over short distances through contact-mediated interactions or over long distances by being secreted in the environment. Many individual guidance cues can function both as repellents and attractants and bifunctionality can depend on a variety of factors such as the intracellular state of the growth cone, differential expression of receptor complexes, and cross talk between intracellular signaling cascades (reviewed in Huber et al. 2003). The four major families of axon guidance molecules include Netrins, Semaphorins, Slits and Ephrins. Netrins are a family of proteins that direct axon outgrowth during embryogenesis and are bifunctional axon guidance cues. There are six netrins in vertebrates and netrins 1-4 are secreted protein while the other two are GPI-linked (glycosylphosphatidylinositol) proteins. Netrins can have their effects through several receptors including DCC (deleted in colorectal cancer), Unc-5, and Neogenin. Semaphorins (Sema) constitute a large family of axon guidance molecules. The semaphorins family is divided into 8 subclasses and four of these (classes 3-7) are found in vertebrates. All semaphorins share a characteristic 'sema' extracellular domain. Semaphorins are bifunctional axon guidance cues and play various roles during neural development. Semaphorins can either be secreted, transmembrane or GPI-linked. While transmembrane and GPI-linked semaphorins signal through Plexins, secreted semaphorins signal via a receptor complex

composed of a neuropilin and a plexin family member. A third family of classical axon guidance molecules is the ephrins. Eph tyrosine kinases, receptors for the ephrins, are encoded by the largest family of receptor tyrosine kinase genes. These receptors are divided in two subclasses, EphA receptors, which bind the GPI-linked ephrin-As and EphB receptors which bind to transmembrane ephrin-Bs. Since ephrins are membrane attached, ephrin-Eph interactions are contact mediated. Interestingly, ephrin/Eph complexes can transduce signals bidirectionally into both receptor (Eph)-expressing cells and ligand (ephrin)-expressing cells termed "forward" and "reverse" signaling, respectively. Both forward and reverse signaling of Ephrin-Eph are essential for axon guidance during neural development. Another major family of axon guidance molecules is the Slits and their receptor Robos. Since Slit and Robo axon guidance molecules are the major focus of this thesis, this family will be further discussed in details later in this chapter.

At the beginning of my graduate studies, our understanding of the molecular mechanisms that regulate wiring of axons in the olfactory system was somewhat cursory. I became interested in identifying axon guidance cues that could regulate the targeting of OSN axons in the dorso-ventral axis of the OB. My analyses suggested that the Slit family of proteins could regulate this specific targeting decision. My results presented in Chapters 2-4 demonstrate that Slits and their receptor Robo-2 play critical roles in the wiring of the olfactory system. Furthermore, they demonstrate that proper formation of a glomerular map in the OB is essential in the regulation of specific innate behaviors in mice.

This chapter will focus on providing the necessary background to the studies presented in chapter 2-4. I will first briefly describe the organization of the olfactory system and the mechanisms that regulate the expression of ORs. This will be followed by a summary of our current knowledge of the mechanisms that regulate axonal guidance in the olfactory systems as well as a discussion of how odorant information is processed by the olfactory system. I will then briefly describe the Slit family of axon guidance molecules and our current understanding of their role in the development of the nervous system. The chapter will conclude with the thesis rational and objectives.

## ESTABLISHING NEURONAL IDENTITY OF OSNS

The mouse olfactory system must detect and discriminate a large number of odorants in order to survive because the odorants convey important information about the environment such as location and quality of food, or presence of predators and potential mates. To distinguish among a wide range of odor molecules, the main olfactory system (MOS) is divided into two parts: the olfactory epithelium (OE) where the first order neurons reside and the OB where second order neurons will relay the information to higher structures of the brain. OSNs are the only neurons that have direct physical contact with the environment. This contact occurs on specialized cilia that project from the sensory neuron dendrites into the mucus covering the OE. Inhaled odorants will bind to one of 1000 ORs present in the dendrites of OSNs which are located in the lumen of the nasal cavity and the depolarization signals are transmitted to the OB (Buck and Axel 1991). ORs are G protein coupled receptors with seven-transmembrane domains and transduce odorant-binding signals to neuronal activity via cyclic-AMP (cAMP) signaling.

There are two basic yet very important principles for the organization of MOS. The first principle is that the majority of OSNs express a single OR gene in a mutually exclusive (Malnic et al. 1999; Serizawa et al. 2000) and monoallelic manner (Chess et al. 1994; Ishii et al. 2001) to establish the neuronal identity of OSNs. The second principle is in the targeting of OSN axons to the OB where OSNs expressing the same OR will extend unbranched axons and converge into a specific glomerulus in the OB making synaptic connections with the dendrites of mitral/tufted cells (second order neurons or projection neurons) (Ressler et al. 1994; Vassar et al. 1994; Mombaerts et al. 1996). A glomerulus is a neuropile structure where OSN axons and dendrites of second order neuron make synaptic connections. Therefore, one glomerulus is innervated by axons expressing a single OR which is critical for the odor detection and processing. Furthermore, one odorant can bind to different ORs and a given OR can respond to different odorants (Malnic et al. 1999; Oka et al. 2006). As a result, different odorants inhaled by the animals will activate different ORs and in turn activate unique patterns of glomeruli in the OB (Mori et al. 2006). Therefore, this discrete organization of the olfactory system allows the mammalian brain to detect and differentiate a large range of odorants.

How is the neuronal identity of OSNs established? It has been proposed that OR gene choice is a stochastic event but similarly to zebrafish (Barth et al. 1996; Kratz et al. 2002), OR expression in the mouse does not appear to be stochastic and therefore suggests the existence of different mechanisms to regulate OR expression. OR expression is spatio-temporally regulated throughout development. OR mRNA is expressed as early as E9 by OSNs and the onset of OR expression seems to be asynchronous whereby some ORs are expressed as the first OSNs differentiate whereas others are expressed in the late

embryonic period (Rodriguez-Gil et al. 2010). In addition, the expression of OR genes is spatially regulated in different regions of the OE (Iwema et al. 2004; Miyamichi et al. 2005). This topographic restriction of expression appears as early as E13 in the OE suggesting that by E13, OSN progenitors are already topographically and lineage restricted (Rodriguez-Gil et al. 2010). It is therefore possible that different transcription factors such as Msx1 and Foxg1 that are also regionally expressed in the OE might differentially regulate the expression of ORs in regions of the OE (Norlin et al. 2001; Duggan et al. 2008). So what are the exact mechanisms that regulate the expression of a single OR per OSN? Both positive and negative regulations appear to play important roles in the decision of which functional OR is expressed. For positive regulation, a cis-acting enhancer 'H' which contains two homeodomain sequences and one O/E (Olf1/EBF TF)-like sequence, was found to be crucial to activate OR gene expression within the MOR28 cluster by physically interacting with one OR gene promoter (Serizawa et al. 2003; Nishizumi et al. 2007). To further ensure that only one OR receptor is expressed, a negative feedback mechanism is present where OR gene expression prevents activation of other endogenous OR genes through an OR protein-dependent feedback mechanism (Serizawa et al. 2003; Feinstein et al. 2004; Lewcock and Reed 2004; Shykind et al. 2004; Nguyen et al. 2007; Fleischmann et al. 2008). However, how OR proteins regulate the negative feedback is yet to be elucidated.

## AXON GUIDANCE EVENTS IN THE WIRING OF THE MAMMALIAN OLFACTORY SYSTEM

In order to ensure an accurate representation of the activation state of the large number of ORs, OSNs expressing a single OR project their axons to two symmetrically bilateral glomeruli out of an estimated 1800 glomeruli in the OB (Royet et al. 1988; Ressler et al. 1993; Vassar et al. 1993). Since OSNs expressing a specific receptor are randomly dispersed across one of four partially overlapping regions of the OE rather than strictly limited to, axonal convergence of axons expressing the same OR must take place at the level of the OB (Figure 1A). How do OSN axons select their target glomeruli in such a complex three-dimensional target field? The target choice of OSN axons appears to rely on a combination of molecular determinants that first promote segregation of axons into broad regions of the OB to form a crude topography and then favor their sorting and convergence into specific glomeruli.

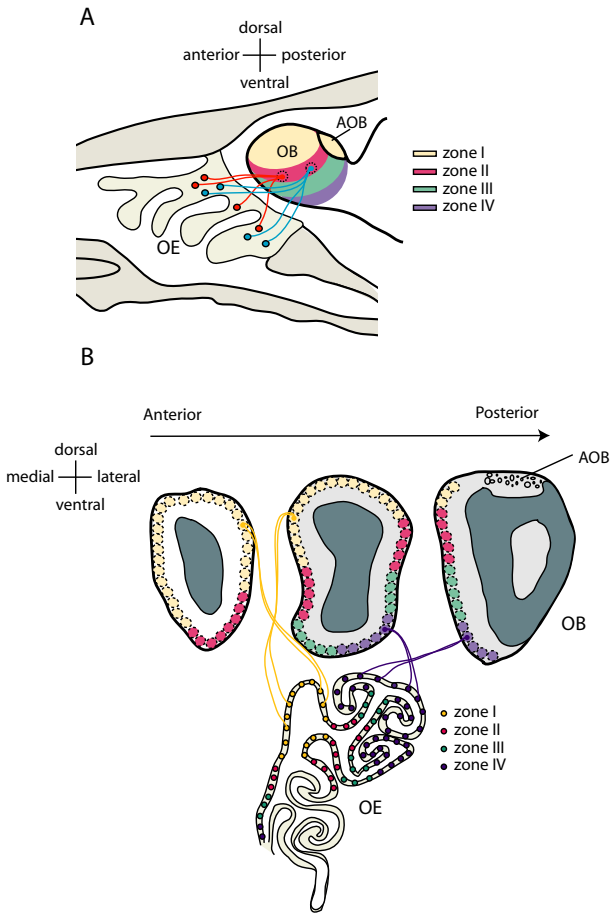


***Figure 1: Axonal projections in the main olfactory system.***

*A. OSNs (closed red and blue circles) located throughout the OE extend axons that synapse with dendrites of second-order neurons inside neuropil structures termed glomeruli (dashed circles) within the OB. Axons of OSNs expressing the same ORs (red or blue) converge to innervate specific glomeruli in the OB along the antero-posterior axis. The approximate positions of zones in the dorso-ventral axis of the OB are represented with different colors. AOB: accessory olfactory bulb.*

*B. OSNs expressing the same OR are scattered within spatially defined but partially overlapping zones of the OE. Schematic representations of a coronal section through the*

*OE and of sections through the OB at three different antero-posterior positions are shown. For simplicity, the zones are shown with distinct colors and overlap is not represented. OSNs located in the dorso-medial region of the OE (yellow circles) (zone I) innervate glomeruli (dashed circle) in the dorsal aspect of the OB while OSNs located in the ventro-lateral region of the OE (purple circles) (zone IV) project their axons to glomeruli in the ventral aspect of the OB. OSNs located in zones II (red circles) and zone III (green circles) project their axons to corresponding zones in the OB. The numbering of zones is according to the nomenclature (Sullivan et al. 1995). OSNs expressing the same OR (yellow or purple) innervate bisymmetrically located glomeruli on the medial and lateral sides of the OB at two different positions along the antero-posterior axis.*

*Axonal projections in the dorso-ventral axis of the olfactory bulb (OB)*

OSN axons projecting along the surface of the OB must accurately innervate glomeruli that are positioned at specific coordinates in the dorso-ventral, antero-posterior, and medio-lateral axes of the OB. There is good evidence supporting a direct spatial relationship between the location of an OSN cell body inside the OE and the dorso-ventral position of the glomerulus it innervates in the OB.

Early in situ hybridization experiments suggested that each OR gene is expressed in a limited number of OSNs that are located in one of four defined regions of the OE termed zones (Strotmann et al. 1992; Ressler et al. 1993; Vassar et al. 1993; Strotmann et al. 1994). These zones were proposed to be spatially restricted and to span the olfactory epithelium from the dorso-medial (zone I) to the ventro-lateral (zone IV) region of the OE (Figure 1B) (Sullivan et al. 1996). More recent in situ hybridization experiments

suggest that OR gene expression is continuous and overlapping in certain regions across the dorso-medial to ventro-lateral axis of the OE (Norlin et al. 2001; Iwema et al. 2004; Miyamichi et al. 2005). Dye-tracing experiments revealed a correlation between the location of OSNs in the OE and their projections in the dorso-ventral axis of the OB (Astic and Saucier 1986; Saucier and Astic 1986; Miyamichi et al. 2005). The concept of zone-to-zone axonal projections is also supported by immunohistochemistry and in situ hybridization experiments demonstrating that OSNs located in the dorso-medial region of the OE project their axons to the dorsal aspect of the OB (Gussing and Bohm 2004; Tsuboi et al. 2006). Hence, the correlation observed between glomerular positioning in the dorso-ventral axis of the OB and the location of OSN cell bodies in the dorso-medial to ventro-lateral axis of the OE suggest that spatial information may be provided through the differential expression of molecules that regulate the growth and targeting of axons.

The concept of zone-to-zone axonal projections raises the possibility that OSNs located in the four regions of the OE may express different molecular determinants that allow their axons to segregate in the dorso-ventral axis of the OB. However, recent in situ hybridization experiments suggest that OR gene expression is continuous and overlapping across the dorso-medial to ventro-lateral axis of the OE rather than strictly restricted to four specific zones (Gussing and Bohm 2004; Miyamichi et al. 2005; Tsuboi et al. 2006). This observation raises the possibility that graded expression of a receptor across the dorso-medial to ventro-lateral axis of the OE may direct the dorso-ventral targeting of axons in the OB. To examine this possibility, we evaluated the pattern of expression of various axon guidance receptors in the OE and observed that Robo-2, a receptor for Slit chemorepellents, is expressed in a high dorso-medial to low ventro-

lateral gradient in the OE throughout development and in the adult. Furthermore, the chemorepellent Slit-1 is expressed in the ventral region of the OB (Figure 2A). The exact role of Slit-1 and Robo-2 in the targeting of the OSN axons to the dorso-ventral axis of the OB will be discussed in details in the chapter 2.

Previous reports have shown that Neuropilin-2 (Npn) could be involved in the segregation of OSN axons to the dorsoventral axis of the OB (Norlin et al. 2001; Walz et al. 2002; Cloutier et al. 2004). Recently, two studies have shown that indeed, Npn-2 and its ligand Sema3F are involved in the targeting of OSN axons along dorso-ventral axis of the OB (Takahashi et al. 2010; Takeuchi et al. 2010). Interestingly, like Robo-2, Npn-2 is also expressed in a graded manner in the OE. Npn-2 expression mirrors the expression pattern of Robo-2 in such a way that Npn-2 is expressed in a high ventro-lateral to low dorso-medial in the OE (Figure 2A). Moreover, OSNs located in zone 1 send their axons very early during development of the OB and OSNs present in zone 4 expressing Npn-2 project axons later during embryogenesis (Takeuchi et al. 2010). It has been proposed that OSN axons targeting to the dorsal region of the OB (zone 1) secrete the chemorepellent Sema3F and therefore repel OSN axons expressing Npn-2 to the ventral region of the OB (Takeuchi et al. 2010). Ablation of either Sema3F or Npn-2 expression in the mouse leads to ectopic innervations of the dorsal region of the OB by OSNs that normally innervate the ventral part of the OB.

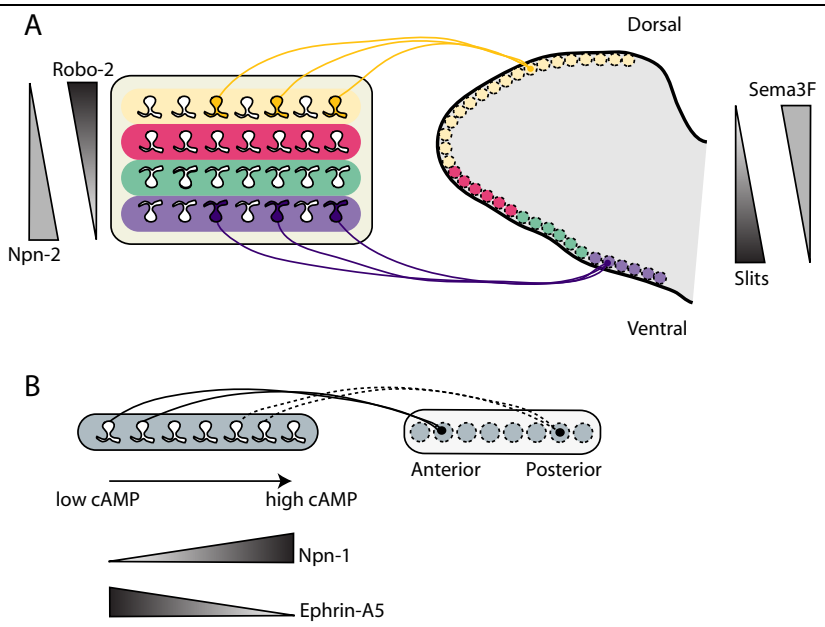


***Figure 2: Control of OSN axonal targeting by axons guidance cues.***

*A. Axonal targeting within the dorso-ventral axis of the OB is controlled by the graded expression of axon guidance cues and their receptors. The graded expression of the Slit receptor Robo-2 in a high dorso-medial (yellow) to low ventro-lateral (purple) gradient*

*within the OE is required to segregate axons emanating from OSNs in the dorso-medial region of the OE to the dorsal aspect of the OB. Expression of Slit-1 in the ventral region of the OB prevents Robo-2-expressing axons from entering the ventral region of the OB. It is likely that other axon guidance receptors may be expressed in an opposite gradient to Robo-2 in the OE and serve to regulate the targeting of ventrally-projecting axons in response to the graded expression of other repellents in the OB.*

*B. Axonal targeting in the antero-posterior axis of the OB is controlled through the differential expression of axon guidance molecules in OSNs. OR-mediated signaling modulates the levels of cAMP present in OSNs, which controls expression of specific*

*axon guidance molecules such as Npn-1 and Ephrin-A5 through a transcriptional mechanism. OSNs containing high levels of cAMP express high levels of Npn-1 and low levels of Ephrin-A5 and as a result innervate glomeruli in more posterior regions of the OB within a specific zone. In contrast, OSNs containing low levels of cAMP express low levels of Npn-1 and high levels of Ephrin-A5 and project their axons to glomeruli located in the anterior part of the OB. The exact mechanism whereby differential expression of Npn-1 and Ephrin-A5 controls the anterior-posterior targeting of axons remains to be determined.*

*Axonal projections in the medio-lateral axis of the OB*

In addition to targeting to the correct zone within the OB, OSN axons expressing the same OR innervate two symmetrically positioned glomeruli on either the medial or lateral side of the OB. Retrograde labeling experiments suggest that there is a loose correlation between the location of an OSN within each zone of the OE and the position of the glomerulus it innervates in the medio-lateral axis of the OB (Levai et al. 2003). For example, OSNs projecting axons to a medial glomerulus are grouped within subregions of a specific OE zone. It is therefore possible that differential expression of axon guidance cues can also regulate the medio-lateral segregation of these axons.

The secreted chemorepellent Sema3A has been shown to direct the medio-lateral targeting of OSN axons. Sema3A is expressed in the nerve layer in the ventral aspect of the OB as well as in mitral cells of the OB (Pasterkamp et al. 1998; Schwarting et al. 2000). The Sema3A receptor, Npn-1, is expressed in subsets of OSNs and Npn-1-positive axons segregate to either the medial or lateral regions of the OB according to their

targeting position along the antero-posterior axis. In Sema3A mutant mice, the medio-lateral segregation of Npn-1-positive axons is lost leading to changes in the formation of the olfactory map (Schwarting et al. 2000; Taniguchi et al. 2003; Schwarting et al. 2004).

The insulin growth factors, IGF-1 and IGF-2, have also been implicated in the control of medio-lateral targeting in the OB (Scolnick et al. 2008). Genetic ablation of IGFs or IGF-1R leads to a reduction in innervation of the lateral region of the OB. Furthermore, in IGF-1R mutant mice, the subset of axons expressing the P2 OR that normally target to a glomerulus located on the lateral side of the OB innervate a more ventro-medial region of the bulb. Interestingly, the subset of P2-expressing axons that innervate a glomerulus on the medial side of the bulb is unaffected in these mice suggesting that IGF signaling may only be required to guide laterally projecting axons. The exact mechanism through which IGFs control the targeting of these axons is not fully understood. Early in development, IGF-1 is expressed in a low medial to high lateral gradient at the anterior part of the bulb and IGF-1 can attract growing OSN axons in vitro. These observations suggest that IGF-1 could act as an attractant to promote the growth of axons into the lateral region of the bulb. However, while IGF-1R is expressed in OSNs, no gradient of expression that could explain how medially and laterally projecting axons respond differentially has been detected. Hence, the differential responsiveness of OSN axons to IGF may therefore be modulated through yet unidentified mechanisms.

*Axonal projections in the antero-posterior axis of the OB*

In contrast to dorso-ventral and medio-lateral targeting of OSN axons, the position of an innervated glomerulus in the antero-posterior axis of the OB does not appear to correlate with the position of OSN cell bodies within the OE. Changes in the levels of cAMP induced by signaling downstream of OR receptors have been proposed to control the expression of molecules that direct the targeting of OSN axons in the antero-posterior axis of the OB.

ORs are G-protein coupled receptors with seven transmembrane domains that transduce odorant-evoked signals into neuronal activity via activation of adenylyl cyclase type III leading to production of cAMP which activates the cyclic nucleotide gated channels (Imai and Sakano 2008). ORs were proposed to play an instructive role in the targeting of OSN axons based on the observations that ORs are expressed on axon termini and that ablation of their expression leads to defects in OSN axonal convergence in the OB (Mombaerts et al. 1996; Barnea et al. 2004; Strotmann et al. 2004). Furthermore, the genetic ablation of several important components in the odor-evoked signaling pathway does not grossly affect the projections of OSN axons to the OB. For example, mice homozygous for a null mutation in $G_{olf}$ are anosmic but retain a normal map of sensory projections in the OB (Belluscio et al. 1998). Mice bearing a targeted mutation in the alpha subunit of the olfactory cyclic nucleotide gated (CNGA2) ion channel show no defects in the pattern of convergence of olfactory axons for the majority of OR examined (Lin et al. 2000; Zheng et al. 2000).

ORs were proposed to regulate axonal targeting by favoring the coalescence of axons expressing the same ORs (Feinstein et al. 2004; Feinstein and Mombaerts 2004).

New insights into how ORs participate in the targeting of OSN axons were provided by experiments in which G-protein signaling and cAMP levels were altered in OSNs (Imai et al. 2006; Chesler et al. 2007). Expression in OSNs of a mutated OR that does not interact with G proteins or of a non-functional tagged OR leads to a lack of axonal convergence. Interestingly, expression of a constitutively active $G_s$ protein rescues these defects and can also promote axonal convergence, suggesting that G protein signaling in OSNs is sufficient to direct growing axons in the OB (Imai et al. 2006; Chesler et al. 2007). Partial rescue of the wiring defects was also observed by expressing a constitutively active form of PKA suggesting that the position of glomeruli in the anterior-posterior axis of the OB may be regulated by the strength of cAMP/PKA signaling (Lin et al. 2000). An important role for cAMP in axonal targeting was further supported by the observations that genetic ablation of adenylyl cyclase III perturbs the formation of glomeruli and the accurate convergence of OR-specific axons in the anterior-posterior axis of the OB (Col et al. 2007; Zou et al. 2007).

How do changes in cAMP levels contribute to the targeting of axons in specific glomeruli within the OB? Different levels of cAMP/PKA signaling in OSNs may affect transcription and expression of axon guidance molecules at the surface of growing axons. RT-PCR analyses of single OSNs in which cAMP levels have been genetically manipulated revealed the differential expression of several genes including Npn-1 and PlexinA3, two well-characterized receptors for secreted semaphorins (Imai et al. 2006). In addition, Npn-1 expression is reduced in adenylyl cyclase III mutant mice, further supporting the possibility that cAMP signaling controls expression of axon guidance receptors (Col et al. 2007). The expression of other classical axons guidance molecules is

also regulated through OR-signaling dependent control of transcription. EphA5 and EphrinA5 are expressed in non-overlapping populations of OSNs in the OE (Cutforth et al. 2003; Serizawa et al. 2006). In OSNs lacking CNGA2, higher levels of EphrinA5 are observed while expression of EphA5 is decreased (Serizawa et al. 2006). The regulation of the levels of expression of EphrinAs on OSN axons plays an important role in the targeting of axons as ablation of expression of both EphrinA5 and EphrinA3 leads to a shift in innervated glomeruli towards the posterior aspect of the OB (Cutforth et al. 2003). Hence based on these studies, it is conceivable that OSNs expressing specific ORs could contain different levels of cAMP, which in turn affects the expression of different axon guidance molecules that regulate axonal targeting in the anterior-posterior axis of the OB (Figure 2B).

As mentioned above, each OR species generates a unique level of cAMP signals that regulated the level of axon guidance molecules Npn-1 and Sema3A (Imai et al. 2006). Recently, the same group has illustrated that Npn-1 is expressed in OSN axons and it is found in an anterior (low) to posterior (high) gradient in the OB. Using a different transgenic mouse line, they have demonstrated that an increase or decrease of Npn-1 expression in OSNs caused either posterior or anterior glomerular shift (Imai et al. 2009). Furthermore, either in Npn-1 or Sema3A deficient mice, glomeruli positions are affected along antero-posterior axis of the OB (Imai et al. 2009). Interestingly, the same study reported that pretarget axon sorting plays an important role in the targeting of OSN axons along antero-posterior axis of the OB (Imai et al. 2009). The study illustrated that in either Npn-1 or Sema3A KO mouse, the axon sorting within the bundle is perturbed and this caused the glomerular shift along the antero-posterior axis of the OB (Imai et al.

2009). In contrast, for the targeting of dorso-ventral axis of the OB, OSN axons do not need sorting within the bundle because OSN axons targeting zone 1 and OSN axons targeting ventral region of the OB are already presegregated in separate bundles in the OE (Takeuchi et al. 2010).

*Compartmentalization of axons in the olfactory bulb by glycans*

In addition to classical axon guidance molecules, glycans have been proposed to promote the gross compartmentalization of large populations of axons in the OB. In early studies characterizing immunoreactivity to monoclonal antibodies recognizing unique carbohydrate moieties, OSNs were found to express lactosamines (Young et al. 1981; Schwarting and Crandall 1991). While low expression of lactosamines was observed throughout the OE, higher levels of lactosamines were detected in subsets of OSNs located in the dorso-medial regions of the OE (Young et al. 1981; Schwarting and Crandall 1991; Schwarting et al. 1992). The differential expression of lactosamine-containing glycans may therefore influence the segregation of subsets of axons in the OB. The potential role of lactosamines in the patterning of the olfactory system was examined by disrupting their synthesis in mouse. β1,3-N-acetylglucosaminyltransferase I (β3GnTI) belongs to the β2GnT family that is responsible for the initiation and addition of N-acetylglucosamine to growing carbohydrate chains in many tissues (Zhou et al. 1999; Henion et al. 2005). In β3GnTI-deficient mice, early projections of lactosamine-rich OSNs expressing P2 or I7 ORs were unable to properly innervate glomeruli in the OB and remained in the nerve layer adjacent to where they normally target (Henion et al. 2005). In addition to these axon guidance defects, P2 and I7-expressing OSNs were

progressively lost from the OE early in development, suggesting that lactosamines are also required for their survival. Interestingly, expression of lactosamines in a subset of axons may also be required to direct the growth of lactosamine-negative axons in the olfactory bulb. Indeed, ablation of β3GnTI expression leads to the formation of multiple glomeruli by axons expressing the OR M72, which do not normally express lactosamines (Schwarting and Henion 2007).

How do lactosamines control the targeting of axons in the OB? It has been suggested that some members of the galectin family of carbohydrate binding proteins are involved in sorting carbohydrate-expressing axons as they grow towards the OB (Storan et al. 2004). Galectin-1 is expressed in the ECM in the pathway taken by OSNs from the nasal cavity to the OB at embryonic ages when axons are projecting through this region (Tenne-Brown et al. 1998; Crandall et al. 2000). These ECM molecules are expressed in a highly restricted manner such that channel-like regions are formed at the boundaries between areas of high and low expression. Galectin-1 may therefore promote fasciculation of olfactory nerves by restricting the pathway of projection and by promoting axonal adhesion of lactosamine-expressing axons to the ECM (Mahanthappa et al. 1994; Crandall et al. 2000).

The observation that the targeting of lactosamine-negative populations of axons is also affected in β3GnTI raises the possibility that lactosamine-poor OSNs could express lactosamine-interacting molecules which help direct them to their appropriate positions in the OB. After loss of lactosamine expression, these OSN populations would lose crucial cell-cell interactions, potentially explaining why heterogeneous glomerular innervation occurs. Another intriguing possibility is that binding of lactosamines to lactosamine-

interacting molecules modulates the responsiveness of axons to guidance cues expressed in the OB and ECM. The transmembrane protein EVA-1 that contains two predicted galactose-binding ectodomains was shown to modulate the responsiveness of axons to slit in *C. elegans* likely through an interaction with the Robo receptor homolog SAX-3 (Fujisawa et al. 2007). The direct binding of SLT-1, the slit *C. elegans* homolog, to EVA-1 may promote SAX-3 signaling. Human and mouse EVA-1 homologs have been identified but whether these proteins are expressed in the developing olfactory system remains to be established. Hence, it is possible that expression of lactosamines on subsets of OSN axons could modulate the response of these axons or of surrounding axons to Slits that are expressed in the OB.

*Axon-Axon interactions in the formation of glomeruli*

The establishment of a coarse map is followed by the formation of specific glomeruli whereby axons of OSN expressing the same OR converge into one to two glomeruli on each side of the OB. How do like-axons sort into specific glomeruli? One possible mechanism of sorting would involve homotypic interactions between axons expressing the same receptor. While elegant genetic analyses have linked ORs to the establishment of axonal identity, several families of adhesion molecules have recently been implicated in the sorting of like axons to specific glomeruli in the OB. The identification of these molecules has led to a model whereby the sorting of axons may be regulated through the combinatorial expression of several families of cell adhesion molecules. Axons expressing the same set of cell adhesion molecules may fasciculate

together and different strengths of interaction may be generated through combinatorial expression of cell adhesion molecules (Figure 3A).

The Kirrel family of Ig domain containing molecules were first implicated in olfactory axonal pathfinding when some members were shown to be differentially expressed in OSNs using serial analysis of gene expression (SAGE) (Serizawa et al. 2006). Kirrel-2 and 3 are expressed in subsets of OSNs in a roughly complementary fashion. OSNs expressing high levels of Kirrel-2 express low levels of Kirrel-3 and vice versa. Furthermore, both Kirrel-2 and 3 can undergo homophilic interactions but do not interact with each other. Glomeruli innervated by Kirrel-2 and Kirrel-3-positive axons are intermingled in the OB. Overexpression of Kirrel-2 in half of the OSNs expressing a specific OR leads to the splitting of axons into two adjacent glomeruli.

Another cell adhesion molecule reported to be involved in the convergence of axons in glomeruli of the OB is a member of the contactin subfamily of the Ig superfamily, BIG-2. BIG-2, or contactin-4, is a GPI (glycosylphosphatidylinositol) anchored glycoprotein expressed in a subpopulation of OSNs and on axon termini (Kaneko-Goto et al. 2008). Immonostaining analyses on the OB have revealed mosaic expression of BIG-2 on axon termini with some glomeruli expressing high or low levels of BIG-2 while others are BIG-2-negative. Furthermore, BIG-2 expression correlates with OR gene expression in OSNs. Ablation of BIG-2 expression in mice leads to the formation of numerous ectopic glomeruli suggesting that BIG-2 plays a role in the establishment of the glomerular map. Hence the OR-correlated expression of cell adhesion molecules in different classes of OSN may contribute to the sorting and convergence of like axons to specific glomeruli. In addition to Kirrels and BIG-2, the

protocadherin-α (Pcdh-α) has been implicated in the accurate targeting of OSN axons (Hasegawa et al. 2008). Pcdh-α is highly expressed in OSNs and ablation of its expression leads to the disruption of convergence into specific glomeruli. In Pcdh-α null mice, OSN expressing the M71 and MOR23 ORs innervate multiple glomeruli. However, it is unclear how Pcdh-α contributes to the convergence of axons since it is expressed evenly among OSNs.

What mechanism regulates the expression of Kirrels and BIG-2 in different populations of OSNs? An important role for neuronal activity has emerged in the OR-correlated expression of Kirrels and Big-2. In mice with the CNGA2 mutation, random X-inactivation leads to the generation of two populations of OSNs in heterozygous female mice. A subset of OSNs retains expression of CNGA2 while others do not (Zhao and Reed 2001). In these mice, CNGA-2-positive and CNGA-2-negative axons expressing the same OR segregate into two glomeruli in the OB. Immunohistochemical analyses of CNGA2-positive and negative glomeruli revealed lower levels of expression of Kirrel-2 and BIG-2 in CNGA2-negative glomeruli, suggesting that neural activity positively regulates their expression (Serizawa et al. 2006; Kaneko-Goto et al. 2008). In contrast, levels of Kirrel-3 expression were increased in CNGA2-negative glomeruli. Thus neuronal activity may regulate the expression of cell adhesion molecules and of other axon guidance molecules involved in controlling the fasciculation and targeting of OSNs. In keeping with this possibility, the levels of expression of EphrinA5 on subsets of olfactory axons is positively regulated by activity (Serizawa et al. 2006).

Is the combinatorial expression of cell adhesion molecules sufficient to sort OSN axons and promote their convergence into specific glomeruli? In addition to positive

homophilic interactions between OSNs, it is likely that repulsive forces may also contribute to the segregation of axons expressing different ORs (Figure 3B). Indeed, EphrinA5 and its receptor EphA5 are expressed in non-overlapping subsets of OSNs (Serizawa et al. 2006). OSNs expressing high levels of EphA5 express low levels of EphrinA5 and vice-versa. This observation raises the intriguing possibility that populations of axons expressing either EphrinA5 or EphA5 repel each other thereby promoting their segregation. In addition to contact-mediated repulsion, it is possible that controlled secretion of chemorepellents by subsets of axons could also contribute to this process. In combination with adhesive forces, these repulsive forces could serve to promote the segregation and sorting of axons. It remains to be determined whether EphrinA5-EphA5 interactions are required to segregate large populations of OSNs within bundles and whether other families of repulsive molecules also contribute to this process.

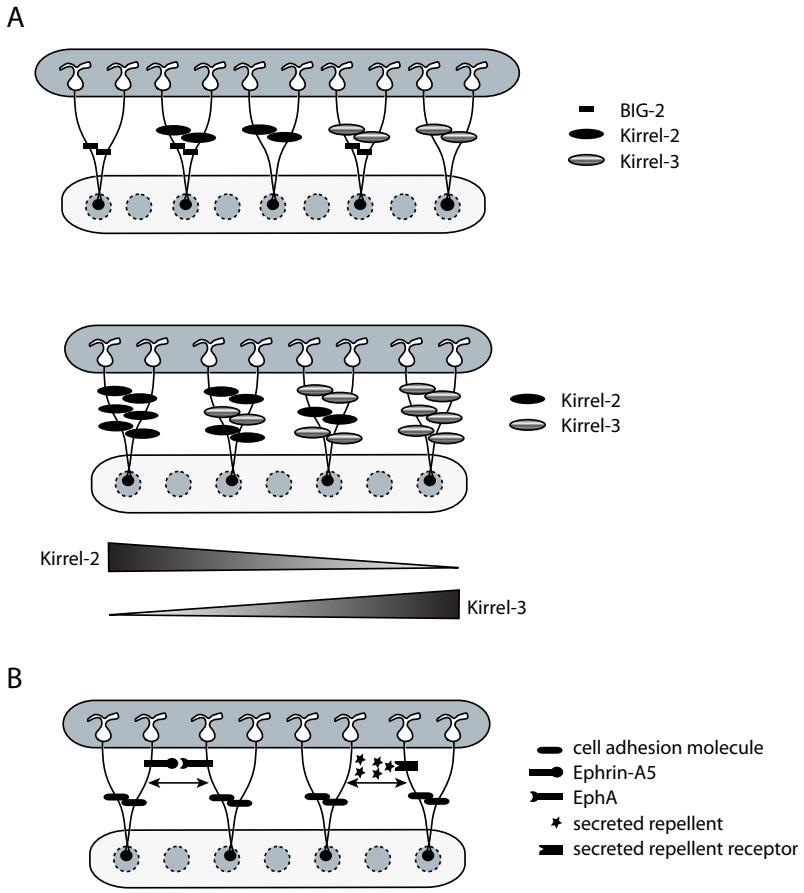


***Figure 3: Sorting of OSN axons to specific glomeruli through a combination of attractive and repulsive forces between axons.***

*A. OSNs expressing the same OR converge into specific glomeruli. The sorting of OR-like axons may be achieved through the combinatorial expression of cell adhesion molecules on axons. Kirrel-2, Kirrel-3, and BIG-2 are differentially expressed in OSNs. The strength of adhesive forces between axons may be directly related to the combination of receptors expressed. For example, while axons expressing BIG-2 alone fasciculate together, adhesive force between axons expressing both BIG-2 and Kirrel-2 are likely to be more robust (top diagram). Furthermore, the graded expression of Kirrel family*

*members in OSNs may also contribute to the differential adhesive properties of their axons (bottom diagram).*

*B. In addition to adhesive forces that favor the fasciculation of like axons, repulsive forces between axons may promote the segregation of axons expressing different ORs into different bundles. Ephrin-A5 is expressed at various levels in different OSNs and may promote repulsion of axons expressing EphA5 receptors. It is also possible that chemorepellents secreted by OSN axons may promote the segregation of axons expressing different ORs within large bundles of axons.*

*Refinement of the sensory map*

Despite the multitude of mechanisms that have evolved to ensure the accurate targeting of axons in the OB, mistargeting of axons and formation of heterogenous glomeruli innervated by axons expressing different ORs are observed in early post-natal animals. As the animal matures, these glomeruli are refined to form homogenous glomeruli innervated by axons expressing a single OR. This refinement process is dependent on olfactory sensory experience. Unilateral naris closure, which decreases both spontaneous and odorant-evoked activity, leads to the persistent presence of heterogenous glomeruli in adult mice (Philpot et al. 1997; Nakatani et al. 2003). The refinement of the map and the disappearance of heterogenous glomeruli through activity-dependent mechanisms occur during a critical period that varies for different subsets of OSNs and that can be accelerated by odorant exposure (Zou et al. 2004; Kerr and Belluscio 2006). In addition to playing a role in the refinement of the sensory map, neuronal activity is

important for the maintenance of OSN connections in the OB (Zhao and Reed 2001; Yu et al. 2004).

*Role of transcription factors (TFs) in the targeting of OSN axons*

One of the critical regulatory events during development of the nervous system is the coordination of proliferation and differentiation of many different cells. A number of transcriptional regulators influence various events to coordinate the formation of diverse structures in the brain. This is especially essential for the formation of the MOS. Transcription factors (TFs) play important roles not only in the proper development of the OE (Guillemot et al. 1993; Xuan et al. 1995; Cau et al. 2000; LaMantia et al. 2000; Tietjen et al. 2003; Hirota and Mombaerts 2004; Kolterud et al. 2004; Theriault et al. 2005; Duggan et al. 2008; Kawauchi et al. 2009) and the OB (Bulfone et al. 1998; Levi et al. 2003; Yoshihara et al. 2005; Laub et al. 2006; Caiazzo et al. 2010) but they also influence the targeting of the OSN axons to the OB.

Recent studies show that the *distalless*-related homeogenes, Dlx-5 and the vertebrate X-linked prd-type homeobox gene, Arx, are not only implicated in the development of the OB, but they are also involved in the targeting of OSN axons to the OB. Both genes play a role in the formation of interneurons in the OB. Furthermore, in Dlx-5 and Arx KO animals, OSN axons fail to contact the OB and fail to establish functional olfactory neural circuitry (Levi et al. 2003; Yoshihara et al. 2005). Additional TFs and transcriptional repressors regulate OSN projections. The mammalian Olf1/EBF (O/E) family of repeated helix-loop-helix TFs, particularly, O/E2 and O/E3, are required for a specific subset of OSN axons to project to the dorsal part of the OB (Wang et al.

2004). *Fez*, a zinc-finger gene encoding a transcriptional repressor, expressed by the OSNS is cell-autonomously required for OSN axon termination into the OB. In *Fez* deficient mice, OSN axons did not reach the OB but instead formed a tangled structure (Hirata et al. 2006; Watanabe et al. 2009). In addition to *Fez*, another zinc finger TF Zfp423/OAZ (O/E associated zinc finger protein) regulates OSN differentiation and axonal targeting (Cheng and Reed 2007). OAZ acts as an inhibitor of O/E TF by binding to O/E and impairing it from interacting with its consensus binding site in olfactory receptor promoters. In OAZ deficient mice, there is a decrease in mature OSN axons failing to reach the OB (Cheng and Reed 2007).

## ODOR INFORMATION PROCESSING TO HIGHER STRUCTURES OF THE BRAIN

Olfactory perception occurs when odorant molecules bind to ORs in the nasal cavity and activate a transduction cascade that leads to the production of action potentials which are transmitted to the brain. This information is then processed in higher structures of the brain to allow for the discrimination of odorants and to elicit cognitive, emotional, hormonal and behavioral responses. One odorant can activate numerous ORs, while a single OR can be activated by several different odorants (Malnic et al. 1999; Oka et al. 2006). Each type of odorant molecule is recognized by the activation of a unique combination of ORs in a combinatorial code. Since OSN axons expressing the same OR, although randomly distributed within different zones in the OE, will converge to a specific glomerulus, this combinatorial code is also maintained in the OB. Therefore,

information coming from randomly distributed populations of active OSNs is consolidated into a discrete spatial map in the OB.

*Importance of the 'Chemotopic' map*

How is this spatial map in the OB organized and more importantly, what is the importance of this glomerular map? In the OB, imaging experiments suggested that different odorants elicit distinct spatial patterns of activity (Uchida et al. 2000; Spors and Grinvald 2002; Xu et al. 2003; Lin et al. 2006; Soucy et al. 2009; Matsumoto et al. 2010). These studies revealed a coarse chemotopic map where glomeruli that are responsive to structurally similar odorant molecules are located within domains, however within these domains neighboring glomeruli possess different odorant specificities. For example, the glomeruli located in the anteromedial domain in the dorsal OB are activated by odorants possessing aliphatic aldehydes and a subset of esters (Uchida et al. 2000). In contrast, glomeruli present in the lateral domain of the dorsal OB are activated by odorants containing different functional groups such as aliphatic alcohols or phenols as well as ketones and a subset of esters (Uchida et al. 2000). Interestingly, these two domains are targeted by OSNs expressing two different classes of ORs (Kobayakawa et al. 2007; Matsumoto et al. 2010).

These two classes of ORs are phylogenetically distinct groups possessing different amino acid sequences (Zhang et al. 2004; Niimura and Nei 2005). All the OSNs located in zones 2-4 express class 2 ORs and these OSN axons target the ventral part of the OB. On the other hand, OSNs present in zone 1 express either class 1 or class 2 ORs and these OSNs project their axons to glomeruli present in the dorsal region of the OB.

OSNs located in zone 1 that express class 1 ORs will target their axons to the most dorsal part of the OB termed the D1 region and OSN axons positive for class 2 ORs will coalesce to glomeruli in the D2 region of the OB which is located just ventral to the D1 domain (Kobayakawa et al. 2007; Bozza et al. 2009; Matsumoto et al. 2010). Therefore, the anteromedial domain in the dorsal OB is innervated by OSNs expressing class 1 ORs (D1) and the lateral domain in the dorsal OB corresponds to the D2 domain.

Why is this chemotopic map important? The chemotopic map might be arranged in such a way so that certain odorants eliciting explicit behaviors activate specific domains like the D1 and D2 domains of the OB. Therefore, the chemotopic map might correspond to functional compartmentalization of OR maps in terms of odor-induced behavioral responses. In animals, the olfactory system plays an important role in predator avoidances as well as discrimination between safe foods and spoiled foods that could be harmful for the animal. Recent studies have shown that D1 glomeruli are activated by an odorant present in spoiled food, 2-methylbutyric (2MB) acid, while D2 glomeruli are activated by a compound present in fox feces, trimethyl-thiazoline (TMT) (Kobayakawa et al. 2007; Matsumoto et al. 2010). Additionally, D2 glomeruli can be activated by 2-sec-Butyl-dihydrothiazole (SBT) and dehydro-exo-brevicomin (DHB) which are well-known urinary odorants that induce aggressive behavioral responses in male mice (Novotny et al. 1985; Matsumoto et al. 2010). Interestingly, these two domains (D1 and D2) were shown to be important for proper processing of aversive odorant information (Kobayakawa et al. 2007). Using a transgenic mouse system, Kobayakawae et al. ablated all OSNs that form synapses in the D1 and D2 region of the OB. The resulting mutant mice lacked innate responses to aversive odorants such 2MB and TMT, but were able to

perform simple odor discrimination tests (Kobayakawa et al. 2007). Therefore, the chemotopic map appears to be divided in a way that odorants eliciting aversive behaviors are grouped in the dorsal part of the OB. It is tempting to speculate that the dorsal region of the OB might also be important for regulating additional innate behaviors such as aggression since D2 glomeruli are also activated by the mouse urinary odorants SBT and DHB. While it remains to be determined whether other regions of the OB are involved in the processing of odorants to elicit specific behaviors in animals, it is likely that the OB is composed of at least two functional modules.

Is the formation of an accurate glomerular map essential for innate behaviors? In *Drosophila*, it is suggested that a hard-wired neural circuit is crucial for the innate odor processing information because these innate behaviors should be developmentally programmed and invariant in different individuals so that even naïve animals could appropriately behave in presence of these odorants (Suh et al. 2004; Stockinger et al. 2005; Fleischmann et al. 2008). While the ablation of OSNs innervating the dorsal part of the OB has shed some light on the role of this region in regulating innate responses to aversive odors, it did not address whether development of an accurate glomerular map is essential for these responses. Studies in Sema3A mutant mice have shown that defects in the spatial pattern of glomeruli can lead to a disruption of the odorant evoked activity map in the OB, but whether this disruption affects behavior in these mice is unknown (Taniguchi et al. 2003). In chapters 3 and 4 of this thesis, I take advantage of a mouse model that I have developed to examine the effect of a disrupted glomerular map on innate behaviors in mice.

*Beyond the OB*

How is the topographic odor map of the OB represented in higher olfactory centers? Mitral and tufted cells of the OB project their axons through the lateral olfactory tract (LOT) and innervate to pyramidal neurons in the olfactory cortex (Haberly and Price 1977). The olfactory cortex is composed of several anatomically distinct areas: anterior olfactory nucleus, piriform cortex, olfactory tubercle and part of the amygdala and entorhinal cortex (Haberly and Price 1977). Interestingly, no topographic (point-to-point) organization has been observed although mitral and tufted cells within the same area of the OB project their axons in similar target areas (Haberly and Price 1977; Scott 1981; Schoenfeld and Macrides 1984). In addition, projection neurons located in the dorsal part of the OB target their axons to the piriform cortex while mitral/tufted neurons located in the ventral part of the OB tend to target their axons both to the piriform cortex and olfactory tubercle (Scott 1981). Recent studies in *Drosophila* demonstrated that the projection neurons innervating the same glomerulus in the antennal lobe (comparable to the OB) target similar areas in higher structures of the brain (Jefferis et al. 2007; Lin et al. 2007). Additionally, projection neurons innervating different glomeruli exhibit discrete but overlapping distributions of axonal arbors (Jefferis et al. 2007; Lin et al. 2007). In zebrafish, mitral cell neurons innervating the same glomerulus exhibit similar axonal trajectories and projection neurons innervating different glomeruli target distinct but overlapping areas in higher structures of the brain (Miyasaka et al. 2009). Even though there is no clear topographic map like in the OB, OB projection neurons seem to target the olfactory cortex in a somewhat orderly manner.

How is the odor information processed in the olfactory processing center, more specifically in the piriform cortex? Many studies used electrophysiological recordings, analysis of odorant evoked Fos gene expression and optical recordings to examine how odorants are represented in the piriform cortex (Illig and Haberly 2003; Rennaker et al. 2007; Poo and Isaacson 2009; Stettler and Axel 2009). The studies show that odorants evoke activity in a sparse spatially scattered manner across piriform cortex neurons without any topographic patterns in which cells selectively respond to a given odorant (Illig and Haberly 2003; Rennaker et al. 2007; Poo and Isaacson 2009; Stettler and Axel 2009). However, the odorants will evoke unique and distributed activity patterns by an ensemble of neurons (Stettler and Axel 2009). Therefore, the chemotopic map present in the OB is not exactly maintained but reorganized in higher olfactory centers. Since the connections from the OB to the piriform cortex appear random without any clear stereotypic projections, the representation of the quality of an odorant is probably acquired through experiences. Indeed, this appears to be the case where odor discrimination and perception of odor quality are lost in a patient following bilateral resection of medial temporal lobes which included the piriform cortex (Eichenbaum et al. 1983). This patient is the well-known amnesiac H.M.. H.M. was able to detect odor and was also capable of discriminating different odor intensity, however, he was unable to discriminate or identify odor (Eichenbaum et al. 1983). In addition, in rat and also in *Drosophila*, the piriform cortex was found to be essential for odor discrimination (Mushroom body is the equivalent of piriform cortex in *Drosophila*) (Hasselmo and Barkai 1995; Saar et al. 2001; Wilson 2001; Wilson and Stevenson 2003; Jortner et al. 2007; Murthy et al. 2008). However, odorants can elicit innate behavioral responses

suggesting that a second area of the brain must receive stereotyped connections and predetermined inputs from the OB. Indeed, in *Drosophila*, avoidance responses elicited by a stress odorant was not abolished when the mushroom body was ablated, however, conditioned (learned) olfactory avoidance was affected (Suh et al. 2004). Furthermore, odorant eliciting male courtship behavior activates a very stereotyped pathway in the OS where the projection neurons will target its axons to protocerebrum and also to the mushroom bodies (Stockinger et al. 2005). In the zebrafish, using high-resolution $Ca^{2+}$ imaging and electrophysiological recordings, it was found that mitral cells targeted two different regions in the higher structure of the brain: the subpallial target area and the pallial area homologous to the olfactory cortex (Yaksi et al. 2009). The subpallial target area is connected to limbic structures which suggest that odor information processed through the subpallial target area might be involved in the control of general behavioral responses (Wong 1997; Rink and Wullimann 2004). Therefore, different pathways might be involved in processing the quality of different odorants.

Where are the innate behaviors elicited by odorants processed in the mouse brain? A number of studies have investigated the neural basis of fear-related behavior and have established that the amygdala, the bed nucleus of the stria terminalis (BNST), the periaqueductal gray and other nuclei are responsible for the processing of fear responses (Fendt and Fanselow 1999; Ledoux 2000; Walker and Davis 2002). One potent inducer of innate fear behavior in rodents is TMT (Vernet-Maury et al. 1984; Kobayakawa et al. 2007). TMT is present in fox feces and it is very effective in eliciting fear in naïve rodents (Vernet-Maury et al. 1984; Kobayakawa et al. 2007). As mentioned above, TMT activates glomeruli present in the D2 region of the OB, which is essential to elicit innate

avoidance behaviors of the mouse in the presence of TMT (Kobayakawa et al. 2007; Matsumoto et al. 2010). Several studies indicate that the TMT-induced fear response involves the BNST (Fendt et al. 2003; Kobayakawa et al. 2007; Coryell et al. 2008; Ziemann et al. 2009).

## SLIT AND ROUNDABOUT (ROBO) AXON GUIDANCE MOLECULES

The Slit family of axon guidance molecules and their receptors, the Robos, were originally identified as potent regulators of commissural axon pathfinding (Brose et al. 1999; Hummel et al. 1999; Kidd et al. 1999; Li et al. 1999). The structure of Slit is conserved across many species including C. elegans, zebrafish, chickens, and mammals (Li et al. 1999; Hao et al. 2001; Yeo et al. 2001). In mice, three different Slit family members have been identified (Li et al. 1999). Robos are transmembrane type 1 receptors that are also conserved across species (Kidd et al. 1998; Brose et al. 1999; Li et al. 1999; Lee et al. 2001; Vargesson et al. 2001). In mice, four Robo molecules have been identified and characterized (Robo-1, Robo-2, Robo-3 and Robo-4). In contrast to Robo-1, Robo-2 and Robo-3 that are highly expressed in the nervous system, Robo-4 is strictly expressed outside the CNS during embryonic development (Park et al. 2003). All three members of the Slit family have been proposed to bind Robo-1, Robo-2 and Robo-3 with similar affinity while an interaction with Robo-4 has yet to be observed (Brose et al. 1999; Li et al. 1999; Sabatier et al. 2004). In addition to playing a key role in guiding growing axons, Slits are also implicated in the regulation of cell migration, dendritic growth, and cell polarity in the nervous system. They are also important for the development of structures outside the nervous system including kidney, diaphragm, heart,

lung and blood vessels (Xian et al. 2001; Liu et al. 2003; Park et al. 2003; Yuan et al. 2003; Grieshammer et al. 2004; Bedell et al. 2005; Zhang et al. 2009).

*Role of Slit/Robo axons guidance molecules in the CNS*

The role of Slit axon guidance molecules has been best studied in the *Drosophila* nerve cord and in the mouse spinal cord. One of the most studied systems for the role of axon guidance is the commissural axon pathfinding in the vertebrate spinal cord. In the spinal cord, commissural neurons are born in the dorsal spinal cord and send their axons ventrally toward the floor plate where they cross the midline and project anteriorly on the contralateral side. Commissural axons are attracted to the midline by the floor plate secreted molecules Netrin-1 and Sonic Hedgehog (Shh) (Tessier-Lavigne and Goodman 1996; Dickson 2002; Charron et al. 2003). In both Drosophila and mice, Slits are expressed and secreted by the floor plate and their Robo receptors are expressed on commissural axons (Rothberg et al. 1990; Holmes et al. 1998; Itoh et al. 1998; Brose et al. 1999; Dickson and Gilestro 2006). Ablation of Slit or Robo expression leads to aberrant crossing of commissural axons at the midline as well as re-crossing of some of these axons (Seeger et al. 1993; Kidd et al. 1998; Long et al. 2004). Expression of Slits at the midline is critical to promote the exit of commissural axons from the midline to the contralateral side. In addition, Slits prevent these axons from re-crossing the midline while they grow longitudinally towards the lateral funiculus. The responsiveness of commissural axons to Slits is tightly regulated to ensure that these axons are not repelled from the midline before crossing. In *Drosophila*, expression of the multipass transmembrane protein Comm downregulates expression of Robos on the axons prior to

midline crossing preventing Slit-mediated repulsion (Keleman et al. 2002; Keleman et al. 2005). In mice, an alternatively spliced form of Robo-3, Robo-3.1, is thought to block Slit-Robo signaling prior to midline crossing thereby preventing repulsion (Chen et al. 2008). Upon crossing, Slit-mediated repulsion takes place following the expression of Robo at the surface of axons in *Drosophila* and Robo-3.1 downregulation in mice (Keleman et al. 2002; Long et al. 2004; Chen et al. 2008). In *Drosophila*, following commissural axon midline crossing, axons turn longitudinally and sort into three lateral pathways parallel to the midline. Gain and loss of function experiments have shown that expression of all three Robo receptors is critical for the proper formation of three lateral pathways (Rajagopalan et al. 2000; Simpson et al. 2000; Spitzweck et al. 2010). It was originally proposed that combinatorial expression of the three Robo receptors regulates the segregation of axons into these three lateral pathways, however, recently only the level of Robo receptors and not the combinatorial expression of the three Robo has been shown to be important for the segregation of axons (Rajagopalan et al. 2000; Simpson et al. 2000; Spitzweck et al. 2010). This initial observation raised the interesting possibility that combinatorial expression of Robos in OSNs may regulate the segregation of OSNs into different regions within the OB.

*Slits and Robos in the development of the olfactory systems*

In the olfactory systems, Slits regulate both the processes of axonal navigation and cell migration. The formation of the OB is dependent on the migration of neuronal precursor cells from the subventricular zone (SVZ) to the developing OB. The interneurons which populate the OB are also continuously generated throughout the life

of the animal. Their progenitors are born in the SVZ of the cerebral cortex and migrate toward the OB via the rostral migratory stream (RMS) (Luskin 1998). Neuroblasts in the SVZ as well as in the RMS express Robo-2 and Robo-3 (Nguyen-Ba-Charvet et al. 2004). Slit secreted from the septum and choroid plexus orient these migrating neuroblast cells to properly target to the OB (Hu 1999; Wu et al. 1999; Nguyen-Ba-Charvet et al. 2004; Sawamoto et al. 2006).

Mitral and tufted neurons of the OB project their axons to various regions of the brain by forming a discrete bundle of axons termed the lateral olfactory tract (LOT). The developing LOT grows away from the midline and posteriorly at the surface of the telecephalon (Schwob and Price 1984; Pini 1993; López-Mascaraque et al. 1996). The septum and olfactory cortex were shown to secrete molecules that repel LOT axons *in vitro* (Pini 1993). This repulsive activity was later proposed to be provided by Slits and ablation of Slit-1 and Slit-2 leads to improper formation of the LOT (Li et al. 1999; Nguyen-Ba-Charvet et al. 2002). Furthermore, the LOT is severely disorganized in the Robo-1 and Robo-2 double mutant mice further substantiating a role for Slit repulsion in the development of this axonal tract (Fouquet et al. 2007).

Slits and Robos also play a critical role in the guidance of axons projecting from the sensory neurons of the vomeronasal organ of the accessory olfactory system (AOS). Vomeronasal sensory neurons (VSN) located in the basal region of the vomeronasal organ express Robo-1 and Robo-2 and Slits are expressed in the AOB where VSN axons form synapses (Knöll et al. 2003; Cloutier et al. 2004; Prince et al. 2009). Basal VSNs expressing Robo-2 strictly innervate the posterior region of the AOB and avoid the anterior region. In Robo-2-deficient mice, a subset of basal VSN axons are mistargeted

to the anterior region of the AOB (Prince et al. 2009). Examination of Slit mutant mice revealed that Slit-1 and Slit-2, but not Slit-3, are required for the Robo-2-mediated segregation of basal VSN axons to the posterior region of the AOB (Prince et al. 2009).

## RATIONALE AND OBJECTIVES

At the onset of my graduate studies, few lines of evidence pointed to a potential role for the Slit family of proteins in regulating wiring of OSN axons in the main olfactory system. First Slits and Robos had been shown to be expressed in structures of the olfactory system (Marillat et al. 2002). Second, Slits and Robos were implicated in the precise targeting of OSN axons in *Drosophila* and later in zebrafish (Jhaveri et al. 2004; Miyasaka et al. 2005). Based on these observations, I hypothesized that Slit-Robo signaling may direct the formation of connections in the complex target field that is represented by the mouse OB. The following chapters will examine three different questions relating to the role of Slits and their receptors in the wiring of OSN axons.

OBJECTIVE 1: DO SLITS AND ROBOS REGULATE THE SEGREGATION OF AXONS WITHIN SPECIFIC REGIONAL COMPARTEMENT OF THE OB?

I have performed a detailed analysis of the expression patterns of Slits and Robos in the OS. Using Slit and Robo null mice, I demonstrated that Slit-1 and Robo-2 are essential to segregate subsets of axons to the dorsal region of the OB. These results are presented in Chapter 2.

OBJECTIVE 2: ARE SLITS AND ROBOS REQUIRED FOR THE PRECISE CONVERGENCE OF AXONS INTO SPECIFIC GLOMERULI OF THE OB?

I examined the requirement for Slit-1 and Robo-2 in the targeting of specific populations of axons innervating zones 1, 2, and 4 of the OB. I have shown that Robo-2 is required for the formation of specific glomeruli and for preventing ectopic glomeruli from forming in specific regions of the OB. These results are presented in Chapter 3 and 4.

OBJECTIVE 3: IS THE STEREOTOPIC OLFACTORY MAP REQUIRED FOR PROPER PERCEPTION OF AVERSIVE ODORS BY MICE?

I examined whether the formation of an accurate glomerular map in the dorsal region of the OB is essential to mediate innate avoidance behaviors in mice by taking advantage of some of the mouse models I developed. I have shown that disruption of the glomerular map in the DII region of the OB leads to reduced avoidance to a specific aversive compound TMT. These results are presented in Chapter 3.

# CHAPTER 2

## Requirement for Slit-1 and Robo-2 in zonal segregation of olfactory sensory neuron axons in the main olfactory bulb

**Jin hyung Cho**[1], Manon Lépine[1], William Andrews[2], John Parnavelas[2], Jean-François Cloutier[1].

[1]*Montreal Neurological Institute, McGill University, Montreal, Quebec, Canada*
[2]*MRC Centre for Developmental Neurobiology, King's College London, London, UK*

**PREFACE**

This chapter was published as a research article in the Journal of Neuroscience (Cho et al. 2007). As described in Chapter 1 above, there is a strong correlation between the location of OSNs within the OE and the targeting of their axons along the dorsal-ventral axis of the OB (Miyamichi et al. 2005). However, the exact molecular mechanism that regulates the innervation of OSN axons along the dorsal-ventral axis of the OB was not fully understood. The main objective of this chapter was to determine the involvement of different members of the Slit and Robo families of axon guidance molecules in the targeting of OSN axons along the dorsal to ventral axis of the OB. In this study, we provide evidence that Slit-1 and Robo-2 are essential for the segregation of a subset of OSN axons to the dorsal region of the OB.

*Acknowledgements*

We thank Alyson Fournier, David Ginty, and Timothy Kennedy for comments on the manuscript and members of the Cloutier lab for helpful discussions. We are thankful

to David Ornitz for Slit cDNA clones, Alain Chédotal for Robo cDNA clones, Tyler Cutforth for the OMP cDNA clone, and Zhiua Zhou and Linda Buck for the M50 and M5 cDNA clones. We also thank Marc Tessier-Lavigne for his generous gift of Slit-1 and Robo-2 mutant mice, Jeffrey Esko for providing us with the Slit-3 mutant mice with permission from David Ornitz, and David Ginty for Synapsin-1 Cre mice. This work was supported by the Canadian Institutes for Health Research, the Fonds Québécois pour la Recherche sur la Nature et les Technologies, and the Canada Foundation for Innovation. J.-F.C. holds a Canada Research Chair in developmental neurobiology.

**ABSTRACT**

The formation of precise stereotypic connections in sensory systems is critical for the ability to detect and process signals from the environment. In the olfactory system, olfactory sensory neurons (OSNs) project axons to spatially defined glomeruli within the olfactory bulb (OB). A spatial relationship exists between the location of OSNs within the olfactory epithelium (OE) and their glomerular targets along the dorsal-ventral axis in the OB. The molecular mechanisms underlying the zonal segregation of OSN axons along the dorsal-ventral axis of the olfactory bulb are poorly understood. Using *robo-2*$^{-/-}$ and *slit-1*$^{-/-}$ mice, we examined the role of the Slit family of axon guidance cues in the targeting of OSN axons during development. We show that a subset of OSN axons that normally project to the dorsal region of the OB mistarget and form glomeruli in the ventral region in *robo-2*$^{-/-}$ and *slit-1*$^{-/-}$ mice. In addition, we show that the Slit receptor, Robo-2, is expressed in OSNs in a high dorso-medial to low ventro-lateral gradient across the OE, and that Slit-1 and Slit-3 are expressed in the ventral region of the OB. These

results indicate that the dorsal-to-ventral segregation of OSN axons are not solely defined by the location of OSNs within the OE but also relies on axon guidance cues.

## INTRODUCTION

The accurate representation of stimuli from the environment relies on the formation of precise connections between sensory neurons in the periphery and second-order neurons in the central nervous system. Such stereotyped connections are crucial for the specific detection and perception of odorant molecules by the olfactory system. OSNs that are located in the OE form highly stereotyped connections with second-order neurons within the OB. OSNs distributed within four spatially distinct zones of the OE project axons to four specific regions of the olfactory bulb (Strotmann et al. 1992; Ressler et al. 1993; Vassar et al. 1993; Ressler et al. 1994; Strotmann et al. 1994; Vassar et al. 1994; Mombaerts et al. 1996; Sullivan et al. 1996; Tsuboi et al. 1999). While these zones are defined based on the segregated patterns of expression of odorant receptors in OSNs there exists a certain degree of overlap in the expression patterns of olfactory receptors (OR) within some of these zones (Norlin and Berghard 2001; Iwema et al. 2004; Miyamichi et al. 2005). Nonetheless, there is a strong correlation between the location of the OSN cell bodies within the OE and the targeting of their axons along the dorsal-ventral axis of the OB (Astic and Saucier 1986; Saucier and Astic 1986; Miyamichi et al. 2005). OSNs positioned in the dorso-medial aspect of the OE project to the dorsal region of the OB while neurons located in the ventro-lateral region of the OE innervate the most ventral

region of the OB (Figure 1 N). The molecular mechanisms that orchestrate the segregation of OSN axons within distinct zones of the OB remain to be defined.

Within spatially-defined zones of the OB, axons of OSNs expressing the same odorant receptor converge into two bilateral and stereotypically conserved glomeruli (Ressler et al. 1994; Vassar et al. 1994; Mombaerts et al. 1996). OR expression is required for convergence of OSN axons onto specific glomeruli within the OB (Mombaerts et al. 1996). Although the exact mechanism by which ORs regulate this convergence has not been fully defined, they may promote sorting of axons by favoring coalescence of axons expressing the same OR (Feinstein et al. 2004; Feinstein and Mombaerts 2004). Alternatively, OR-derived cAMP signals can regulate glomerular targeting of OSN axons (Imai et al. 2006).

Since the OB is a three dimensional structure, OSN axons must target to specific glomeruli by responding to signals that direct their growth along the medial-lateral, anterior-posterior, and dorsal-ventral axes of the OB. In addition to ORs, several families of axon guidance cues have emerged as important regulators of axonal targeting during formation of stereotyped connections in the olfactory system. Members of the secreted semaphorin family and their receptors, the neuropilins, have been implicated in the development of OSN projections. (de Castro et al. 1999; Pasterkamp et al. 1999; Renzi et al. 2000; Schwarting et al. 2000; Walz et al. 2002; Cloutier et al. 2004; Schwarting et al. 2004). Indeed, Sema3A is required for appropriate medial to lateral targeting of OSN axons (Schwarting et al. 2000). Furthermore, differential expression of Ephrin A family members on OSN axons are required for their accurate anterior-to-posterior targeting in

the OB (Cutforth et al. 2003). However, the molecules involved in the control of dorsal-to-ventral targeting of OSN axons within the OB have yet to be identified.

Members of the Robo family of axon guidance cue receptors have been implicated in the targeting of OSN axons in Drosophila and Zebrafish (Jhaveri et al. 2004; Miyasaka et al. 2005). Moreover, we have previously demonstrated that the Slit and Robo families of axon guidance cues can promote zonal segregation of vomeronasal axons in the accessory olfactory system in mice (Cloutier et al. 2004). We therefore evaluated whether Slit-Robo signaling controls zonal segregation of OSNs in the main olfactory bulb. To evaluate the roles of Slits and Robos in the development of the olfactory system, we have defined their patterns of expression in the olfactory system and have analyzed OSN projections in mice lacking Slit ligands and the Slit receptor Robo-2. Our results show that Slit-1 and Robo-2 are essential for dorsal-ventral segregation of OSN axons within the OB.

## MATERIALS AND METHODS

### *Animals*

Embryonic day E16 and E18 mouse embryos were obtained from timed-pregnant females purchased from Charles River (Saint-Constant, Canada). Date of vaginal plug was considered as E0. *Robo-2*, *slit-1*, and *slit-3* mutant mice have been described (Plump et al. 2002; Yuan et al. 2003; Grieshammer et al. 2004) and were generously provided by Dr. Marc Tessier-lavigne (*robo-2* and *slit-1*) and Dr. Jeff Esko (*slit-3*). The floxed *robo-2* mutant mouse has previously been described (Lu et al., 2007)

*Generation of Robo-2 antibody*

Anti-Robo-2 antibodies were produced by immunizing rabbits with a synthetic peptide from the C-terminal region of Robo-2 (CLRGSHQRNANDLLDI) coupled to keyhole limpet hemocyanin. Rabbits were immunized with 250ug of coupled peptide in complete Freunds adjuvant and boosted every 2-3 weeks with 100ug of coupled peptide. Serum was collected and antibodies were purified with an affinity column prepared using the SulfoLink kit from Pierce (Rockford, IL). The specificity of the purified antibodies for Robo-2 was determined by immunoblot analysis using extracts of Robo-1- or Robo-2-transfected 293T cells (data not shown) and by immunostaining on sections of olfactory bulbs from E18 wild-type and *robo-2*$^{-/-}$ mice (Figure S1).

*In situ hybridization*

Nonradioactive, dioxygenin-labeled cRNA probes with either sense or antisense orientation were synthesized by in vitro transcription using DIG labeling mix (Roche, Mannheim, Germany) according to the manufacturer's recommendations. Probes were synthesized from cDNA clones encoding *robo-1* and *robo-2* (Brose et al. 1999), *slit-1*, *slit-2* and *slit-3* (Yuan et al. 1999), *OMP* (Cutforth et al. 2003), *NQO-1* (Est image #:3586888), *rig-1*(Est image #:6834877), *OCAM* (PCR-amplified coding region), and *M50* (Zou et al. 2001). To prepare *M49*, *L45, K21, and M72*-specific cRNA probes, DNA fragments of the coding sequences were PCR-amplified from C57Bl6 genomic DNA and subcloned into the pBluescript vector. The primer sets used were the following: *M49* (5'-CCGAATCGTTTGGGAGGAGGCTT-3'; 5'-CACTCGAGAGCTCTTCCTAGTACC-

3'); *L45* (5'-CCGAATTCACGAGAGCATCACAGG-3'; 5'-CACTCGAGGCAATAATTCCATAGA- 3'); K21 (5'-CCGAATCATGCCCCTCTTCTTC-3'; 5'-CACTCGAGGCTCAATGTTTTTCTC-3'); M72 (5'-CCGAATCGAGGGCTAACTAACAG-3'; 5'-CACTCGAGCAGTGCG-GTCTTCACC-3'). For in situ hybridization on E16 and E18 embryos, as well as P0 mice, fresh frozen brains were cryosectioned at 20 um and sections were allowed to dry for two hours. Following fixation, sections were processed as previously described (Cloutier et al. 2002). For in situ hybridization on adult (3 to 4 month old) olfactory epithelium, mice were transcardially perfused with phosphate-buffered saline (PBS) containing 4% paraformaldehyde. The nasal cavity was dissected, post-fixed in PFA containing 0.5M EDTA in PBS for three to five days for decalcification, and cryoprotected in PBS containing 30% sucrose before freezing. The olfactory epithelium was cryosectioned at 20 um and sections were processed as previously described (Cloutier et al. 2002).

*Immunohistochemical Procedures*

Adult mice were anesthetized and perfused transcardially with ice-cold PBS containing 4% paraformaldehyde. Brains were dissected, postfixed for 3 to 5 hours in perfusion solution, and cryoprotected in PBS containing 30% sucrose. Alternatively, E16 and E18 embryos, and P0 mouse heads were immersion-fixed overnight in PBS containing 4% paraformaldehyde followed by cryoprotection in PBS containing 30% sucrose. The samples were cryosectioned (20 um), mounted on superfrost plus microscope slides and allowed to dry for one hour. The sections were rinsed twice in TBS (50 mM Tris-HCl

[pH 7.6] and 150 mM NaCl), microwaved ten times thirty seconds in 100mM Tric-HCl pH10 for antigen retrieval, and allowed to cool down for 20 minutes at room temperature. The sections were then blocked for 2 hours in TNT (50 mM Tris-HCl [pH 7.6], 500 mM NaCl, and 0.5% triton X-100) containing 10% fetal bovine serum (FBS), and incubated overnight with primary antibody at $4^0$C in TNT/10% FBS using the following dilutions: anti-OCAM (1:100) (BD Biosciences), anti-NQO-1 (1:100) (Abcam), anti-SV2 (1:1000) (Developmental Studies Hybridoma Bank), and anti-Robo-2 (1:350). After rinsing in TBS, primary antibody was detected with the appropriate Alexa-488 or Alexa-546-conjugated secondary antibody (1:500; Molecular Probes) in TNT/10% FBS.

*Analysis of the position of NQO-1-positive glomeruli in adult olfactory bulbs*

Adult mice were anesthetized and perfused transcardially with ice-cold PBS containing 4% paraformaldehyde. Brains were dissected, postfixed for 3 to 5 hours in perfusion solution, and cryoprotected in PBS containing 30% sucrose. Brains were then laid flat, ventral side down, in a rectangular chamber and a cut was made perpendicular to the surface of the cortex at similar rostro-caudal levels. The olfactory bulbs and remaining forebrain were then mounted with the cut side of the forebrain lying flat on a chuck for cryosectioning. OBs from three-month old mice were cryosectioned (20μm) in the coronal plane and sections were collected on microscope slides over a distance of 1000μm along the rostro-caudal axis starting 800μm from the tip of the OB. All sections were immunostained with NQO-1 and OCAM antibodies and counter-stained with Hoescht as described above. The position of all NQO-1-positive glomeruli in the OB was determined using an Image J plug-in as previously described (Schaefer, M. et al 2001).

An NQO-1-positive glomerulus was defined as a region of the neuropil that contains NQO-1-positive immunorecativity and that is surrounded by periglomerular cells. Briefly, images of every other sections were imported into Adobe Photoshop software (Adobe Systems, Mountain View, CA) for mapping of glomeruli. The radial angle of each NQO-1-positive glomeruli was measured after setting the origin for each section. The origin was set at one-third the distance between the mitral cell layer in the dorsal region of the OB and the mitral cell layer in the ventral region of the OB. A scatter plot was constructed that shows the location of each NQO-1-positive glomerulus with degrees (angle) on the y axis and the rostro-caudal distance on the y-axis.

## RESULTS

*Robo-2 expression by olfactory sensory neurons*

The molecular cues that coordinate the zonal segregation of OSN axons in the OB are unknown. Previous studies showed that Robo-2 is expressed in the OE during early development (Marillat et al. 2002). To begin to assess the involvement of Slits and their receptors, the Robos, in guidance of OSN projections, we performed in situ hybridization analyses of the *robo* family members *robo-1*, *robo-2,* and *rig-1* to determine their patterns of expression in the developing olfactory system.

While *rig-1* is not expressed in the OE, *robo-1* expression is restricted to the basal lamina surrounding the OE (Figure 1 A, B). *rig-1* expression was detected in other structures on these sections including the retina (data not shown). In contrast to *rig-1* and *robo-1*, *robo-2* is highly expressed in the OE at E16 (Figure 1 C) and E18 (data not

shown), developmental ages when OSN axons have reached the OB and have begun to form protoglomeruli, respectively. Interestingly, *robo-2* expression in the OE at E16 is graded with high levels detected in the dorso-medial region and low levels in the ventro-lateral region (Figure 1 C). OE regions expressing high levels of *robo-2* overlap with the region containing *NQO-1*-expressing OSNs, which are located in zone I of the OE according to the nomenclature defined by Sullivan et al. (1996) (Figure 1 C, D) (Gussing and Bohm 2004). *Robo-2* expression also partially overlaps regions of the OE containing *OCAM*-expressing OSNs that define zones II to IV of the OE (Figure 1 C, E) (Alenius and Bohm 1997; Yoshihara et al. 1997). To further ask whether OSNs located in specific zones of the OE express *robo-2*, we compared its pattern of expression to the expression of specific OR in the adult OE. In contrast to *OMP*, and as observed at E16, *robo-2* expression is graded in the adult OE with the highest levels of expression observed in the dorso-medial region of the OE (Figure 1 F, G). We compared *robo-2* expression to the expression of molecules expressed in specific zones of the OE: *NQO-1* (zone I), *OCAM* (zones II to IV), *M49* (zone II), *L45* (zone III), and *M50* (zone IV) (Figure 1 I-M) (Sullivan et al., 1996). This comparison revealed that OSNs located in zones I and II of the OE express the highest levels of *robo-2*, while OSNs of zones III express lower levels, and OSNs in zone IV do not express detectable levels of *robo-2*.

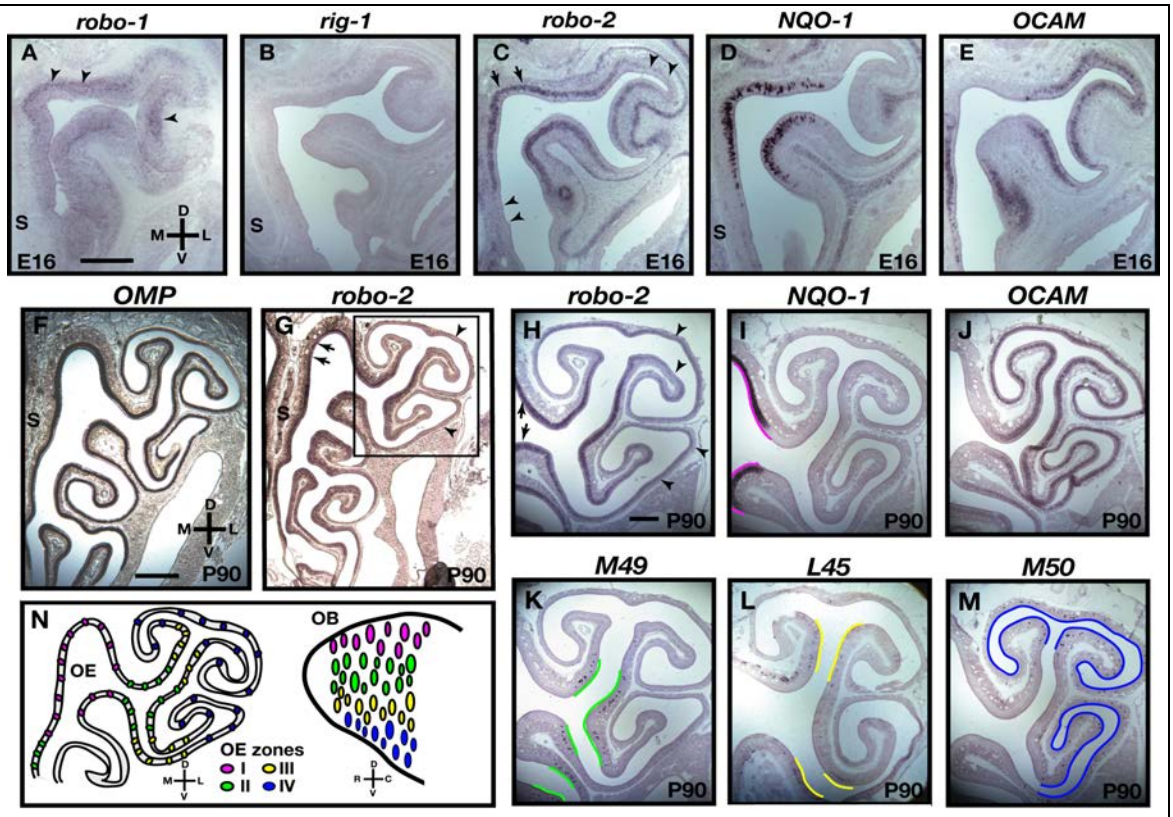


***Figure 1. Expression of Robo family members in the olfactory epithelium.***

*In situ hybridization of coronal sections of olfactory epithelium isolated from embryonic day (E)16 (A-E) and adult mice (P90) (F-M) with cRNA probes specific for robo-1 (A), rig-1 (B), robo-2 (C, G and H), NQO-1 (D and I), OCAM (E and J), OMP (F), M49 (K), L45 (L), and M50 (M).*

*(A-G) Expression of robo-1 is restricted to the basal lamina of the olfactory epithelium (A, arrowheads) while rig-1 is not expressed in the olfactory epithelium (B). Interestingly, in contrast to OMP, which is equally expressed throughout the olfactory epithelium, robo-2 is expressed in a gradient with high levels of expression in the dorso-medial regions of the olfactory epithelium (arrows) and low levels in the ventro-lateral regions*

*(arrowheads) of E16 (C) and adult olfactory epithelium (G and H). (H-M) robo-2 expression is confined to zones I to III of the olfactory epithelium. A higher magnification of a region of the olfactory epithelium (boxed in G) where all four zones of the olfactory epithelium are represented is shown in panels H-M. The expression pattern of robo-2 was compared to the expression pattern of specific olfactory epithelium zonal markers that include NQO-1 (zone I) (I), OCAM (zones II-IV) (J), M49 (zone II) (K), L45 (zone III) (L), and M50 (zone IV) (M). robo-2 is expressed in a high to low gradient in olfactory sensory neurons located in zones I (arrows) to IV (arrowheads) respectively. Regions of the olfactory epithelium expressing the different zonal markers are traced with a colored line on the apical surface of the olfactory epithelium to represent the four zones (zone I: magenta; zone II: green; zone III: yellow; zone IV: blue). S: septum. Scale bars: 250μm (A-E, H-M); 500μm (F, G).*

*(N) Diagram representing the spatial relationship between the location of olfactory sensory neurons within the olfactory epithelium (OE) and their target glomeruli within the olfactory bulb (OB). Olfactory sensory neurons located in the dorso-medial regions of the olfactory epithelium (magenta) project axons to glomeruli in the dorsal region of the olfactory bulb, while olfactory sensory neurons in the ventro-lateral region of the olfactory epithelium (blue and not shown) project axons to the ventral aspect of the olfactory bulb. D: dorsal; V: ventral; L: lateral; M: medial; R: rostral; C: caudal.*

In order to address whether the graded expression of *robo-2* observed in OSNs of the OE is reflected by the distribution of Robo-2 protein on axons targeting to the OB, we

generated antibodies against a carboxy-terminal peptide of Robo-2. Immunohistochemical analysis using these Robo-2-specific antibodies revealed that Robo-2 is highly expressed on OSN axons that project to the dorsal (Figure 2 A, D, G, J) and dorso-medial (Figure 2 M, P) aspects of the OB at E16 and E18. No immunoreactivity was detected in sections of OB from *robo-2*$^{-/-}$ mice demonstrating that our antibody specifically recognizes Robo-2 (Figure S1 D, F). A large proportion of OSN axons that express high levels of Robo-2 originate from OSNs located in zone I of the OE that express NQO-1 (Figure 2 A-C, G-I, M-O). Robo-2 is also expressed, albeit at lower levels, on OSN axons that target more ventrally in the OB. While some of the Robo-2-positive axons express OCAM, a subset of OCAM-positive axons that target to the most ventral aspect of the OB are devoid of Robo-2 expression (Figure 2 D-F, J-L, P-R). This observation is consistent with the results obtained by in situ hybridization showing overlap of *robo-2* and *OCAM* expression in zone II of the OE (Figure 1 H, J, K). Taken together, these observations indicate that Robo-2 is a candidate for imparting guidance information to OSN axons as they project to the OB.

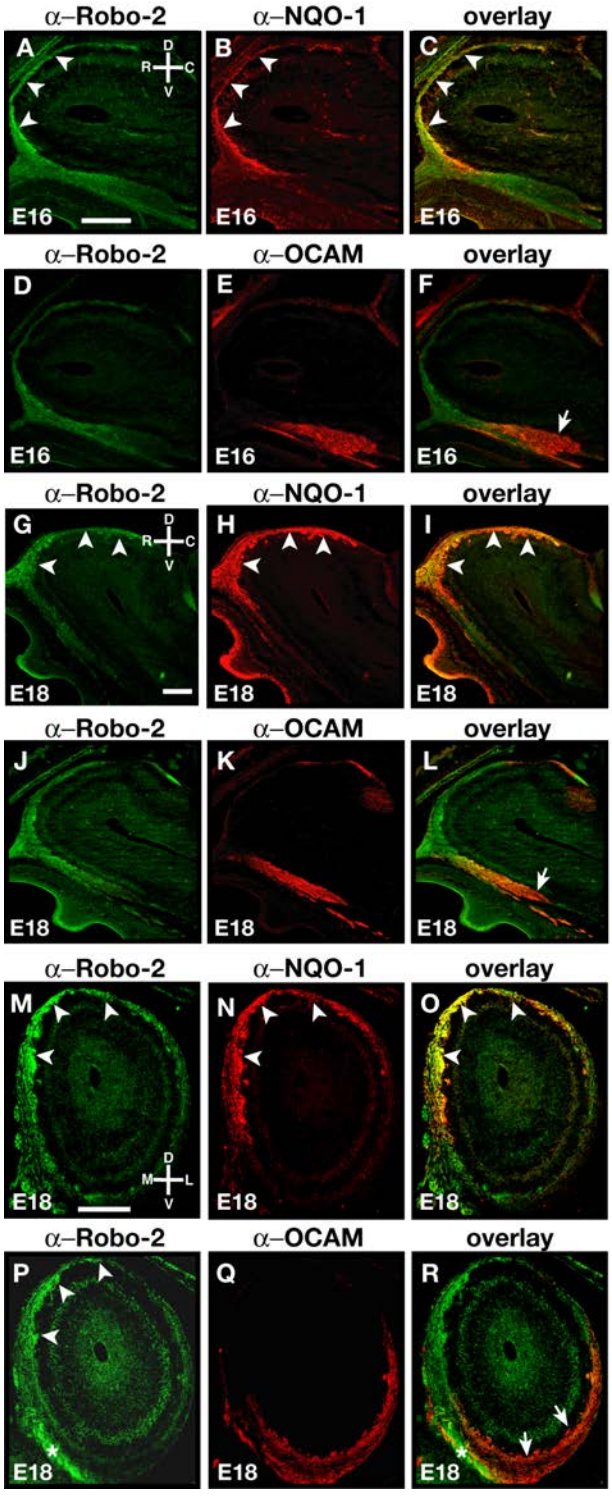


***Figure 2. Targeting of Robo-2-expressing olfactory sensory neuron axons in the olfactory bulb.***

*(A-L) Parasagital sections of olfactory bulbs from E16 (A-F) and E18 (G-L) embryos stained with anti-Robo-2 (A, C, D, F, G, I, J, L), anti-NQO-1 (B, C, H, I), and anti-OCAM (E, F, K, L). At E16 and E18, olfactory sensory neuron axons expressing high levels of Robo-2 are observed in the dorsal and rostral regions of the OB (A, D, G, J). Robo-2 is also expressed at lower levels on a subset of axons targeting the ventral region of the olfactory bulb. NQO-1-expressing axons, originating from zone I of the olfactory epithelium, that target to the dorsal region of the OB, express high levels of Robo-2 (B, C, H, I) (arrowheads). A subset of OCAM-expressing axons that originate from zones II to IV of the olfactory epithelium and target to the ventral region of the olfactory bulb do not express Robo-2 (arrow) (E, F, K, L).*

*(M-R) Coronal sections of olfactory bulbs from E18 embryos stained with anti-Robo-2 (M, O, P, R), anti-NQO-1 (N, O), and anti-OCAM (Q, R). At E18, olfactory sensory neuron axons expressing high levels of Robo-2 are observed in the dorso-medial regions of the OB (arrowheads) while lower levels of Robo-2 expression is observed on olfactory sensory neuron axons targeting to the ventro-lateral region of the OB. As observed in sagital sections (G-L) NQO-1-positive axons express high levels of Robo-2 (arrowheads) (M-O) while a subset of OCAM-positive axons do not express Robo-2 (arrows) (P-R). Robo-2-positive axons restricted to the nerve layer are marked with asterisk in P and R. D: dorsal; V: ventral; R: rostral; C: caudal; M: medial; L: lateral. Scale bars: 250μm.*

*Expression of slits in the ventral region of the olfactory bulb*

The graded expression of *robo-2* across the OE suggests that axons of OSNs located in specific regions of the OE may respond differently to Robo-2 ligands expressed in their target field. In situ hybridization experiments revealed that two members of the Slit family of proteins are expressed in the OB. *Slit-2* expression is not detected in sagital sections of the OB at E16 and E18, while *slit-1* and *slit-3* are highly expressed in the ventral region of the OB (Figure 3 A-L). *Slit-2* expression was detected in other regions of the brain in the same sections, including the developing cortex (data not shown). Interestingly, while *slit-1* expression is restricted to a small subset of cells located in the ventral most region of the OB at E18, the distribution of *slit-3* expression remains unchanged at this later stage of development (Figure 3 D, F). Similar patterns of expression were observed in coronal sections of the OB where *slit-1* and *slit-3* are highly expressed in the ventro-lateral region and at lower levels in the ventro-medial region of the OB (Figure 3 G, I, J, L). This pattern of expression of the Slit-1 and Slit-3 chemorepellents supports the possibility that axons of Robo-2-expressing OSNs are guided towards the dorsal region of the OB through Slit-Robo repulsion.

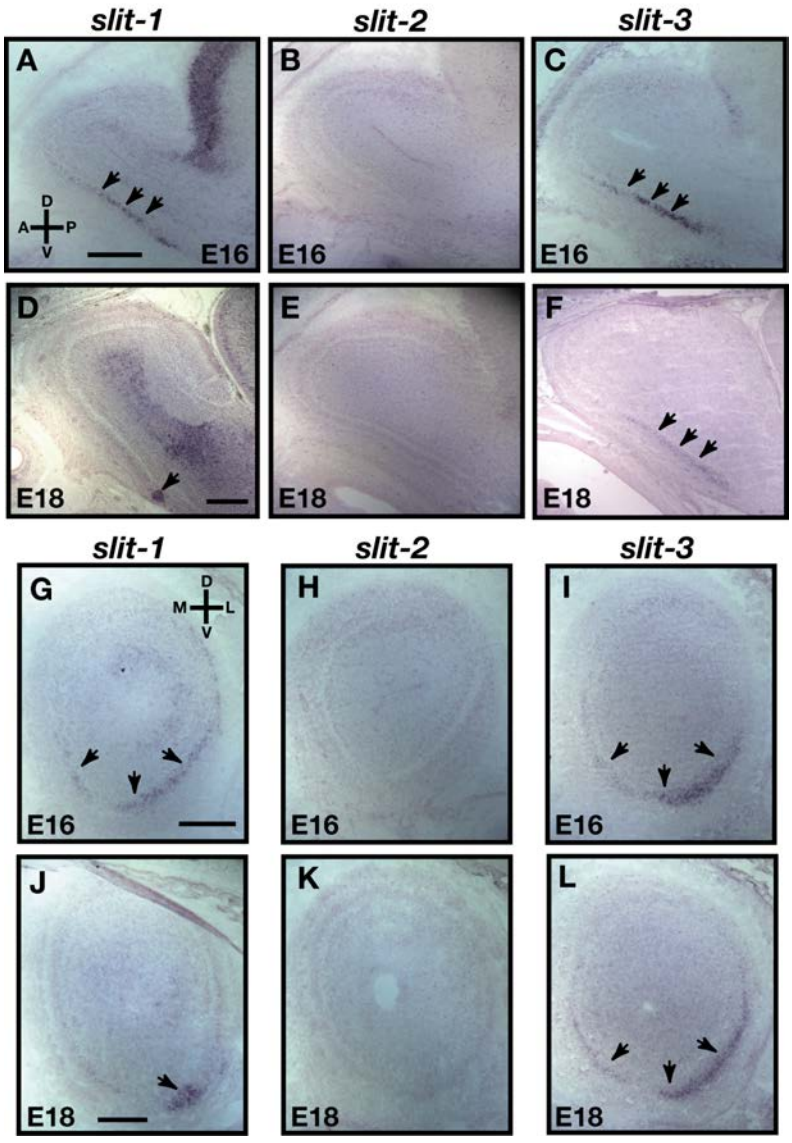


***Figure 3. Expression of slits in the olfactory bulb.***

*(A-L) In situ hybridization of parasagital (A-F) and coronal (G-L) sections of olfactory bulb at embryonic day E16 (A-C and G-I) and E18 (D-F and J-L) with cRNA probes specific for slit-1 (A, D, G, J), slit-2 (B, E, H, K) and slit-3 (C, F, I, L). At E16, while slit-2 is not expressed in the olfactory bulb (B, H), slit-1 (A, G) and slit-3 (C, I) are expressed in the ventral region of the olfactory bulb (arrows). These patterns of expression are*

*maintained at E18 for slit-2 (E, K) and slit-3 (F, L), while slit-1 expression is restricted to the most ventral region of the OB at E18 (D, J) (arrows). D: dorsal; V: ventral; L: lateral; M: medial; R: rostral; C: caudal. Scale bars: 250μm.*

*OSN projections are disorganized in Robo-2$^{-/-}$ mice*

We next examined the integrity of olfactory projections in mice harboring a null mutation in *robo-2*. In light of the perinatal lethality of *robo-2$^{-/-}$* mice, we performed our analyses at P0 when OSN axons have begun to form glomeruli within the OB (Grieshammer et al., 2004). At this stage of development, the OB of *robo-2$^{-/-}$* mice is smaller and their accessory olfactory bulb is underdeveloped when compared to *robo-2$^{+/+}$* mice. Nonetheless, in most *robo-2$^{-/-}$* mice analyzed, the majority of OSN axons have reached and innervated the OB. To evaluate the accuracy of OSN axon targeting, sagital and coronal sections of OB from P0 *robo-2$^{+/+}$*, *robo-2$^{+/-}$* (data not shown) and *robo-2$^{-/-}$* mice were stained with NQO-1 and OCAM antibodies to visualize axons originating from OSNs located in zone I and zones II to IV of the OE, respectively. In wild-type mice, NQO-1- and OCAM-expressing OSN axons are segregated to the rostro-dorsal and ventral regions of the OB, respectively (Figure 4 A-C). A similar segregation of NQO-1- and OCAM-expressing axons is observed in coronal sections where these axons target to the dorso-medial and ventro-lateral aspects of the OB, respectively (Figure 4 G, I). In contrast, a subset of NQO-1-expressing OSN axons project inappropriately to the ventral region of the OB in *robo-2$^{-/-}$* mice (Figure 4 D, F, J, L, M, O). Ectopic NQO-1-positive axons are detected at several levels along the rostro-caudal axis of the OB in all mice

analyzed (Figure 4 and Figure S3). However, we did not observe any mistargeted OCAM-expressing OSN axons in the most dorsal region of the OB in *robo-2*$^{-/-}$ mice (Figure 4 E, F, K, L, N, O). Nonetheless, we observed that some regions of the ventral OB that are normally innervated by OCAM-expressing axons lack innervation in these mice (Figure 4 K, L, N, O). The severity of this defect varies from animal to animal with some mice having small regions that lack innervation (6 out of 11 mice) (Figure 4 K, L) and others lacking innervation in a large part of the ventral region of the OB (Figure 4 N, O). In mice lacking innervation in the ventral region of the OB, OCAM-expressing axons appear to remain trapped in the olfactory nerve layer and do not enter the glomerular layer of the OB (data not shown).

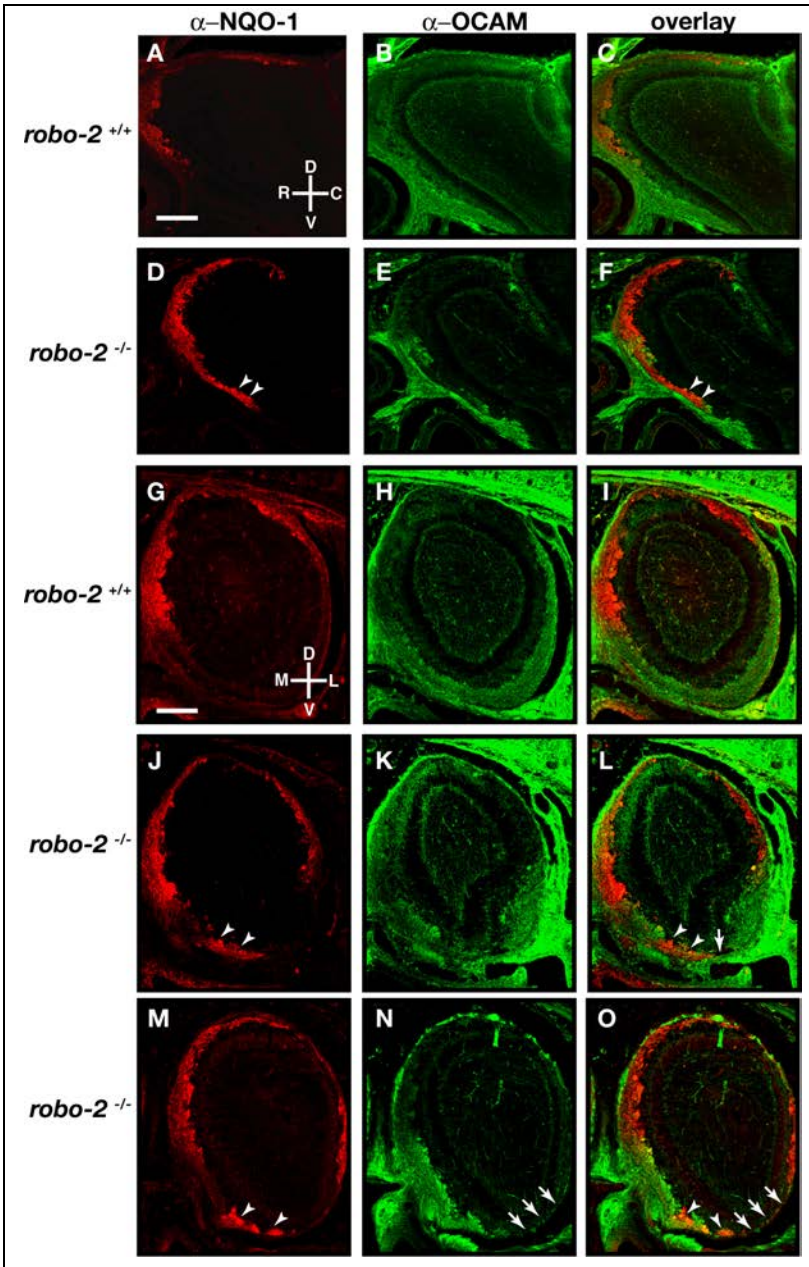


***Figure 4. Olfactory sensory neuron projections are disorganized in robo-2$^{-/-}$ mice.***

*Parasagital (A-F) and coronal (G-O) sections of olfactory bulbs from post-natal day P0 robo-2$^{+/+}$ (A-C, G-I) and robo-2$^{-/-}$ mice (D-F, J-O) were stained with anti-NQO-1 (A, C, D, F, G, I, J, L, M, O) and anti-OCAM (B, C, E, F, H, I, K, L, N, O). In robo-2$^{-/-}$ mice, NQO-1-expresing axons are restricted to the rostral and dorsal region of the olfactory*

*bulbs (A, G) while OCAM-expressing axons target the ventral region of the olfactory bulbs (B, H). A subset of NQO-1-expressing axons is mistargeted to the ventral region of the olfactory bulbs in robo-2$^{-/-}$ mice (arrowheads) (D, F, J, L, M, O). In addition, some regions of the ventral olfactory bulb that are innervated by OCAM-expressing axons in robo-2$^{+/+}$ mice lack innervation in robo-2$^{-/-}$ mice (arrows). N=9 robo-2$^{+/+}$, 3 robo-2$^{+/-}$, 11 robo-2$^{-/-}$. D: dorsal; V: ventral; L: lateral; M: medial; R: rostral; C: caudal. Scale bars: 250μm.*

To determine whether mistargeted NQO-1-positive axons observed in the ventral region of the OB in *robo-2*$^{-/-}$ mice result from deregulated expression of NQO-1 or of other robo family members in OSNs, we assessed the patterns of expression of *NQO-1*, *OCAM, robo-1, and rig-1* in the OE of these mice. As observed in wild-type mice, *NQO-1* expression is restricted to the dorso-medial region of the OE while OCAM expression is restricted to more ventro-lateral regions of the OE in *robo-2*$^{-/-}$ mice (Figure 5 A, C, D, F). Furthermore, as observed in wild-type mice, *robo-1* and *rig-1* are not expressed in the OE of *robo-2*$^{-/-}$ mice (Figure 5 K, N). Hence, ablation of Robo-2 expression does not affect the expression patterns of *NQO-1*, *OCAM*, *robo-1*, and *rig-1* in OSNs. In addition the zonal segregation of zone I OR expression was unaltered in *robo-2*$^{-/-}$ mice (Figure S2). These results indicate that Robo-2 is required for the accurate targeting of NQO-1-expressing OSN axons to the dorsal region of the OB.

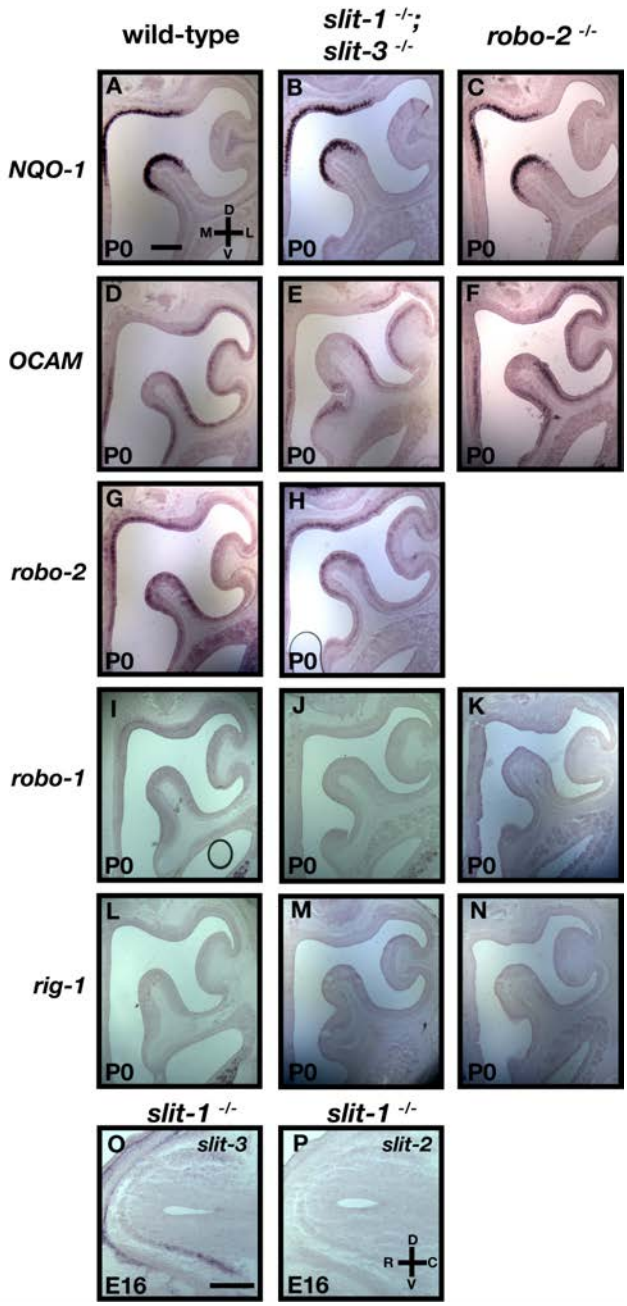


***Figure 5. Expression of NQO-1 and OCAM are unaltered in robo-2$^{-/-}$ and slit-1$^{-/-}$; slit-3$^{-/-}$ mice.***

*(A-N) In situ hybridization of coronal sections of olfactory epithelia from post-natal day P0 wild-type (A, D, G, I, L), slit-1$^{-/-}$;slit-3$^{-/-}$ (B, E, H, J, M), and robo-2$^{-/-}$ (C, F, K, N)*

*mice with cRNA probes specific for NQO-1 (A-C), OCAM (D-F), robo-2 (G, H), robo-1 (I-K), and rig-1 (L-N). robo-2 is expressed in a gradient in the OE with high levels of expression in the dorso-medial region of the OE and low levels in the ventro-lateral region in wild-type (G) and slit-1$^{-/-}$;slit-3$^{-/-}$ (H) mice. NQO-1 is expressed in the dorso-medial region while OCAM is expressed in the ventro-lateral region of the olfactory epithelium in wild-type (A, D), slit-1$^{-/-}$;slit-3$^{-/-}$ (B, E), and robo-2$^{-/-}$ (C, F) mice. Both robo-1 and rig-1 are not expressed in the olfactory epithelium in wild-type (I, L), slit-1$^{-/-}$;slit-3$^{-/-}$ (J, M), and robo-2$^{-/-}$ (K,N) mice. N= 5 robo-2$^{-/-}$; n=5 slit-1$^{-/-}$;slit-3$^{-/-}$.*

*(O-P) In situ hybridization of parasagital sections of olfactory bulbs from E16 slit-1$^{-/-}$ embryos with cRNA probes specific for slit-3 (O) and slit-2 (P). While slit-3 is expressed in the ventral region of the olfactory bulb, slit-2 is not expressed in the olfactory bulb of slit-1$^{-/-}$ embryos. N=3 slit-1$^{-/-}$. D: dorsal; V: ventral; L: lateral; M: medial; R: rostral; C: caudal. Scale bars: 250μm.*

*Mistargeting of NQO-1-expressing OSN axons in Slit-1 mutant mice*

The distribution of Slits in the OB, combined with the defects observed in the projections of OSN axons in *robo-2*$^{-/-}$ mice, suggests that Slits provide guidance information to OSN axons. To determine whether Slits are required for the segregation of NQO-1-expressing axons to the dorsal region of the OB, we analyzed these projections in *slit-1* or *slit-3* mutant mice, as well as in *slit-1*; *slit-3* double mutant mice. In contrast to what we observed in *robo-2*$^{-/-}$ mice, the size of the OB is unaffected in *slit-1*$^{-/-}$ mice at P0. However, a subset of *slit-3*$^{-/-}$ and *slit-1*$^{-/-}$*; slit-3*$^{-/-}$ mice analyzed showed a slight reduction

in the size of their OBs. For axon targeting analysis, sagital sections of P0 OB from wild-type, *slit-1*$^{-/-}$, *slit-3*$^{-/-}$, and *slit-1*$^{-/-}$*; slit-3*$^{-/-}$ mice were immunostained with NQO-1 and OCAM antibodies to visualize the two populations of OSN axons. While NQO-1-expressing axons are accurately segregated to the rostro-dorsal regions in sagital sections of the OB in wild-type and *slit-3*$^{-/-}$ mice (Figure 6 A, C, H, J), a subset of NQO-1-expressing axons mistarget to the most caudo-ventral region of the OB in *slit-1*$^{-/-}$ and *slit-1*$^{-/-}$*; slit-3*$^{-/-}$ mice (Figure 6 D, F, K, M). Similar results were observed in coronal sections of the OB. Whereas NQO-1-expressing axons are restricted to the dorso-medial region of the OB in wild-type mice, a subset of NQO-1-positive fibers are detected in the ventral region of the OB in *slit-1*$^{-/-}$ and *slit-1*$^{-/-}$*; slit-3*$^{-/-}$ mice (Figure 6 N, O, P). Mistargeted axons were observed in all mutant mice analyzed and at several levels along the rostro-caudal axis (Figure S3). Interestingly, the defects observed in *slit-1*$^{-/-}$*;slit-3*$^{-/-}$ mice were similar in severity to those seen in *slit-1*$^{-/-}$ mice, suggesting that Slit-3 is not required for targeting of NQO-1-expressing OSN axons. Furthermore, the defects observed are not due to deregulated expression of *NQO-1*, *OCAM*, and *robo* family members in the OE or of *slits* in the OB of these mice (Figure 5 B, E, H, J, M, O, P). In addition the zonal segregation of zone I OR expression was unaltered in *slit-1*$^{-/-}$ mice (Figure S2). Since Slit-1 is expressed at high levels in the ventral region of the OB, these results suggest that Slit-1 is required to prevent NQO-1-positive axons, which express high levels of Robo-2, from innervating the ventral region of the OB.

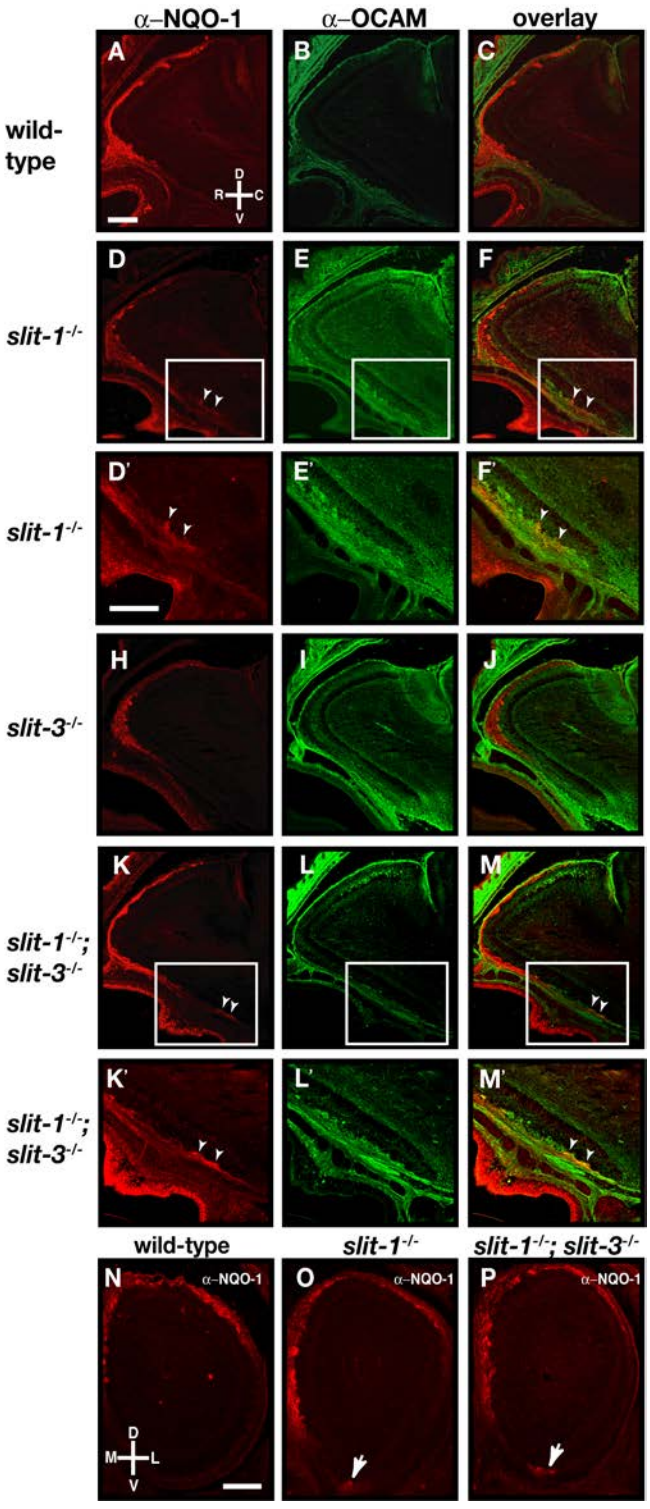


***Figure 6. Loss of zonal targeting of NQO-1-expressing olfactory sensory neuron axons within the olfactory bulb in slit-1$^{-/-}$ mice.***

*(A-M) Parasagital sections of olfactory bulbs from post-natal day P0 wild-type (A-C), slit-1$^{-/-}$ (D-F), slit-3$^{-/-}$ (H-J), and slit-1$^{-/-}$;slit-3$^{-/-}$ (K-M) mice stained with anti-NQO-1 (A, C, D, F, H, J, K, M) and anti-OCAM (B, C, E, F, I, J, L, M). In wild-type animals, NQO-1-expressing axons are restricted to the rostro-dorsal region of the OB (A, C) and OCAM-expressing axons target to the ventral region of the olfactory bulb (B, C). While NQO-1-expressing axons are properly targeted to the dorsal region of the olfactory bulb in slit-3$^{-/-}$ mice (H, J), a subset of NQO-1-expressing axons mistarget to the most ventral region of the olfactory bulb in slit-1$^{-/-}$ mice (D, F) (arrowheads). In slit-1$^{-/-}$; slit-3$^{-/-}$ mice, NQO-1-expressing axons are also observed in the ventral region of the olfactory bulb (K, M) (arrowheads). High-powered magnifications of ectopically projecting NQO-1-expressing axons (insets in D, F, K, and M) are shown in D', F', K', and M'. N=8 wild-type, n=5 slit-1$^{-/-}$, n=8 slit-3$^{-/-}$, and n=7 slit-1$^{-/-}$; slit-3$^{-/-}$.*

*(N-P) Coronal sections at similar rostro-caudal levels of olfactory bulbs isolated from post-natal day P0 (N-P) wild-type (N), slit-1$^{-/-}$ (O), and slit-1$^{-/-}$;slit-3$^{-/-}$ (P) mice stained with anti-NQO-1 (N-P). In wild-type mice, NQO-1-expressing axons innervate the dorso-medial region of the olfactory bulb. In slit-1$^{-/-}$ and slit-1$^{-/-}$;slit-3$^{-/-}$ mice, a subset of NQO-1-expressing axons are mistargeted to the ventral region of the olfactory bulb (arrows). N= 8 wild-type, n=8 slit-1$^{-/-}$, and n=5 slit-1$^{-/-}$;slit-3$^{-/-}$. D: dorsal; V: ventral; L: lateral; M: medial; R: rostral; C: caudal. Scale bars: 250μm.*

*Mistargeted NQO-1 axons form glomeruli in Slit and Robo-2 mutant mice*

Our analyses of axonal projections in Robo-2 and Slit mutant mice at P0 shows that a subset of NQO-1-expressing axons ectopically enter the glomerular layer to form protoglomeruli in the ventral region of the OB in *robo-2*$^{-/-}$, *slit-1*$^{-/-}$, and *slit-1*$^{-/-}$;*slit-3*$^{-/-}$ mice (Figure 4 D, J, M and Figure 6 D, K, O, P). However, it is unclear whether these axons are retained or pruned during maturation of the glomerular map. Since *slit-1*$^{-/-}$ and a subset of *slit-1*$^{-/-}$;*slit-3*$^{-/-}$ mice survive to adulthood, we analyzed the targeting accuracy of NQO-1 axonal projections in adult mice. In contrast to wild-type mice, in which all NQO-1-positive glomeruli are located in the dorso-medial region of the OB, NQO-1-positive glomeruli are detected in the ventral region of the OB in both *slit-1*$^{-/-}$ and *slit-1*$^{-/-}$;*slit-3*$^{-/-}$ mice (Figure 7 A, B, C, I, J, K, P, Q). Ectopic NQO-1-positive glomeruli are observed in the ventral region of OB sections representing a large proportion of the rostro-caudal axis of the OB in *slit-1*$^{-/-}$ and *slit-1*$^{-/-}$;*slit-3*$^{-/-}$ mice (Figure 7 Q, data not shown). In addition, whereas a sharp border is observed between NQO-1- and OCAM-positive glomeruli in the medial side of the OB in wild-type mice, NQO-1- and OCAM-positive glomeruli are often intermingled in *slit-1*$^{-/-}$ and *slit-1*$^{-/-}$;*slit-3*$^{-/-}$ mice (Figure 7 K, data not shown). These defects were observed in adult mice up to eight months of age, suggesting that they are unlikely to result from a delayed maturation of the glomerular map (Figure S4) (Zou et al, 2004). Interestingly, while the majority of ectopically targeted NQO-1-expressing axons form homogenous glomeruli containing strictly NQO-1-positive axons, heterogenous glomeruli containing both NQO-1- and OCAM-positive axons are also observed in all mutant mice analyzed (Figure 7 M, N). Furthermore, NQO-1-expressing axons that ectopically target to the ventral region of the OB are SV2-

positive, which is consistent with the possibility that they form synapses within glomeruli (Figure 7 O).

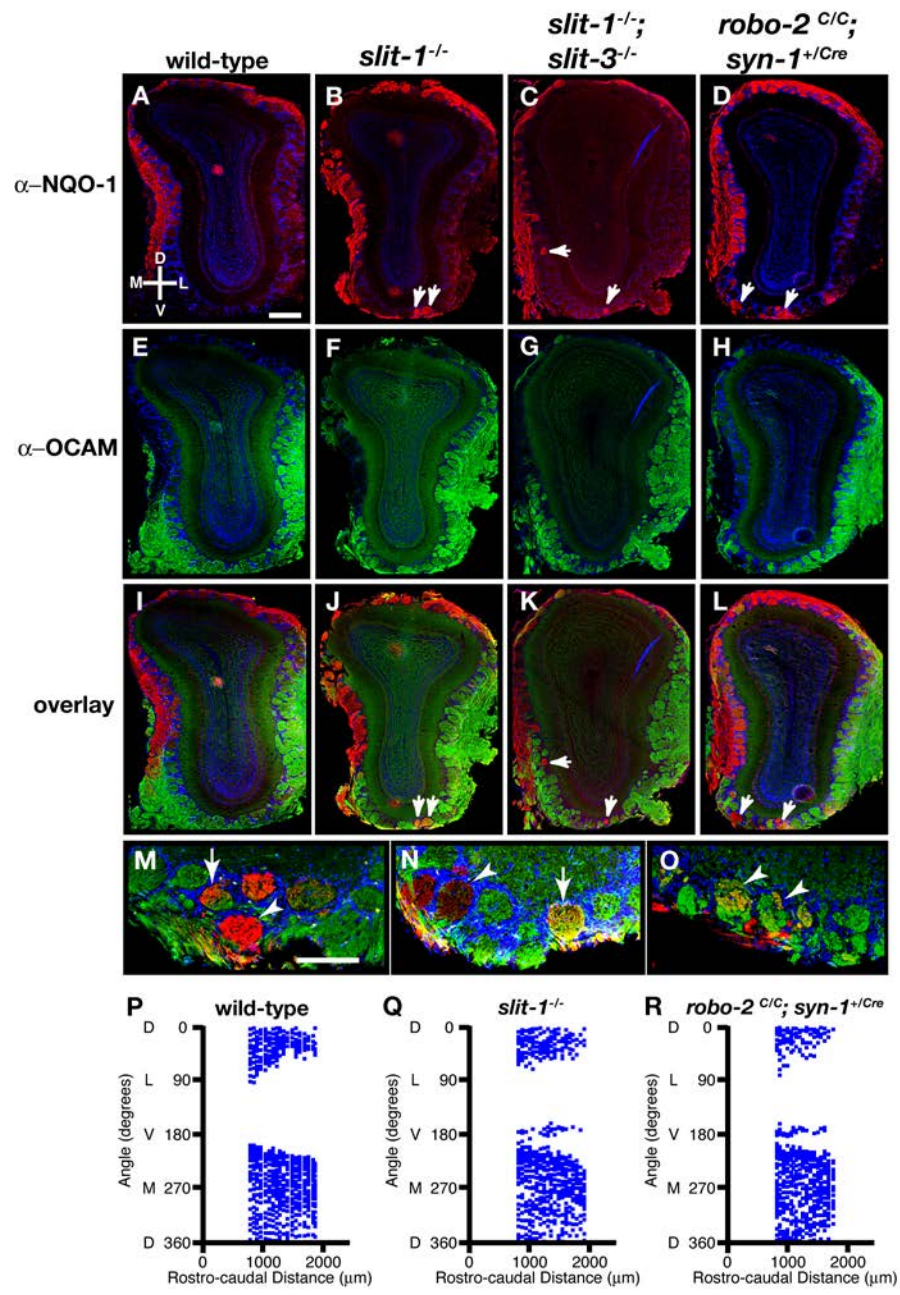


***Figure 7. Mistargeted axons of NQO-1-expressing olfactory sensory neurons innervate glomeruli in the ventral region of the olfactory bulb in slit and robo-2 mutant mice.***

*Coronal sections at similar rostro-caudal levels of olfactory bulbs isolated from 8 to 12 week-old wild-type (A, E, I), slit-1$^{-/-}$ (B, F, J, M-O), slit-1$^{-/-}$;slit-3$^{-/-}$ (C, G, K), and robo-2$^{c/c}$;syn-1$^{+/cre}$ (D, H, L) mice stained with anti-NQO-1 (A-D, I-L, M, N, O), anti-OCAM (E-H, I-L, M, N), anti-SV2 (O), and Hoescht (A-O). In wild-type mice, NQO-1-expressing axons innervate glomeruli restricted to the dorso-medial region of the olfactory bulb (A, I) and OCAM-expressing axons innervate glomeruli in the ventro-lateral region of the olfactory bulb (E, I). In slit-1$^{-/-}$ (B, J), slit-1$^{-/-}$;slit-3$^{-/-}$ (C, K), and robo-2$^{c/c}$;syn-1$^{+/cre}$ (D, L) mice, a subset of NQO-1-expressing axons are mistargeted to glomeruli in the ventral region of the olfactory bulb (arrows). NQO-1-expressing axons that target ectopically in the ventral region of the OB in slit-1$^{-/-}$ mice form both homogenous (arrowheads) and heterogenous glomeruli (arrows) (M, N), and are positive for the pre-synaptic marker SV2, suggesting they form synapses (arrowheads) (O). N=10 wild-type, n=14 slit-1$^{-/-}$, n=9 slit-1$^{-/-}$;slit-3$^{-/-}$, and n=4 robo-2$^{c/c}$;syn-1$^{+/cre}$. Scale bars: (A-L) 250μm; (M-O) 140μm.*

*(P-R) Scatter plots showing the mapping of the positions of NQO-1-positive glomeruli in the olfactory bulb of an adult wild-type (P), slit-1$^{-/-}$ (Q), and robo-2$^{c/c}$;syn-1$^{+/cre}$ (R) mouse. The relative positions of glomeruli containing NQO-1-positive axons were assessed in olfactory bulb sections isolated over a rostro-caudal distance of 1000 μm starting at 800 μm from the tip of the olfactory bulb. While NQO-1-positive glomeruli are absent in the ventral region of the olfactory bulb (V-180 degree angle) from a wild-type mouse, NQO-1-positive glomeruli are consistently observed in the most ventral region of the OB in slit-1$^{-/-}$ and robo-2$^{c/c}$;syn-1$^{+/cre}$ mice . Shown are representative plots from a*

*single olfactory bulb for each genotype (n=4 olfactory bulbs from 2 mice of each genotype). D: dorsal; V: ventral; L: lateral; M: medial.*

The perinathal lethality of *robo-2*$^{-/-}$ mice precluded us from evaluating the requirement for Robo-2 in the development of accurate NQO-1-expressing axonal projections in the adult olfactory glomerular map. We therefore selectively ablated expression of Robo-2 in neurons by generating *robo-2* conditional null mice that express the Cre recombinase under the control of the pan-neuronal *synapsin-1* promoter (Hoesche et al., 1993, 1995; Cloutier et al. 2004; Lu et al. 2007). *robo-2*$^{C/C}$*; synapsin-1*$^{Cre/+}$mice survive until adulthood and their OBs are fully innervated by NQO-1- and OCAM-expressing axons. As observed in Slit mutant mice, a subset of NQO-1-positive axons mistarget to glomeruli in the ventral region of the OB in *robo-2*$^{C/C}$*; synapsin-1*$^{Cre/+}$mice (Figure 7 D, L, R). Together, these results show that Slit-1 and Robo-2 are required for the accurate formation of the mature olfactory glomerular map.

## DISCUSSION

The detection of sensory inputs requires the formation of stereotypic connections between sensory neurons in the periphery and second-order neurons of the central nervous system. A spatial relationship exists between the location of OSNs within the OE and their target glomeruli within the OB. OSNs of the dorso-medial aspect of the OE project dorsally within the OB while OSNs located in the ventro-lateral region of the OE send their axons to more ventral targets in the OB (Astic and Saucier 1986; Saucier and

Astic 1986; Miyamichi et al. 2005). While the molecular mechanism underlying the accurate sorting of these axons within the OB during development has not been identified, axon guidance cues represent good candidates to regulate this process. Our results show that the axon guidance receptor Robo-2 is expressed in a high dorso-medial to low ventro-lateral gradient in the OE. Furthermore, the Robo-2 ligands, Slit-1 and Slit-3, are expressed at high levels in the ventral aspect of the OB, and both Slit-1 and Robo-2 expression are required for the segregation of NQO-1-expressing OSN axons to the dorsal region of the OB (Figure 8). Taken together, our results demonstrate that Slit-1 and Robo-2 are required for accurate dorsal-to-ventral targeting of OSN axons within the OB.

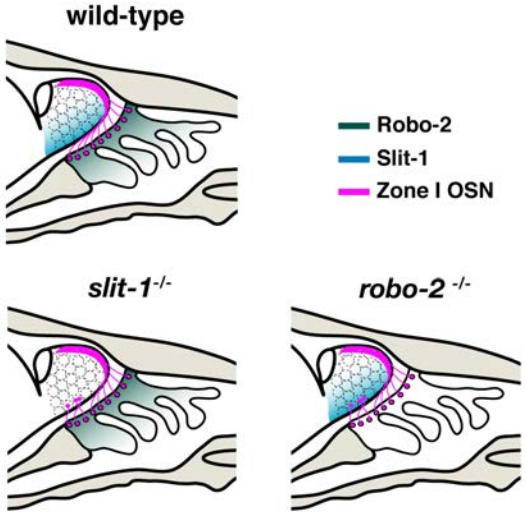


***Figure 8: Slit-1 and Robo-2 are required for the segregation of zone I OSN axons to the dorsal region of the OB.***

*Representation of zone I OSN projections in wild-type, slit-1$^{-/-}$, and robo-2$^{-/-}$ mice. NQO-1-expressing zone I OSNs (magenta) located in the dorsal region of the OE project their axons to the dorsal aspect of the OB. The high dorsal to low ventral graded expression of*

*Robo-2 (green) in OSN of the OE promotes the segregation of NQO-1-expressing axons to the dorsal region of the OB. Zone I OSN axons may be repelled by the Robo-2 ligand Slit-1, which is expressed in the ventral region of the OB. Loss of either Robo-2 or Slit-1 expression leads to mistargeting of a subset of zone I OSN axons to the ventral aspect of the OB.*

*Expression patterns of Robo-2 and Slits in the olfactory system*

OSNs expressing a specific OR are scattered within four spatially distinct zones of the OE (Strotmann et al. 1992; Ressler et al. 1993; Vassar et al. 1993; Ressler et al. 1994; Strotmann et al. 1994; Vassar et al. 1994; Mombaerts et al. 1996; Sullivan et al. 1996; Tsuboi et al. 1999). While initial studies suggested that these zones only partially overlap at their boundaries, recent results suggest that OR expression domains form a continuous gradient in the OE (Miyamichi et al. 2005). This observation raises the possibility that the dorso-ventral segregation of OSN axons within the OB may be regulated through graded expression of axon guidance receptors in the OE and of their ligands in the OB. Consistent with this notion, our results show that the Slit receptor, Robo-2, is expressed in a gradient across the OE. The high dorso-medial to low ventro-lateral expression of Robo-2 in the OE suggests that its expression may regulate dorso-ventral targeting of OSNs within the bulb. While the axon guidance receptor Npn-2 is expressed in a gradient in specific regions of the OE (Norlin et al. 2001), our result represents the first example of an axon guidance receptor being expressed in a gradient across the defined zones of the OE. OSN axons expressing varying levels of Robo-2 may

therefore respond differentially to the expression of Slits in the OB. Indeed, our results show that Slit-1 and Slit-3 are expressed in the ventral region of the developing OB at the stages of development when OSN axons reach and begin to enter the OB. Secretion of Slits by cells in the ventral region of the OB, possibly by mitral cells, may promote the formation of a high ventral to low dorsal gradient of Slit proteins in the OB (Fig. 8). The levels of Robo-2 expressed on an OSN axon may therefore dictate its targeting location in the dorso-ventral axis in response to a gradient of slit proteins within the OB.

*Slit-1 and Robo-2 control dorso-ventral segregation of olfactory sensory neuron axons in the olfactory bulbs*

The graded pattern of expression of Robo-2 in the OE and the expression of its ligands Slit-1 and Slit-3 in the OB suggest Slit-Robo signaling may direct targeting of OSN axons within the OB. Since Robo-2 is highly expressed in OSNs located in the dorso-medial region of the OE that express NQO-1, we evaluated the accuracy of targeting of NQO-1-expressing axons in *robo-2*$^{-/-}$, *slit-1*$^{-/-}$, and *slit-3*$^{-/-}$ mice. Our analyses revealed that a subset of NQO-1-expressing axons mistarget to the ventral region of the OB in the absence of Robo-2. Furthermore, Slit-1, but not Slit-3 is required to segregate axons of NQO-1-expressing OSNs to the dorsal region of the OB. Indeed, ablation of both Slit-1 and Slit-3 does not lead to more severe defects in targeting of NQO-1-expressing axons when compared to the single ablation of Slit-1, indicating that Slit-1 is the major contributor to Robo-2-mediated segregation of OSN axons within the OB. This observation suggests that different members of the Slit family may bind to Robos with

various efficiencies in vivo despite having similar binding affinities for these receptors in vitro. Alternatively, Slit-1 and Slit-3 may be secreted at different levels in the ventral region of the OB. Nonetheless, we cannot exclude the possibility that Slit-3 is required for sorting of OCAM-expressing axons within the more ventral regions of the OB.

In contrast to NQO-1-expressing OSN axons, the ventral segregation of OCAM-expressing OSN axons does not appear to be grossly affected in *slit-1*$^{-/-}$ and *robo-2*$^{-/-}$ mice. Indeed, we did not observe mistargeting of OCAM-expressing axons to the more dorsal region of the OB in these mice. This observation raises the interesting possibility that another set of guidance cues may promote the segregation of OCAM-expressing axons to the ventral region of the OB. While OCAM-expressing axons appear to be properly segregated to the ventral region of the OB, it is possible that these axons mistarget within this region in *slit-1*$^{-/-}$ and *robo-2*$^{-/-}$ mice. In fact, if Slit-1-Robo-2 signaling is required for the zonal segregation of all OSN axons within the OB, we would expect that targeting accuracy within OCAM-positive regions of the OB (zones II to IV) should also be affected. Moreover, our analyses of NQO-1-positive axonal projections in mutant mice do not exclude the possibility that Slit-1-Robo-2 signaling can also control targeting of OSN axons in other axes of the OB. To address these questions, it will be necessary to evaluate the accuracy of targeting of specific populations of OSN axons in *slit-1*$^{-/-}$ mice using OR-taulacZ reporter mice.

While the mistargeting of NQO-1-expressing axons to the ventral region of the OB observed in *robo-2*$^{-/-}$ mice is likely to result from the inability of OSN axons to respond to Slits in the OB, we cannot exclude the possibility that the stunted development of the OB observed in *robo-2*$^{-/-}$ mice may also affect axonal targeting. Nonetheless, the

observation that ablation of Slit-1 expression also leads to mistargeting of NQO-1-expressing axons, despite the normal size (Schwarting et al. 2000) of the OB in *slit-1*$^{-/-}$ mice, strongly suggests that Slit-1-Robo-2 interactions are required for accurate targeting of these axons within the bulb. Future experiments involving the genetic ablation of Robo-2 expression exclusively in OSNs should shed more light on the cell autonomous requirement of Robo-2 for segregation of OSN axons in the OB.

We also cannot exclude the possibility that expression of a specific subset of zone I ORs may be lost in *slit-1*$^{-/-}$ and *robo-2*$^{-/-}$ mice, leading to the mistargeting of this subset of axons. However, OSN axons lacking OR expression have previously been shown to remain in the olfactory nerve layer and do not enter glomeruli in the OB (Wang et al., 1998). Since the NQO-1-expressing axons that erroneously target to the ventral region of the OB in *slit-1*$^{-/-}$ and *robo-2*$^{C/C}$*; Syn-1*$^{Cre/+}$ mice coalesce into glomeruli and appear to form synapses, they are likely to still express an OR.

It is interesting to note that in addition to the mistargeting of a subset of NQO-1-expressing axons within the OB, *robo-2*$^{-/-}$ mice show additional defects that are not observed in Slit-1$^{-/-}$ mice. These include smaller olfactory bulbs and a lack of innervation of some regions that are innervated by OCAM-expressing axons in wild-type mice. This observation would suggest that Robo-2 may have both Slit-1-dependent and -independent functions during development of OSN projections. Indeed, Robo-2 has been shown to have the capacity to function as an adhesion molecule and could therefore be involved in promoting the sorting of axons in the nerve layer as well as their entry into the glomerular layer of the OB (Hivert et al. 2002). Alternatively, these differences in phenotypes may result from the differential expression of Robo-2 in several types of cells such as neurons

or glia. Our observation that selective ablation of Robo-2 expression in neurons does not affect innervation of the OB by OCAM-expressing axons seems to support this possibility.

*Axon guidance cues in the generation of the glomerular map*

The formation of stereotypic connections between olfactory sensory neurons and mitral/tufted cells within the OB is tightly regulated. The glomerular map that is formed requires axons to find their precise target within a complex three-dimensional field. This accurate targeting relies on the expression of ORs in OSNs and on their ability to respond to axonal guidance cues. Several axon guidance molecules such as Sema3A (Schwarting et al. 2000; Schwarting et al. 2004), EphrinAs (Cutforth et al. 2003), and now Slits, appear to be required for proper development of the glomerular map. While Ephrin As have been implicated in the regulation of anterior-posterior targeting of OSN axons (Cutforth et al. 2003), Sema3A is required for accurate medial-lateral compartmentalization of OSN axons within the OB (Schwarting et al. 2000; Schwarting et al. 2004). Here, we provide evidence that Slit-1-Robo-2 signaling promotes the zonal segregation of OSNs in the dorsal-ventral axis of the OB. It is likely that Slit-1 and Robo-2 collaborate with other families of axon guidance cues to direct accurate dorsal-ventral targeting of OSN axons within the bulb. Indeed, our observation that a large proportion of NQO-1-expressing axons target appropriately to the dorsal region of the OB in the absence of Slit-1 or Robo-2 suggests that long-range attractant cues may also promote their segregation to the dorsal region of the OB.

In addition to axon guidance cues, expression of OR plays a critical role for the accurate coalescence of axons into specific glomeruli (Mombaerts et al. 1996). It has

been proposed that ORs may regulate targeting of OSN axons through OR-mediated interactions between OSN axons (Feinstein et al. 2004; Feinstein and Mombaerts 2004). Our observation that the mistargeted NQO-1-positive axons observed in adult *slit-1*$^{-/-}$ and *robo-2*$^{C/C}$*;Syn-1*$^{+/Cre}$ mice form heterogenous glomeruli with OCAM-positive axons suggests that expression of an OR is not sufficient to ensure homogenous coalescence of axons into glomeruli. It is possible that Slit-1-Robo-2 signaling serves to promote the initial segregation of OSN axons in the dorsal-ventral axis of the OB, which is followed by coalescence of axons into glomeruli through OR-mediated interactions. However, recent results suggest that OR-dependent G protein signaling leading to changes in intracellular cAMP levels can also regulate the anterior-posterior targeting of OSN axons within the OB (Imai et al. 2006). While it is unclear how OR-induced G protein signaling mediates this effect, it may do so by modulating signals generated by axon guidance receptors. For example, in *Drosophila*, expression of an activated form of the G protein dgqα3 antagonizes Robo signaling, thereby leading to axonal pathfinding defects at the midline (Ratnaparkhi et al., 2002). Alternatively, the regulation of intracellular cAMP levels may be important for expression of specific axon guidance molecules and their receptors, such as Neuropilin-1 (Imai et al. 2006). Interestingly, modulating cAMP levels does not affect the dorso-ventral targeting of OSN axons suggesting that Robo-2 expression in OSNs is unlikely to be regulated by intracellular levels of cAMP (Imai et al. 2006). OR molecules may also promote the accurate coalescence of axons by regulating the expression of homophilic adhesion molecules and repulsive guidance cues, such as Ephrin As, in OSNs (Serizawa et al. 2006).

Taken together, our results demonstrate that the dorsal-ventral segregation of OSN axons within the OB is not only dependent on the anatomical locations of OSNs within the OE, but also on their ability to process guidance information provided by their surroundings. Further studies will address potential interactions between the different families of axon guidance molecules involved in the development of connectivity in the olfactory system.

**SUPPLEMENTAL FIGURES**

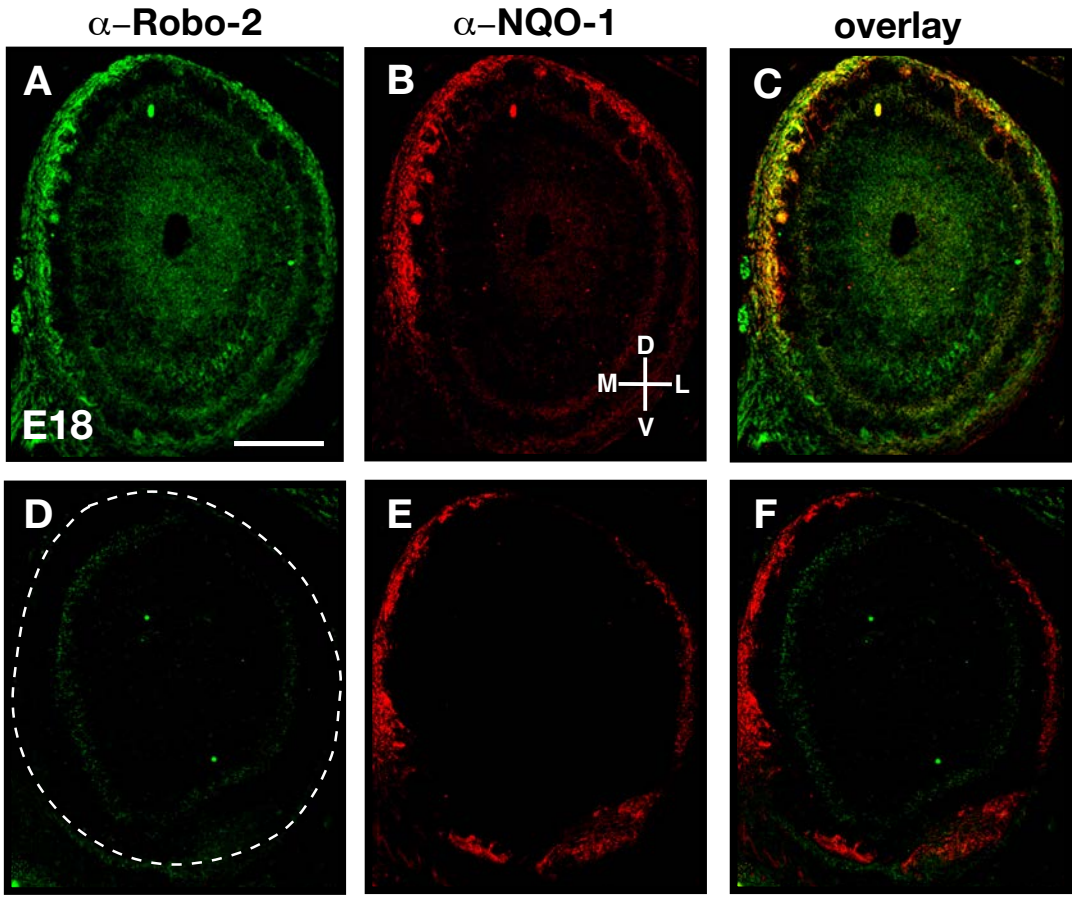


***Supplemental Figure 1: Characterization of Robo-2 antibodies.***

*Coronal sections of olfactory bulbs from E18 wild-type (A-C) and robo-2$^{-/-}$ (D-F) mice stained with anti-Robo-2 (A, C, D, F) and anti-NQO-1 (B, C, E, F). While the Robo-2 antibody detects olfactory sensory neuron axons in wild-type mice (A, F), no staining is observed in robo-2$^{-/-}$ mice (D, F). In D, the olfactory bulb is traced with a white dashed line. D: dorsal; V: ventral; R: rostral; C: caudal.*

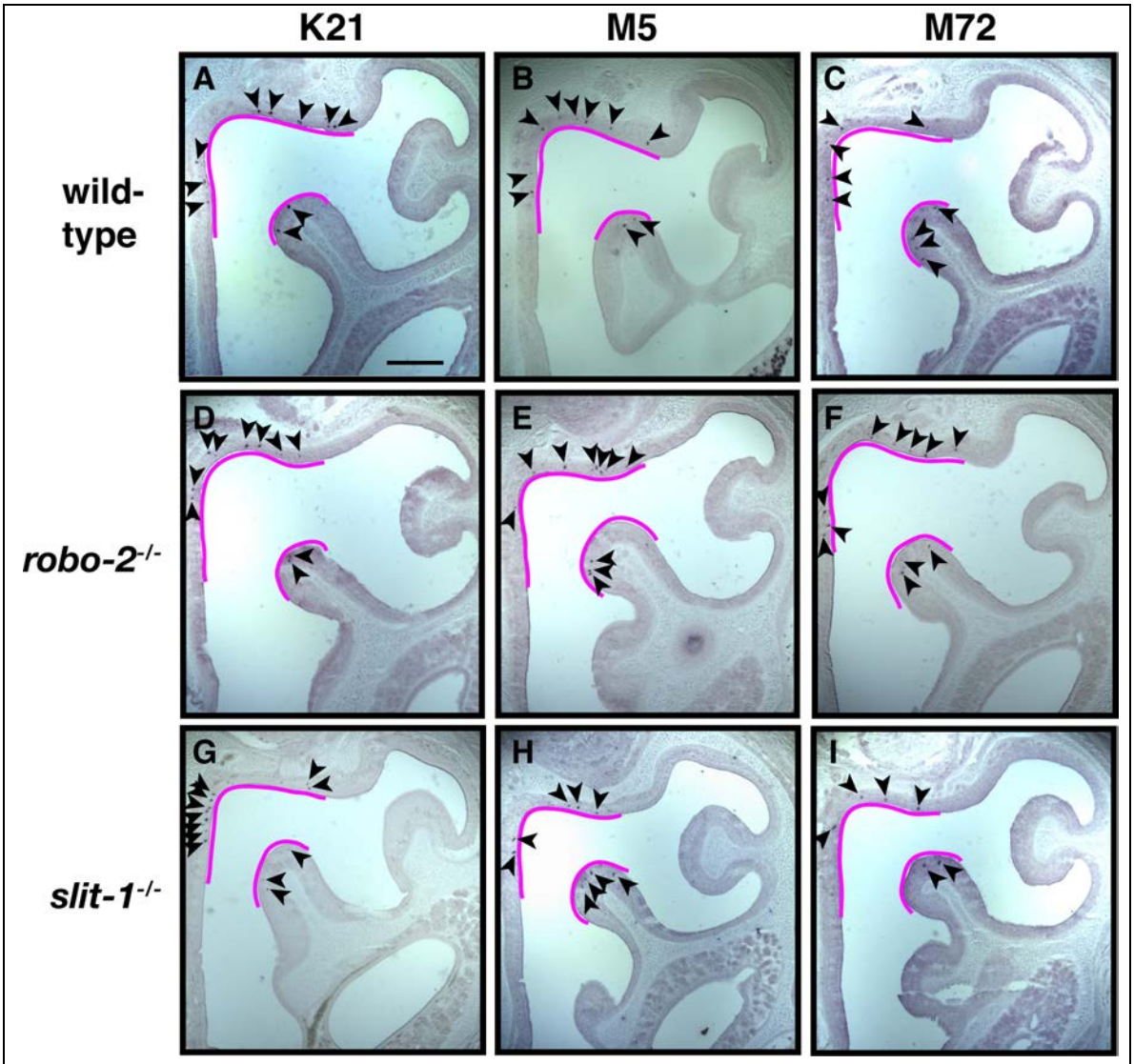


***Supplemental Figure 2: Zonal segregation of zone I OR expression is unaltered in slit-1$^{-/-}$ and robo-2$^{-/-}$ mice.***

*In situ hybridization of coronal sections of olfactory epithelia from post-natal day P0 wild-type (A-C), robo-2$^{-/-}$ (D-F), and slit-1$^{-/-}$ (G-I) mice with cRNA probes specific for K21 (A, D, G), M5 (B, E, H), and M72 (C, F, I). All three receptors are expressed in zone I of the OE (Sullivan et al., 1996; Zheng et al. 2000). The expression of K21, M5, and M72 is restricted to the dorso-medial region of the OE (zone I) in wild-type, robo-2$^{-/-}$,*

*and slit-1$^{-/-}$ mice. The location of zone I is represented by a magenta line on the apical side of the OE. The delineation of zone I was determined by performing NQO-1 in situ hybridization on sections adjacent to the sections presented (data not shown). N=3 wild-type, n= 3 robo-2$^{-/-}$; n=3 slit-1$^{-/-}$.*

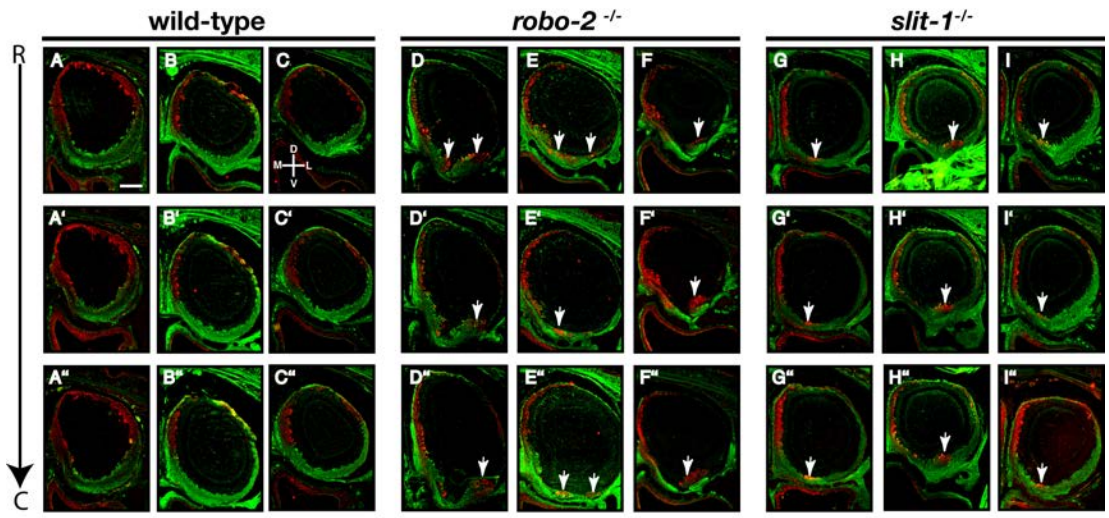


***Supplemental Figure 3: NQO-1-expressing olfactory sensory neuron axons mistarget to the ventral region at several levels along the rostro-caudal axis of the olfactory bulb in slit-1$^{-/-}$ and robo-2$^{-/-}$ mice.***

*Coronal sections (20μm) of olfactory bulbs from three different post-natal day P0 wild-type (A-C) robo-2$^{-/-}$ (D-F), and slit-1$^{-/-}$ (G-I) mice were stained with anti-NQO-1 and anti-OCAM. Sections at three different levels of the rostro-caudal axis of the olfactory bulb are shown for each mouse. The rostral (R) and caudal (C) sections shown are separated by 160μm. In wild-type mice, NQO-1-expressing axons are restricted to the dorso-medial region of the olfactory bulb in this segment of the OB while OCAM-expressing axons target the ventral region of the olfactory bulbs (A-C''). A subset of NQO-1-expressing axons is mistargeted to the ventral region of the olfactory bulbs in robo-2$^{-/-}$ and slit-1$^{-/-}$ mice (arrows) (D-F'', G-I'') at all three levels of the rostro-caudal axis shown. D: dorsal; V: ventral; L: lateral; M: medial; R: rostral; C: caudal. Scale bars: 250μm.*

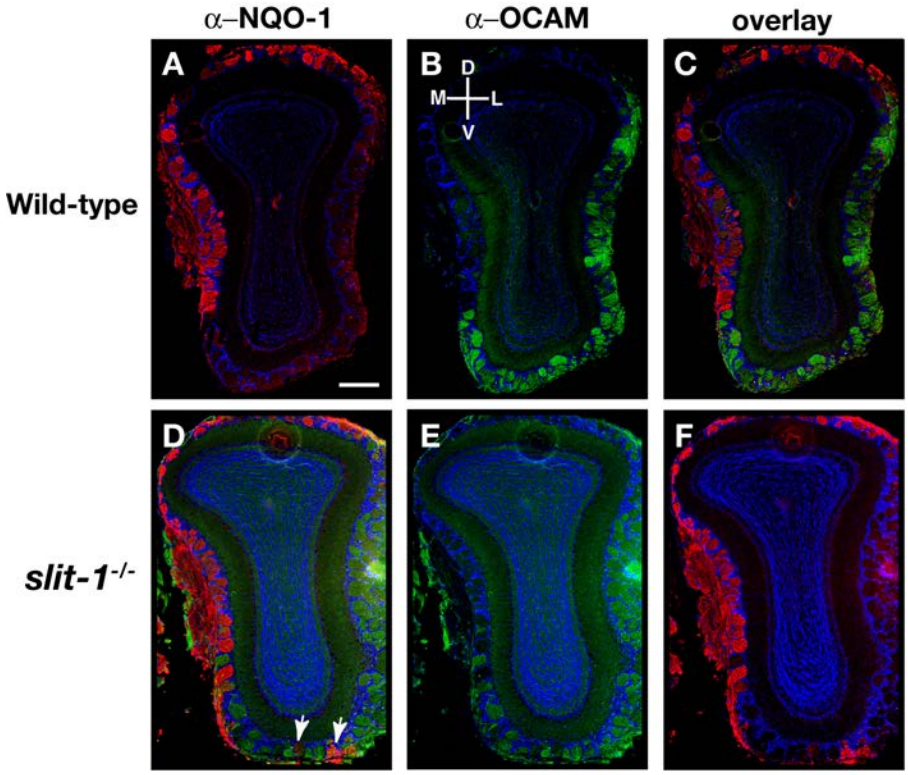


***Supplemental Figure 4: Mistargeted NQO-1-expressing olfactory sensory neuron axons are detected in the ventral region of the olfactory bulb in 8-month old slit-1$^{-/-}$ mice.***

*Coronal sections at similar rostro-caudal levels of olfactory bulbs isolated from 8 month-old wild-type (A-C), and slit-1$^{-/-}$ (D-F) mice stained with anti-NQO-1 (A, C, D, F), anti-OCAM (B, C, E, F) and Hoescht (A-F). In wild-type mice, NQO-1-expressing axons innervate glomeruli restricted to the dorso-medial region of the olfactory bulb (A, C) and OCAM-expressing axons innervate glomeruli in the ventro-lateral region of the olfactory bulb (B, C). In slit-1$^{-/-}$ mice, a subset of NQO-1-expressing axons are mistargeted to glomeruli in the ventral region of the olfactory bulb (D, F) (arrows). N=2 wild-type and n=2 slit-1$^{-/-}$. D: dorsal; V: ventral; M: medial, L: lateral. Scale bar: 250μm.*

# CHAPTER 3

## The pattern of glomerular map formation defines responsiveness to aversive odorants in mice

**Jin hyung Cho**[1], Janet E.A. Prince[1], Tyler Cutforth[2], and Jean-François Cloutier[1]

[1]*Montreal Neurological Institute, McGill University, Montreal, Quebec, Canada*
[2] *Department of Molecular, Cellular, and Developmental Biology, U.C. Santa Cruz, Santa Cruz, CA, USA*

### PREFACE

This chapter is a manuscript that is currently being revised for resubmission to the Journal of Neuroscience after an initial round of very positive reviews. In the previous chapter, we demonstrated that: (1) Robo-2 is expressed in a graded manner in the OE and Slit-1 is expressed in the OB, (2) Slit-1-Robo-2 signaling is crucial for the accurate innervation of NQO-1 expressing OSN axons (zone 1) to the dorsal region of the OB. A study by Kobayakawa et al., in 2007 demonstrated that zone 1 of the OB is subdivided in two different regions; DI and DII, and that OSNs innervating these regions are essential for the processing of aversive odorants in mice (Kobayakawa et al. 2007). In this chapter we examine the role of Robo-2 in the targeting of OSNs axons innervating the DI and DII regions along the dorsal to ventral axis of the OB. We also performed behavioral studies to investigate the requirement of accurate innervation in the olfactory sensory map for the processing of aversive odorants.

*Acknowledgements*

We would like to thank Bill Andrews and John Parnavelas for providing us with the Robo-2 mouse line and Thomas Bozza for the S50-tau-GFP and M72-tau-lacZ mouse lines. We also thank Don Van Meyel for comments on the manuscript and Armen Saghathelyan for discussions on olfactory behavior tests. This work was supported by the Canadian Institutes for Health Research, the Fonds Québécois pour la Recherche sur la Nature et les Technologies, and the Canada Foundation for Innovation. J.H.C. holds a studentship from the Fonds de Recherche en Santé du Québec. J.E.A. Prince held a Master's studentship from the Natural Sciences and Engineering Research Council of Canada and holds a Ph.D. studentship from the Fonds Québécois pour la Recherche sur la Nature et les Technologies. J.-F.C. holds a Canada Research Chair in developmental neurobiology.

**ABSTRACT**

In many species, the detection and recognition of odors is critical to regulate behaviors that are essential for survival, such as foraging for food and avoidance of predators. The formation of complex stereotypic connections between olfactory sensory neurons (OSNs) and second order neurons in the olfactory bulb (OB) is believed to be important for accurate odorant information processing. In mice, ablation of OSNs that innervate the dorsal region of the OB leads to a loss of avoidance behavior in response to aversive and predator odorants (Kobayakawa et al., 2007). It remains to be determined whether the accurate formation of a glomerular map in this region of the OB is required for these innate responses. Here, we have generated mice that lack expression of the axon

guidance receptor Robo-2 in OSNs and found that ablation of Robo-2 expression leads to mistargeting of subsets of OSN axons within the dorsal region of the OB. Furthermore, these mice show decreased avoidance behavior toward the predator odorant trimethyl-thiazoline (TMT). Our results indicate that the pattern of glomerular innervation in the OB is critical for innate behavioral responses in mice.

## INTRODUCTION

Odor recognition is mediated by OSNs located in the olfactory epithelium (OE). OSNs project their axons to the OB where they make synaptic connections with second-order neurons in neuropil structures termed glomeruli (Mombaerts, 2006). Odorants are detected by olfactory receptors (ORs) expressed on OSNs (Buck and Axel, 1991; Zhao et al., 1998). Each OSN expresses a single type of OR, and axons of OSNs expressing the same OR coalesce into stereotypically conserved glomeruli (Ressler et al., 1994; Vassar et al., 1994; Mombaerts et al., 1996; Malnic et al., 1999; Serizawa et al., 2003). The formation of the glomerular map is dependent on the expression of ORs, adhesion molecules and axon guidance cues by OSNs (reviewed in Mombaerts, 2006 and Cho et al., 2009; Imai et al., 2009; Tsuboi et al., 2009; Takahashi et al. 2010; Takeuchi et al. 2010). The spatial arrangement of glomeruli within the OB is believed to contribute to the coding of odor information (Mori et al., 2006; Johnson and Leon, 2007).

The dorsal OB receives input from OSNs located in the dorsomedial region of the OE that express either class I or class II odorant receptors. Class I and class II ORs are phylogenetically distinct and their glomeruli are segregated into the DI and DII regions of the dorsal OB, respectively (Figure 1 a) (Zhang et al., 2004; Miyamichi et al., 2005;

Tsuboi et al., 2006; Kobayakawa et al., 2007; Bozza et al., 2009). Activation of glomeruli in these two regions has been linked to innate avoidance responses to aversive odors such as those emanating from spoiled food and predator urine (Kobayakawa et al., 2007). Mitral cells are projection neurons that receive inputs from OSNs, and the majority of mitral cells located in the dorsal region of the OB innervate the cortical amygdala, suggesting it could process olfactory information that illicits innate behaviors (Miyamichi et al., 2010).

Here, we have examined whether formation of an accurate glomerular map is required for responsiveness to aversive cues. Our results indicate that the pattern of glomerular innervation in the DII region of the dorsal OB is critical for avoidance of predator odorants in mice.

## MATERIALS AND METHODS

### *Animals*

Embryonic day 18 (E18) mouse embryos were obtained from timed pregnant females purchased from Charles River (Saint-Constant, Québec, Canada). The following mouse strains have been described previously: floxed *robo-2* mutant (Lu et al., 2007), OMP-Cre (Eggan et al., 2004), S50-tau-GFP (Bozza et al., 2009), and M72-tau-lacZ (Zheng et al., 2000). MOR1-3-ires-tau-lacZ and MOR174-9-ires-GFP mice were generated by standard homologous recombination methods using the self-excising ACN cassette to remove the neo marker during germline transmission in male chimeras (Bunting et al., 1999). For all analyses performed, *robo-2*$^{+/+}$*; OMP-Cre* and *robo-2*$^{+/lox}$*; OMP-Cre* mice were used as controls and compared to *robo-2*$^{lox/lox}$*; OMP-Cre* mice.

*Fluorescence* in situ *hybridization*

Nonradioactive, digoxigenin (DIG)-labeled or fluorescein-labeled cRNA probes were synthesized from cDNA clones encoding *robo-2* (Brose et al., 1999), *MOR1-3*, or *MOR174-9*. The coding sequences of *MOR1-3* and *MOR174-9* were PCR amplified from C57BL/6 genomic DNA using the following oligonucleotides: *MOR1-3*, 5'-TCCTACTGACGGGCTTTCTG-3' and 5'-CATGCTTTCCAAACCT-GTGA-3'; *MOR174-9*, 5'-AGATGGAAATCACAGTGGGG-3' and 5'-CACAG-AGGCCACTTTTACGG-3'. Sections of OE were processed as described previously (Schaefer et al., 2001; Ishii et al., 2004; Prince et al., 2009).

*Analysis of the position of OR-positive glomeruli in adult olfactory bulbs*

Adult mice (3 months old) were anesthetized and perfused transcardially with ice-cold PBS containing 4% paraformaldehyde. Brains were processed as described previously and all sections were collected on microscope slides over the complete rostrocaudal axis of the OB (Cho et al., 2007). Sections were immunostained with NQO-1 antibodies (1:100; Abcam, Cambridge, MA), and GFP (1:250; Invitrogen, Carlsbad, CA) or β-gal antibodies (1:250; MP biomedicals, Solon, OH), and counterstained with Hoechst. The position of GFP- or β-gal-positive glomeruli in the OB was determined using an NIH Image J plug-in as previously described (Schaefer et al., 2001). Briefly, images of sections containing GFP- or β-gal-positive glomeruli were imported into Adobe Photoshop software (Adobe Systems, Mountain View, CA) for mapping of glomeruli. The radial angle of each GFP- or β-gal-positive glomerulus was measured after setting the origin for each section. The origin was set at one-third the distance between the mitral

cell layer in the dorsal region of the OB and the mitral cell layer in the ventral region of the OB. A scatter plot was constructed that shows the location of GFP- or β-gal-positive glomeruli in all OBs analyzed in the dorsoventral axis with degrees (radial angle) on the y-axis. The mean radial angle for each identified glomerulus was measured and compared between control and *robo-2*$^{lox/lox}$*;OMP-Cre* mice using an unpaired t-test.

*Immunohistochemical procedures*

E13 and E14 mouse embryos or P0 mouse heads were fixed in 4% paraformaldehyde for 12 hours and cryoprotected in PBS containing 30% sucrose. 20mm sections were incubated with anti-OMP (1:1000) (Wako Chemicals USA, Richmond, VA), anti-Robo-2 (1:350), anti-βgal (1:250), or anti-βIII tubulin (1:1000) (Promega, Madison, WI). After rinsing in TBS, sections were incubated with the appropriate Alexa-488- or Alexa-546-conjugated secondary antibody (1:500; Invitrogen, Carlsbad, CA).

*X-Gal staining*. For whole-mount X-Gal staining, three-month old adult mice were perfused transcardially with ice cold PBS containing 4% paraformaldehyde, 2 mM $MgSO_4$, and 5 mM EGTA. Whole olfactory bulbs were washed twice for 15 minutes in 0.1M phosphate buffer containing 2mM magnesium sulfate, 0.01% sodium deoxycholate, and 0.02% Nonidet P40 and processed for X-Gal staining. Samples were incubated in 0.1M phosphate buffer containing 2mM magnesium sulfate, 0.01% sodium deoxycholate, and 0.02% Nonidet P40, 5mM $K_3Fe(CN)_6$, 5mM $K_4Fe(CN)_6$, and 1 mg/ml X-Gal for 1 hour to overnight at 37$^{o}$C.

*Innate olfactory preference and avoidance tests*

For these tests, we followed the published method with slight modifications (Kobayakawa et al., 2007). Three month old male *robo-2*$^{lox/lox}$*; OMP-Cre* and control littermates were used only once in each test. Individual mice were habituated to the experimental environment for thirty minutes and then to the test cage (30 X 18 X 13 cm) for an additional ten minutes. After the habituation period, a filter paper (2 X 2 cm) scented with water was introduced and the time each mouse spent investigating the filter paper during a 3 minute test period was measured. The filter paper was taken out and, after a 10 minute waiting period, replaced with one scented with test odorant. The investigation time for the odorant-scented filter paper was measured for 3 minutes.

For the innate olfactory avoidance test, the test cage was visually separated into two areas (1:3) using masking tape on the outside of the cage to discern the two areas during analysis. After habituation, a filter paper (2 X 2 cm) scented with water was introduced in the part of the cage containing the smaller region and the duration of time spent by the mouse in the larger part of the cage measured over a 3-minute test period. The filter paper was taken out, replaced with a filter paper scented with test odorant and the duration of time spent by the mouse in the large region of the cage was measured. The time spent in the large compartment with the water control was subtracted from the value obtained with odorants to give the recorded avoidance time. Mouse behavior was recorded with a digital video camera for analysis. Odorants used for these analyses were: TMT (7.65M) **(**Phero Tech Inc., Delta, BC**),** 2-Methylbutyric acid (2MB) (8.7M) **(**Sigma**),** and peanut butter (10% w/v). Statistical analyses were performed using unpaired t-tests.

Aversion conditioning with LiCl was adapted from a published procedure (Kobayakawa et al., 2007). *robo-2*$^{lox/lox}$*; OMP-Cre* mice were exposed to TMT (7.65M) for 3 minutes and their avoidance times calculated as described above. For aversive conditioning, 0.5M LiCl solution was immediately injected (20 ml kg$^{-1}$) into the peritoneal cavity after testing. Two days later, the mice were subjected to the olfactory avoidance test with TMT, and avoidance times were measured. A paired t-test was performed for statistical analysis.

**RESULTS**

*Robo-2 is required for the targeting of MOR174-9 and M72 OSN axons in the OB*

We have previously shown that the axon guidance receptor Robo-2 is highly expressed in OSNs located in the dorsomedial region of the OE, and that Robo-2 is required to prevent dorsally-projecting OSN axons from inappropriately innervating the ventral region of the OB (Cho et al., 2007). *In situ* hybridization analyses revealed that OSNs located in the dorso-medial region of the OB expressing either class I or class II ORs express high levels of *robo-2* (Figure 1 B-B'', C-C''). To address whether Robo-2 is required for the accurate coalescence of OSN axons into specific glomeruli, we ablated expression of Robo-2 in OSNs and examined the projections of subpopulations of OSNs that send their axons to the DI and DII regions of the dorsal OB. These subpopulations of OSNs express either of the class I ORs, MOR1-3 and S50, or the class II ORs MOR174-9 and M72.

To ablate expression of Robo-2 in OSNs, we generated *robo-2* conditional mice expressing Cre recombinase under the control of the olfactory marker protein (*OMP)*

promoter. In these mice, Robo-2 expression is ablated in axons of OSNs by E14 but not in cells of the OB (Figure 2 A-P). Importantly, we found no additional Cre-induced recombination in any brain structures of the same *OMP-Cre* mouse (Figure S1). Furthermore, the OBs in these mice were of similar size and contained a comparable number of glomeruli as OBs from control animals (data not shown). To visualize targeting of OSN axons, *Robo-2;OMP-Cre* mice were crossed with mice that express reporter genes in MOR1-3- (tau-lacZ), S50- (tau-GFP), MOR174-9- (GFP), and M72- (tau-lacZ) expressing OSNs.

Examining whole-mount preparations of OBs from *robo-2*$^{lox/lox}$; *OMP-Cre; MOR174-9 tau-GFP*; it appeared that MOR174-9 positive glomeruli are shifted ventrally in the OB when compared to controls (Figure 1 J-M). Furthermore, in *robo-2*$^{lox/lox}$; *OMP-Cre; M72 tau-lacZ* mice, an additional glomerulus is observed on the dorso-lateral side of the OB (Figure 1 N-O'') as well as on the medial side of the OB (data not shown). In contrast, the targeting of MOR1-3- and S50-expressing axons appeared unaffected in mutant mice (Figure 1 D-I).

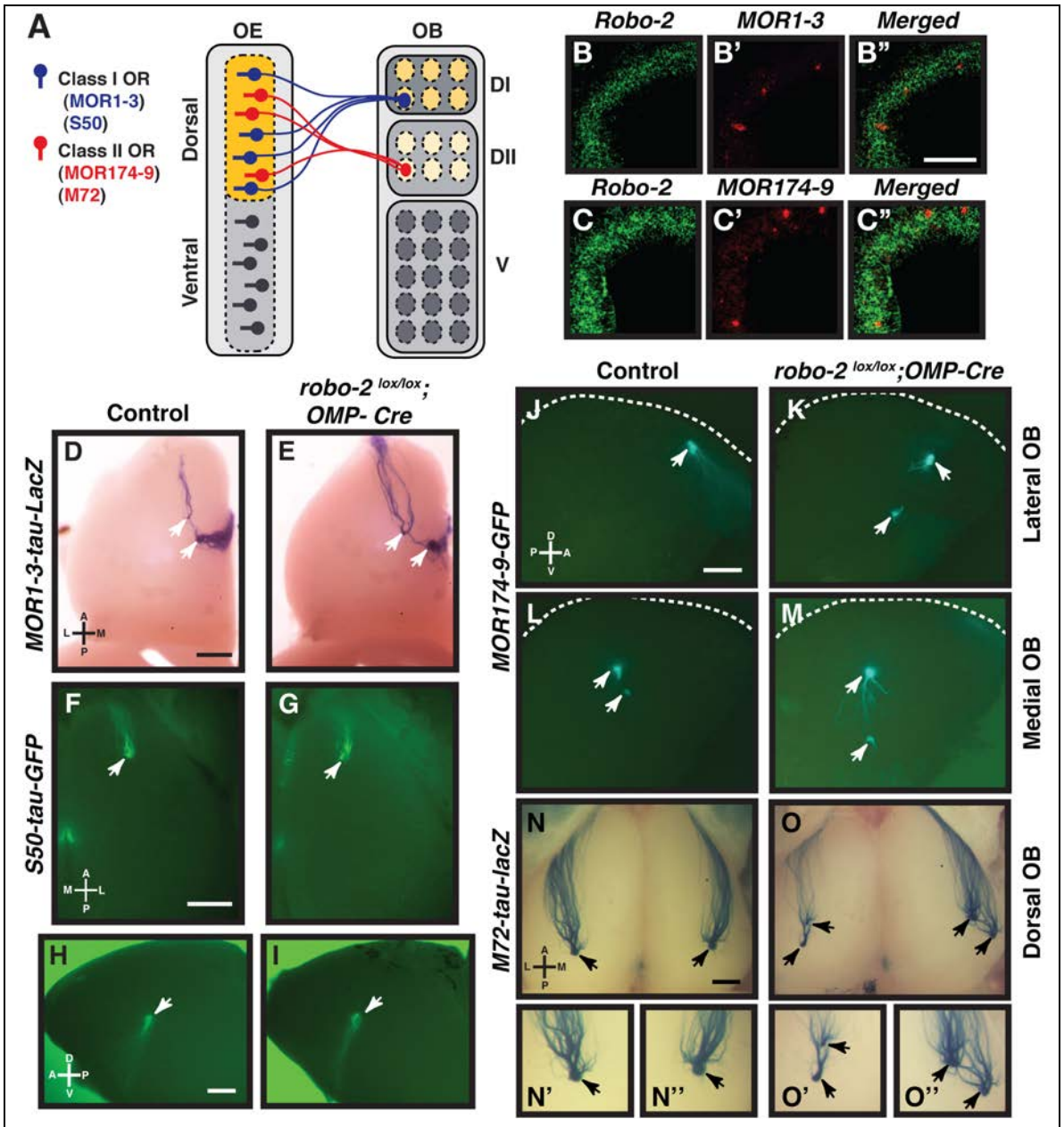


**Figure 1. Robo-2 is expressed in OSNs innervating the dorsal region of the olfactory bulb and is required for the targeting of axons from subsets of OSNs.**

A. Schematic representation of the pattern of innervation of the olfactory bulb by OSNs. OSNs located in the dorsal region of the olfactory epithelium (OE) innervate the dorsal part of the olfactory bulb (OB). In the dorsal OE, OSNs expressing class I ORs, such as

MOR1-3 or S50, send their axons to the DI region of the OB while OSNs expressing class II ORs, such as MOR174-9 or M72, innervate the DII region of the OB.

B, C. *Fluorescent In situ* hybridization of coronal sections of olfactory epithelium isolated from E18 embryos with cRNA probes specific for *robo-2* (B, B'', C, C''), *MOR1-3* (B', B''), and *MOR174-9* (C', C''). OSNs expressing the class I OR, *MOR1-3*, or the class II OR, *MOR174-9*, are located in the dorsomedial region of the OE and express *robo-2*. Scale bar: 100μm.

D-I. Whole-mount X-gal-stained or fluorescent views of MOR1-3-expressing (D, E) and S50-expressing (F-I) OSN projections in adult control (D, F, H) and *robo-2$^{lox/lox}$; OMP-Cre* (E, G, I) mice. MOR1-3-expressing OSN axons target to one or two glomeruli in the most dorsal region of the OB (D, E) (arrowheads). S50-expressing axons innervate glomeruli in the dorsal (F, G) and medial (H, I) regions of the OB (arrowheads). The location of MOR1-3 and S50-positive glomeruli appear unchanged in *robo-2$^{lox/lox}$; OMP-Cre* mice (E, G, I). n= 4 controls and 4 *robo-2$^{lox/lox}$; OMP-Cre.* Scale bars: 500μm. D, Dorsal; V, ventral; L, lateral; M, medial.

J-O. Whole-mount X-gal-stained or fluorescent views of MOR174-9- (J-M) or M72- (N,O) expressing OSN projections in adult control (J, L, N) and *robo-2$^{lox/lox}$; OMP-Cre* (K, M, O) mice. MOR174-9-expressing OSN axons innervate one or two glomeruli on the lateral (J, K) and medial (L, M) sides of the OB (arrowheads). The location of some of these glomeruli appears shifted towards the ventral part of the OB in most *robo-2$^{lox/lox}$; OMP-Cre* mice analyzed when compared to controls. M72-expressing OSN axons innervate one glomerulus on the dorsal (N) and medial (not shown) regions of the OB (arrowheads). In *robo-2$^{lox/lox}$; OMP-Cre* mice, two glomeruli are consistently observed in

the dorsal region of the OB (O). High magnification views of M72-positive glomeruli are shown in panels N', N'', O', and O''. n= 5 control; MOR174-9-GFP, 3 control; M72-tau-lacZ, 5 *robo-2*$^{lox/lox}$*; OMP-Cre*; MOR174-9-GFP, and 3 *robo-2*$^{lox/lox}$*; OMP-Cre*; M72-tau-lacZ mice. The dorsal limit of the OB is indicated by a white dashed line in J-M. Scale bars: 500μm. D, Dorsal; V, ventral; L, lateral; M. medial.

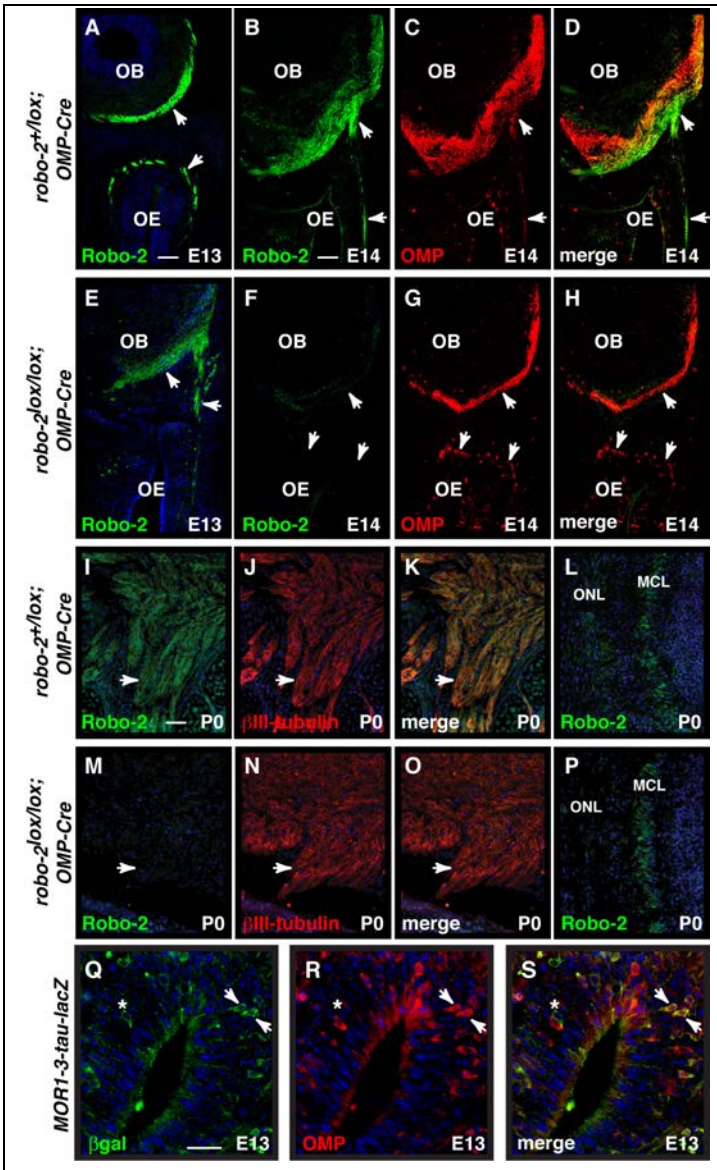


**Figure 2: Ablation of Robo-2 expression in OSN axons.**

A-P Coronal sections of OBs from E13, E14, and P0 *robo-2*$^{+/lox}$*; OMP-Cre* (A-D, I-L) or *robo-2*$^{lox/lox}$*; OMP-Cre* (E-H, M-P) embryos stained with Robo-2 (A, B, D, E, F, H. I, K, L), OMP (C, G, D, H), or β-III tubulin antibodies (J, K, N, O). The Robo-2 expression observed on OSN axons (arrowheads) in *robo-2*$^{+/lox}$*; OMP-Cre* mice (A, B, I) is diminished at E13 (E) and ablated at E14 (F) and P0 (M) in *robo-2*$^{lox/lox}$*; OMP-Cre* mice. In contrast, Robo-2 is still expressed in the mitral cell layer of the OB in *robo-2*$^{lox/lox}$*; OMP-Cre* mice (H). MCL: mitral cell layer. ONL: olfactory nerve layer. Scale bars: 125μm (A-H); 50μm (I-P).

Q-S Coronal sections of OE from E13 MOR1-3-tau-lacZ embryos stained with β-gal (I, K) and OMP (J, K) antibodies. While the majority of MOR1-3-expressing cells also express OMP (arrowheads) at that stage of development, some MOR1-3-positive cells do not express OMP (asterisk). The late onset of OMP expression in a portion of dorsal OSNs may explain the residual expression of Robo-2 observed on OSN axons at E13 in *robo-2*$^{lox/lox}$*; OMP-Cre* mice. Scale bar: 25μm.

To quantify these observations, the location of MOR174-9 and MOR1-3 innervated glomeruli in the OBs of control and *robo-2*$^{lox/lox}$; *OMP-Cre* mice was determined by immunostaining consecutive coronal sections of the OB with GFP or β-gal antibodies. In controls and *robo-2*$^{lox/lox}$; *OMP-Cre; MOR174-9-GFP* mice, one or two glomeruli were detected on both the medial and lateral sides of the OB in most mice analyzed (Figure 3 A-J). In a subset of control (1/14) and *robo-2*$^{lox/lox}$; *OMP-Cre; MOR174-9-GFP* (3/12) mice, a third glomerulus was also observed on the lateral side of the OB. Examination of the location of MOR174-9 glomeruli revealed an overall dorsal

to ventral shift in the distribution of both medial and lateral glomeruli in *robo-2*$^{lox/lox}$; *OMP-Cre; MOR174-9-GFP* mice (Figure 3 K, L). In contrast, we did not observe a significant change in the distribution of MOR1-3 positive glomeruli in the dorsal-ventral axis of the OB in *robo-2*$^{lox/lox}$; *OMP-Cre; MOR1-3 tau-lacZ* mice (Figure 4 A-E).

Our results indicate that Robo-2 is required for the coalescence of MOR174-9 and M72- expressing axons in specific glomeruli but appears dispensable for the convergence of MOR1-3 and S50-expressing axons in the OB. Our data also indicate that the glomerular map within the DII region of the OB is disrupted in *robo-2*$^{lox/lox}$; *OMP-Cre* mice, which may lead to improper processing of odorant signals in this region of the OB.

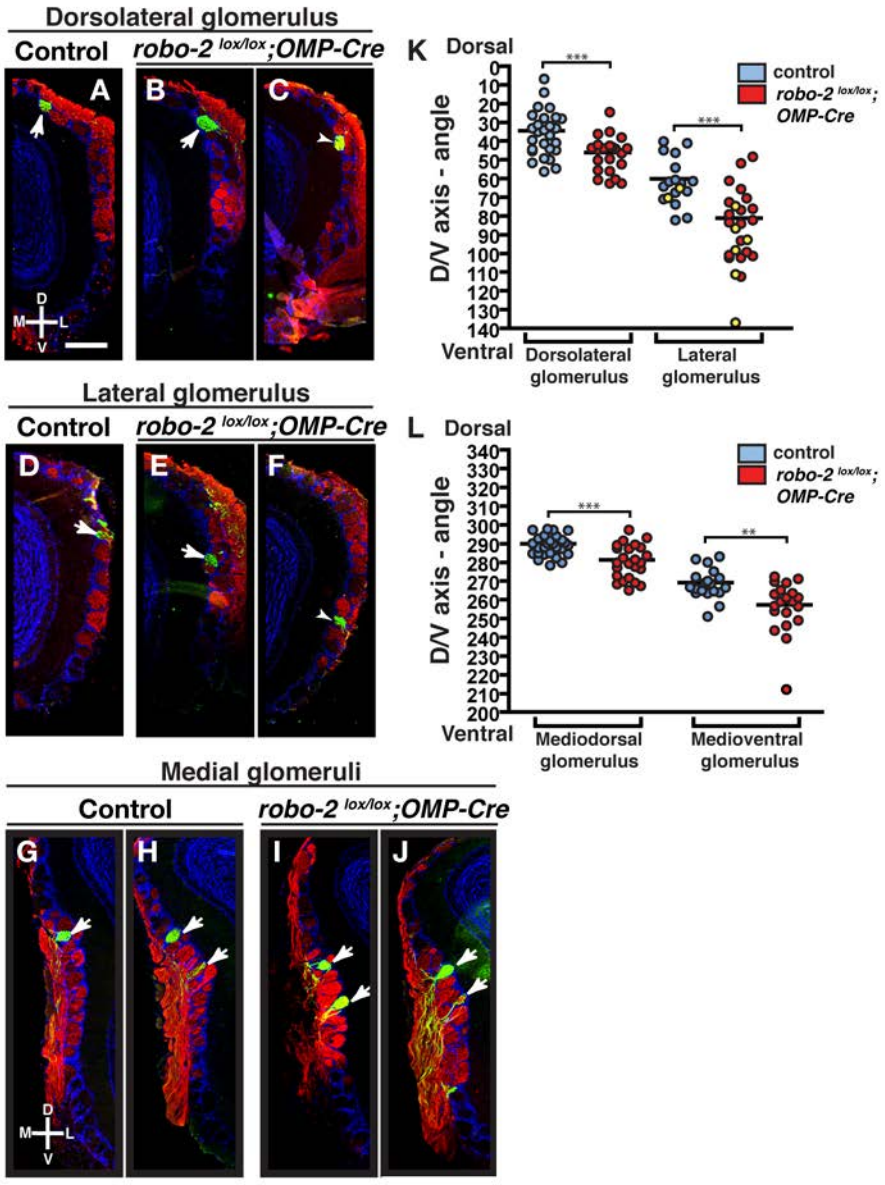


**Figure 3. Robo-2 is required for the targeting of MOR174-9-expressing OSN axons in the OB.**

A-J. Coronal sections of OBs isolated from control (A, D, G, H) and *robo-2*$^{lox/lox}$*;OMP-Cre; MOR174-9-tau-GFP* (B, C, E, F, I, J) mice stained with NQO-1 and GFP antibodies (A-J). NQO-1 antibodies stain axons of OSNs innervating the dorsal region of the OB. On the lateral side of the OB, a GFP-positive glomerulus is consistently observed in the

dorsal region of the OB (A, B, C) and a second GFP-positive glomerulus is observed in approximately half of the OBs analyzed (14/28 controls and 18/25 *robo-2$^{lox/lox}$; OMP-Cre*) (D, E, F). In addition, a third glomerulus was observed more ventrally in two OBs from control mice and in six OBs from *robo-2$^{lox/lox}$; OMP-Cre* mice (shown in yellow on the scatter plot in K). On the medial side of the OB, all OBs analyzed contained at least one GFP-positive glomerulus (G, H) and the majority of OBs analyzed (19/27 for controls and 19/25 for *robo-2$^{lox/lox}$; OMP-Cre* mice) contained two GFP-positive glomeruli (H, J). Furthermore, a few OBs analyzed contained an additional GFP-positive glomerulus (2/28 controls and 6/27 *robo-2$^{lox/lox}$; OMP-Cre*).

K, L. The relative positions of GFP-positive glomeruli in the dorso-ventral axis of the OB on the lateral and medial sides of the OB were assessed and represented on scatter plots (K, L). Parameters are shown as mean ± SEM. The mean location of glomeruli innervated by MOR174-9 expressing axons on both the lateral and medial sides of the OB is shifted ventrally in *robo-2$^{lox/lox}$; OMP-Cre*. Note that the additional glomeruli observed in some bulbs (represented in yellow) were not included in the calculation of the mean. Sections containing glomeruli located close to the mean angle are shown in panels A, B, D, E, G, H, I, and J. In panels C and F, sections with a more severe ventral shift in the location of the glomeruli are shown. Triple asterisk: $P<0.001$. Double asterisk: $P<0.01$. D, Dorsal; V, ventral; L, lateral; M, medial. Scale bar: 250μm.

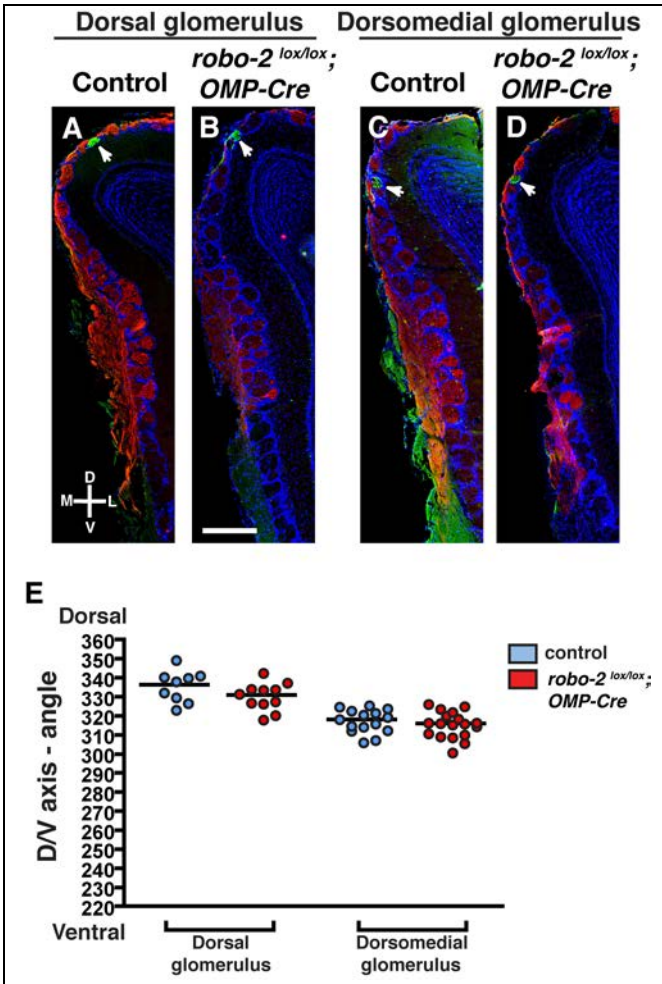


**Figure 4. MOR1-3-expressing OSN axons coalescence accurately in *robo-2*$^{lox/lox}$*; *OMP-Cre* mice.**

A-D. Coronal sections of OBs isolated from control (A, C) and *robo-2*$^{lox/lox}$*;OMP-Cre; MOR1-3-tau-lacZ* (B, D) mice stained with NQO-1 and β-galactosidase antibodies (A-D). A β-galactosidase positive glomerulus is consistently observed in the dorsomedial part of the OB in all mice analyzed (C, D). In addition, a second β-galactosidase positive glomerulus is observed on the dorsal part of the OB in approximately half of the OBs analyzed (9/17 controls and 12/20 *robo-2*$^{lox/lox}$*; OMP-Cre*) (A, B).

E. The relative positions of β-galactosidase-positive glomeruli in the dorsoventral axis of the OB was assessed and represented on a scatter plot. Parameters are shown as mean ± SEM. No significant change was observed in the mean location of MOR1-3 positive glomeruli in *robo-2$^{lox/lox}$; OMP-Cre* mice. Note that in panels A-D sections with glomeruli located approximately at the mean angle are shown. D, dorsal; V, ventral; L, lateral; M, medial. Scale bar: 500μm.

*Reduced innate avoidance behavior in robo-2$^{lox/lox}$; OMP-Cre mice*

The ability of mice to detect and respond to aversive odorants has been linked to the activation of glomeruli in the dorsal region of the OB: ablation of OSNs that innervate this region resulted in a loss of innate avoidance behavior in response to the predator odorant TMT, a component of fox feces, and to the aliphatic acid 2MB, a pungent odorant of spoiled food (Kobayakawa et al., 2007). Furthermore, specific deletion of OSNs innervating the DII region of the OB affected the innate avoidance behavior of mice in response to TMT but did not affect the response to 2MB acid, suggesting that the DII region plays a critical role in the response to TMT (Kobayakawa et al., 2007). To examine whether an accurate glomerular map in the dorsal part of the OB is required for the innate avoidance behavior of mice to TMT and 2MB acid, we performed olfactory preference and avoidance tests on the *robo-2$^{lox/lox}$; OMP-Cre* mice.

For the olfactory preference test, control and mutant mice were placed in the presence of filter paper scented with specific odorants including peanut butter, TMT or 2MB acid. Control and *robo-2$^{lox/lox}$; OMP-Cre* mice responded equally to peanut butter, spending the same amount of time investigating this attractive odorant (Figure 5 A). In

contrast, *robo-2*$^{lox/lox}$*; OMP-Cre* mice had reduced aversive responses to TMT, spending longer durations investigating the TMT-scented paper than control mice (Figure 5 A). Both control and *robo-2*$^{lox/lox}$*; OMP-Cre* mice responded similarly to the aversive odorant 2MB acid. These results therefore suggested that *robo-2*$^{lox/lox}$*; OMP-Cre* mice show a reduced responsiveness to TMT but not to 2MB acid.

We next assessed the innate avoidance behavior of *robo-2*$^{lox/lox}$*; OMP-Cre* mice to TMT and 2MB acid. The *robo-2*$^{lox/lox}$*; OMP-Cre* mice showed a selective decrease in avoidance behavior in response to TMT (Figure 5 B; Movie S1). In contrast, their avoidance response to 2MB acid was similar to control mice (Figure 5 B).

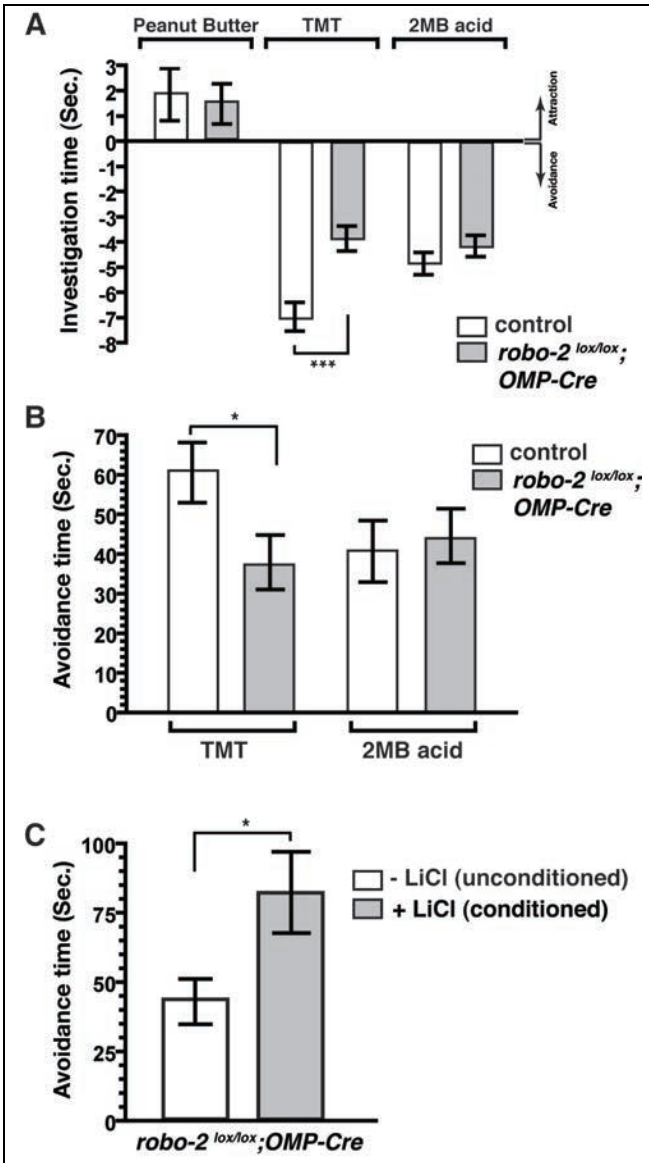


**Figure 5. Reduced avoidance behavior in response to TMT in *robo-2$^{lox/lox}$; OMP-Cre* mice.**

A. Innate olfactory preference test. The duration of time spent by a mouse investigating a filter paper scented with peanut butter, TMT, or 2MB acid was measured over a period of three minutes. The mean investigative time (sec +/- SEM) is shown for each odorant after subtraction of the mean investigative time for water for control (white bar) and *robo-2$^{lox/lox}$; OMP-Cre* (grey bar) mice. An investigative time for an odorant that is less than for

water is defined as an avoidance response. For control mice, n= 14 for peanut butter, 18 for TMT, and 14 for 2MB acid. For *robo-2*$^{lox/lox}$*; OMP-Cre* mice, n= 14 for peanut butter, 20 for TMT, and 14 for 2MB acid. Triple asterisk: P<0.001.

B. Innate olfactory avoidance tests. A test cage was subdivided into two regions (1:3) using a tape marker on the side of the cage. A scented filter paper was placed in the smaller partition and the duration of time spent by each animal in the larger partition of the cage was measured over a period of three minutes. The mean avoidance times (sec +/- SEM) for each test odorant is shown relative to the mean avoidance time for water for control (white bar) and *robo-2*$^{lox/lox}$*; OMP-Cre* (grey bar) mice. For TMT, n= 17 control and 19 *robo-2*$^{lox/lox}$*; OMP-Cre* mice. For 2MB acid, n= 12 control and 12 *robo-2*$^{lox/lox}$*; OMP-Cre* mice. Asterisk: P<0.05. See also Movie S1.

C. Avoidance test after LiCl conditioning. *robo-2*$^{lox/lox}$*;OMP-Cre* mice were aversively conditioned to TMT with a LiCl injection. Mean avoidance times (sec +/- SEM) of a filter paper scented with TMT for unconditioned mice (white bar) is compared to the mean avoidance time for conditioned mice (grey bar) over the three-minute test period. (n= 11 each for unconditioned and conditioned mice). Asterisk: P < 0.05.

Our observation of reduced avoidance behavior of *robo-2*$^{lox/lox}$*; OMP-Cre* mice in response to TMT suggests that responses mediated by the DII region of the OB are disturbed in these mice. Interestingly, responses mediated by the DI region, such as avoidance of 2MB acid, are unaltered in *robo-2*$^{lox/lox}$*; OMP-Cre* mice. In light of the defects observed in the targeting of MOR174-9 and M72 OSN axons in the DII region of the OB of *robo-2*$^{lox/lox}$*; OMP-Cre* mice, it is likely that OSNs expressing other ORs,

including those detecting TMT, are also mistargeted in this region. The reduced avoidance behavior to TMT observed in *robo-2$^{lox/lox}$; OMP-Cre* mice cannot be attributed to a decreased detection of TMT by OSNs since these mice can be conditioned for aversive reactions to TMT by injection of the irritant LiCl (Figure 5 c). It is therefore likely that inaccurate glomerular mapping underlies the behavioral defects observed in *robo-2$^{lox/lox}$; OMP-Cre* mice.

## Discussion

*Regulation of avoidance responses to TMT*

Processing of odorant information in the dorsal region of the OB has been associated with the modulation of innate behaviors in response to aversive and predator odorants. Innate behavior, in contrast to associative behavior, is independent of prior experience and learning and may therefore be hard-wired during development. Here we show that the pattern of coalescence of OSN axons into glomeruli of the DII region of the OB is critical for avoidance responses to the aversive odorant TMT.

We cannot completely exclude the possibility that changes in the wiring of the accessory olfactory system (AOS) may also be a factor in the reduced avoidance response to TMT observed in *robo-2$^{lox/lox}$; OMP-Cre* mice. Indeed we have previously reported that some basal vomeronasal sensory neurons erroneously innervate the anterior region of the accessory olfactory bulb (AOB) in these mice (Prince et al. 2009). TMT exposure induces c-fos activation in target regions of AOB mitral cells including the medial and basolateral amygdala (Day et al., 2004). In addition, TMT-induced responses are blocked by temporary inactivation of the medial amygdala supporting a role for the AOS in this

response (Muller and Fendt, 2006). Therefore, it remains possible that activation of these brain regions contributes to TMT avoidance responses in mice, but it is noteworthy that vomeronasal organ function is not required for this response (Papes et al., 2010).

The dorsal region of the OB is critical for avoidance behavior in response to TMT, but TMT also activates glomeruli in the ventral region of the OB (Kobayakawa et al., 2007). It is therefore possible that, in addition to the defects observed in the DII region, changes in the glomerular map in the ventral region of the OB may also contribute to the reduced avoidance response observed in *robo-2$^{lox/lox}$; OMP-Cre* mice. The future examination of connectivity in the ventral OB of *robo-2$^{lox/lox}$; OMP-Cre* mice as well as the generation of genetically-modified mice bearing a selective disruption of the glomerular map in the ventral OB will help address the role of this region in avoidance responses to TMT.

*Robo-2 in the wiring of the dorsal region of the olfactory bulb*

The formation of the glomerular map in the DII region of the OB is regulated in part by the axon guidance receptor Npn-1, which controls the anterior-posterior targeting of OSN axons within this region (Imai et al., 2009). Our results show that Robo-2 is required for the dorsal-ventral positioning of MOR174-9 innervated glomeruli as well as for the accurate coalescence of M72-expressing axons in the DII region of the OB. It is therefore likely that expression of Robo-2 and Npn-1, combined with the expression of specific ORs and cell adhesion molecules, can promote the coalescence of axons into specific glomeruli of this OB region. Our analyses suggest that Robo-2 is dispensable for the targeting of OSN axons in the DI region of the OB. However we cannot exclude the

possibility that residual levels of Robo-2 protein remain on these axons in *robo-2*$^{lox/lox}$*; OMP-Cre* mice early during development of these projections, and that this is perhaps sufficient to promote coalescence of these axons onto correct targets. We think this unlikely due to several observations. First, axons that project to the dorsal region of the OB do so prior to E14 but they remain in the nerve layer until the beginning of glomerulogenesis around E15 (Treloar et al., 1999; Treloar et al. 2009; Takeuchi et al., 2010). In *robo-2*$^{lox/lox}$*; OMP-Cre* mice, Robo-2 expression on OSN axons is already greatly reduced at E13 and mostly absent by E14, suggesting that Robo-2 expression is ablated before the coalescence of axons into glomeruli (Figure 2 I-K). Our observation that OMP is expressed by E13 in the majority, but not all, OSNs expressing a specific receptor (MOR1-3) that innervate the DI region may explain the residual expression of Robo-2 observed at that stage (Figure 2 Q-S). It remains formally possible that Cre-mediated ablation of Robo-2 in OSNs that innervate the DI region does not occur quite early enough to affect the targeting of these axons in *robo-2*$^{lox/lox}$*; OMP-Cre* mice. Nonetheless, the OMP-Cre-mediated *robo-2* gene excision provides a unique model to study the effects of selective disruption of the DII glomerular map on responses to aversive odorants.

Overall, our results indicate that formation of a precise glomerular map is essential for innate behavioral responses in mice, and suggest that the circuits regulating these responses exhibit limited plasticity to compensate for any miswiring that may take place during development.

**SUPPLEMENTAL FIGURE**

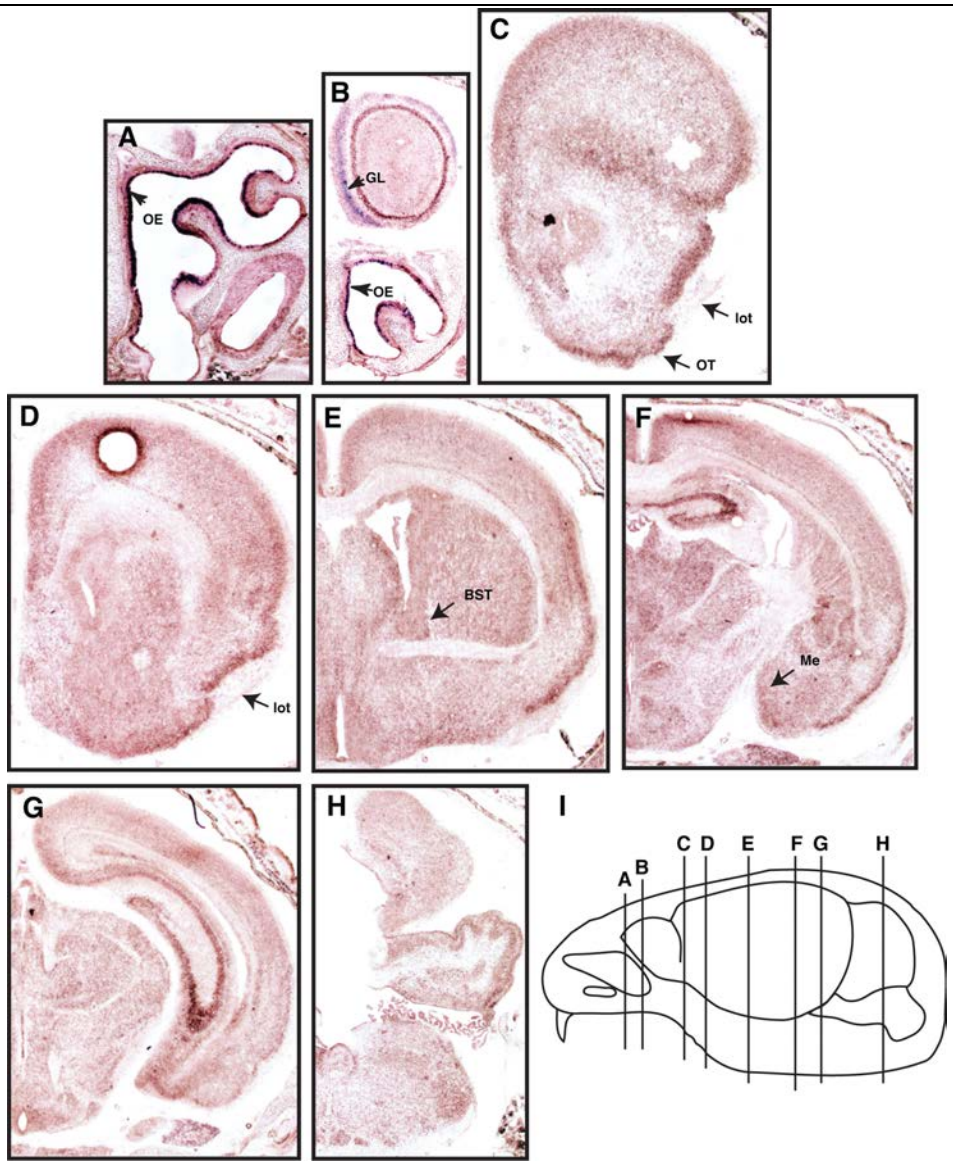


***Supplemental figure 1: Specificity of Cre-induced recombination in OMP-Cre mice.***

*An OMP-cre mouse was crossed with a Rosa-Stop-LacZ reporter mouse to examine cre-induced recombination in the OE and brain. LacZ expression in coronal sections of the nasal cavity or brain of a P0 mouse was detected by X-gal staining and sections were counterstained with eosin to facilitate identification of brain regions. LacZ expression (arrowhead) was detected in the OE and in the glomerular layer (GL) of the OB (A, B)*

*but not in other parts of the brain (C-H). The approximate locations of sections shown in A-H is presented in I. OT: olfactory tubercle. lot: lateral olfactory tract. BST: bed nucleus of the stria terminalis. Me: Medial amygdala.*

***Movie S1: Innate avoidance test in response to TMT.***

*This movie shows the response of control and robo-2$^{lox/lox}$; OMP-Cre littermates to a filter paper scented with the predator odor TMT. In contrast to the control mouse, which shows a freezing response, the robo-2$^{lox/lox}$; OMP-Cre mouse shows a reduced avoidance.*

*Supplemental experimental Procedures*

*Animals*

The *ROSA-26-LacZ* mouse line has been previously described [1].

*X-Gal staining*

For whole-mount X-Gal staining, three-month old adult mice were perfused transcardially with ice cold PBS containing 4% paraformaldehyde, 2 mM $MgSO_4$, and 5 mM EGTA. For X-Gal staining of sections, heads from P0 mice were immersion fixed in 4% paraformaldehyde, 2 mM $MgSO_4$, and 5 mM EGTA and cryoprotected in PBS containing 30% sucrose. 20μm sections were collected on slides and allowed to dry for one hour before processing. Both whole olfactory bulbs and brain sections were washed twice for 15 minutes in 0.1M phosphate buffer containing 2mM magnesium sulfate, 0.01% sodium deoxycholate, and 0.02% Nonidet P40 and processed for X-Gal staining.

Samples were incubated in 0.1M phosphate buffer containing 2mM magnesium sulfate, 0.01% sodium deoxycholate, and 0.02% Nonidet P40, 5mM $K_3Fe(CN)_6$, 5mM $K_4Fe(CN)_6$, and 1 mg/ml X-Gal for 1 hour to overnight at 37$^{o}$C.

*Supplemental reference*

1. Soriano P (1999) Generalized lacZ expression with the ROSA26 Cre reporter strain. Nat Genet. 21:70-71.

# CHAPTER 4

## Slit-1 and Robo-2 regulate the coalescence of subsets of OSN axons within the ventral region of the OB

Jin hyung Cho and Jean-François Cloutier

*Montreal Neurological Institute, McGill University, Montreal, Quebec, Canada*

**PREFACE**

This section explores the role of Slit-1 and Robo-2 in the segregation of OSN axons located in zone 1, 2 and 4 along the dorsal-ventral axis of the OB. As demonstrated in chapter 2 and 3, Robo-2 is expressed in a gradient manner in the OE where OSNs located in zone 1 express the most Robo-2 and OSNs located in zone 2, 3 and 4 display decreasing levels of expression. Since Robo-2 is required for the targeting of DII OSN axons to the dorsal region of the OB, I explored the role of its ligand, Slit-1 in the innervation of DII OSN axons. Additionally, I looked at the requirement of Slit-1 and Robo-2 in the segregation of OSN axons projecting from OSNs located in zone 2 and 4 of the OE to the OB. Here I report that Slit-1 and Slit-2 are expressed in OSN axons and I demonstrate that Slit-1 and Robo-2 are required for the accurate coalescence of OSN axons located in zone 2 and 4 to the OB. In this study, we provide evidence that Slit-1 and Robo-2 are essential for the segregation of an accurate glomerular map in the ventral region of the OB.

*Acknowledgements*

We thank Marc Tessier-Lavigne for providing the *slit-1* and *slit-2* mutant mice, Bill Andrews and John Parnavelas for the floxed *robo-2* mouse, and Tyler Cutforth for the OMP-Cre, MOR28-tau-lacZ, and P2-tau-lacZ mice. We thank Donna Lee for help

with glomeruli counting. This work was supported by the Canadian Institutes for Health Research. J.H.C. holds a studentship from the Fonds de Recherche en Santé du Québec. J.-F.C. holds a Canada Research Chair in developmental neurobiology.

**ABSTRACT**

Olfactory sensory neurons (OSNs) project their axons to second order neurons in the olfactory bulb (OB) to form a precise glomerular map and these stereotypic connections are crucial for accurate odorant information processing by animals. To form these connections, olfactory sensory neuron (OSN) axons respond to axon guidance molecules that direct their growth and coalescence. We have previously implicated the axon guidance receptor Robo-2 in the accurate coalescence of OSN axons within the dorsal region of the OB (Cho et al., 2011). Herein, we have examined whether Robo-2 and its ligands, the Slits, contribute to the formation of an accurate glomerular map within more ventral regions of the OB. We have ablated expression of Robo-2 in OSNs and assessed the targeting accuracy of axons expressing either the P2 or MOR28 olfactory receptors, which innervate two different regions of the ventral OB. We show that P2-positive axons, which express Robo-2, coalesce into glomeruli more ventrally and form additional glomeruli in the OB of *robo-2*$^{lox/lox}$*;OMP-Cre* mice. Interestingly, although MOR28-positive OSNs do not express Robo-2, a reduced number of MOR28-positive glomeruli is observed in the OB of *robo-2*$^{lox/lox}$*;OMP-Cre* mice. We also demonstrate that Robo-2-mediated targeting of P2 axons along the dorsoventral axis of the OB is dependent on Slit-1 expression and propose that, in addition to target-derived Slits, OSN-derived Slits may regulate axonal targeting in the OB. Taken together, our

results demonstrate that Slit-1 and Robo-2 are required for the formation of an accurate glomerular map in the ventral region of the OB.

## INTRODUCTION

Mice can smell and discriminate a vast number of odorants with diverse chemical structures. The detection of these odorants and subsequent processing of the stimulus play important roles in the regulation of behaviors that are essential for survival including avoidance of aversive odorants and food foraging. Odor recognition takes place in the olfactory epithelium (OE) where each olfactory sensory neuron (OSN) expresses one of around 1200 functional olfactory receptors (ORs) that can bind to different odorant molecules (Buck and Axel, 1991; Zhao et al., 1998; Zhang and Firestein, 2002). This olfactory information is then relayed to the central nervous system through the olfactory bulb (OB) where axons of OSNs make synaptic connections with dendrites of second-order neurons located in neuropile structures termed glomeruli. To accurately represent all odor information coming from a large number of ORs, OSNs expressing a single OR project their axons to approximately two specific glomeruli out of an estimated 1800 glomeruli in each OB (Royet et al., 1988; Ressler et al., 1993; Vassar et al., 1993; Mombaerts et al., 1996). Hence, odor information received in the OE can be converted into an activated glomerular map in the OB that is further processed in higher structures of the brain (Mori et al., 2006; Johnson and Leon, 2007; Matsumoto et al., 2010). The formation of an accurate glomerular map is essential for the regulation of innate responses in mice including avoidance of aversive odorants. Mice bearing an ablation of OSNs that innervate the dorsal region of the OB do not avoid aversive odorants such as

trimethyl-thiazoline (TMT) and 2-methyl butyric acid (2MB) (Kobayakawa et al., 2007). Furthermore, disruption of the glomerular map within the DII domain of the OB leads to reduced avoidance responses to the predator odorant TMT (Cho et al., 2011). Whether formation of an accurate glomerular map within the ventral region of the OB is also required for innate responses remains to be determined.

To provide an accurate representation of odorant stimuli, OSNs form highly stereotyped connections with second-order neurons within the OB. OSNs located in four spatially distinct yet overlapping regions of the OE extend their axons to the dorsal and ventral regions of the OB (Royet et al., 1988; Strotmann et al., 1992; Ressler et al., 1993; Vassar et al., 1993; Strotmann et al., 1994; Mombaerts et al., 1996; Sullivan et al., 1996; Tsuboi et al., 1999; Norlin et al., 2001; Iwema et al., 2004; Miyasaka et al., 2005). The dorsal region can be subdivided into two domains, $D_I$ and $D_{II}$, that are innervated by OSNs expressing type I and type II ORs respectively (Kobayakawa et al., 2007; Bozza et al., 2009). There is strong evidence that the position of OSN cell bodies within the OE correlates with the location of glomeruli innervated along the dorsoventral axis of the OB (Astic and Saucier, 1986; Saucier and Astic, 1986; Miyamichi et al., 2005). OSNs residing in the dorsomedial part of the OE project axons to the dorsal region of the OB while OSNs located in the ventrolateral part of the OE extend their axons to the most ventral region of the OB. Two families of axon guidance cues have been implicated in the regulation of axonal targeting in the dorsal-ventral axis of the OB. Robo-2 is necessary for the coalescence of subsets of axons that innervate the dorsal region of the OB (Cho et al., 2007). In contrast, the secreted semaphorin Sema3F and its receptor, Neuropilin-2 (Npn-2) promote the segregation of axons projecting from OSNs located in

the vento-lateral part of the OE to the most ventral region of the OB (Takahashi et al., 2010; Takeuchi et al., 2010).

Other families of axon guidance molecules have also been implicated in directing axonal targeting in the anteroposterior and mediolateral aspects of the OB. Ephrin/Eph A family members control the coalescence of OSN axons in the anteroposterior axis through differential expression of Ephrins in OSNs regulated by OR-derived cAMP (Cutforth et al., 2003; Imai et al., 2006; Serizawa et al., 2006; Col et al., 2007; Zou et al., 2007; Kaneko-Goto et al., 2008). OR-mediated signaling also regulates expression of the Sema3A receptor, Npn-1, whose differential expression in OSN axons promotes the segregation of populations of axons within olfactory nerve bundles and directs anteroposterior targeting (Imai et al., 2006). Sema 3A also controls the mediolateral segregation of OSN axons within the OB (Schwarting et al., 2000; Schwarting et al., 2004). Additional molecules, including cell adhesion molecules and growth factors, have also been implicated in the formation of the glomerular map in the OB (Serizawa et al., 2006; Kaneko-Goto et al., 2008; Scolnick et al., 2008).

While clear alterations in the targeting of OSN axons that express high levels of Robo-2 and innervate the DII region of the OB have been reported in Robo-2 mutant mice (Cho et al. 2011), it remains to be determined whether glomerular map formation in the ventral region of the OB is also affected in these mice. Furthermore, whether Slits regulate Robo-2-dependent coalescence of axons in the OB remains unknown. We have examined the accuracy of coalescence of OSNs expressing either the P2 or MOR28 ORs in mice lacking Slit-1 or Robo-2 expression. We show that Slit-1 and Robo-2 are required for accurate coalescence of P2-expressing OSN axons but are mostly dispensable for the

coalescence of MOR28-expressing axons into specific glomeruli. Furthermore, in contrast to Robo-2, Slit-1 is not required for the glomerular coalescence of OSNs axons in the DII region of the OB and Slit-1$^{-/-}$ mice show robust avoidance responses to the predator odorant TMT. Our results therefore show that Slit-1-Robo-2 signaling can direct the coalescence of subsets of OSN axons in the ventral region of the OB and suggest that other Slit family members may be involved in the Robo-2-dependent targeting of OSN axons in the dorsal region of the OB. In addition, our results indicate that disruption of the glomerular map in the ventral region of the OB does not affect innate responses to aversive odorants.

## METHODS AND MATERIALS

*Animals*

Embryonic day 18 (E18) mouse embryos were obtained from timed-pregnant females purchased from Charles River (Saint-Constant, Quebec, Canada). The floxed *robo-2* (Lu et al., 2007), OMP-Cre mice (Eggan et al., 2004), P2-ires-tau-lacZ (Mombaerts et al., 1996), MOR28-ires-tau-LacZ (Barnea et al., 2004), and MOR174-9-ires-GFP (Cho et al., 2011; Sosulski et al., 2011) have been described previously. For all analyses performed, *robo-2*$^{+/+}$*; OMP-Cre* and *robo-2*$^{+/lox}$*; OMP-Cre* mice; *slit-1*$^{+/+}$ *or slit-1*$^{+/-}$ were used as controls and compared to either *robo-2*$^{lox/lox}$*; OMP-Cre* mice or *slit-1*$^{-/-}$ mice. All mice were in a mixed C57Bl6-129J background.

*Fluorescent* In situ *hybridization*

Nonradioactive, digoxigenin (DIG)-labeled or fluorescein (Flu)-labeled cRNA probes with either sense or antisense orientation were synthesized by *in vitro* transcription according to the recommendations of the manufacturer (Roche, Mannheim, Germany). Probes were synthesized from cDNA clones encoding *robo-2* (Brose et al., 1999), *MOR174-9* (Cho et al., 2011), *P2(MOR263-5)* or *MOR28(MOR244-1)*. To prepare *P2 and MOR28* specific cRNA probes, DNA fragments of the coding sequences were PCR amplified from C57BL/6 genomic DNA and subcloned into the pBluescript vector. The primer sets used were as follows: *P2 (MOR263-5),* 5'-TGTCAGGGAATTTATC-3' and 5'-AGCCTTCACCTCATTA-3'; *MOR28 (MOR244-1)*, 5'-GGAAAAGGCTGTCCTCATCA-3' and 5'-GGGTTCAGCAGAGGGGTTAT-3'. Sections of OE were processed as described previously (Ishii et al., 2004; Prince et al., 2009).

*Immunohistochemical procedures and analysis of the position of OR-positive glomeruli in adult olfactory bulbs*

Adult mice (3 months old) were anesthetized and perfused transcardially with ice-cold PBS containing 4% paraformaldehyde. Brains were processed as described previously and all sections were collected on microscope slides over the complete rostrocaudal axis (Cho et al., 2007). Sections were immunostained with NQO-1 (1:100; Abcam, Cambridge, MA), GFP (1:250; Invitrogen, Carlsbad, CA or Novus, Littleton, CO), β-gal (1:250; MP biomedicals, Solon, OH), Robo-2 (1:350;(Cho et al., 2007)), or OCAM (1:100; BD sciences) antibodies and counterstained with Hoechst. The position of GFP-

or β-gal-positive glomeruli in the OB was determined using an NIH Image J plug-in as previously described (Schaefer et al., 2001; Cho et al., 2007). Briefly, images of sections containing GFP- or β-gal-positive glomeruli were imported into Adobe Photoshop software (Adobe Systems, Mountain View, CA) for mapping of glomeruli. The radial angle of each GFP- or β-gal-positive glomerulus was measured after setting the origin for each section. The origin was set at one-third the distance between the mitral cell layer in the dorsal region of the OB and the mitral cell layer in the ventral region of the OB. A scatter plot was constructed that shows the location of GFP- or β-gal-positive glomeruli in all OBs analyzed in the dorsoventral axis with degrees (radial angle) on the y-axis. The mean radial angle for each identified glomerulus was measured and compared between control and *robo-2*$^{lox/lox}$*;OMP-Cre* or *slit-1*$^{-/-}$ mice using an unpaired t-test.

*Determination of the total number of glomeruli in olfactory bulbs*

Coronal sections (20μm thick) through the whole OB of adult mice were processed for Hoechst straining. The total number of glomeruli, as defined by an area surrounded by periglomerular cell bodies, was counted for all sections obtained. Since the diameter range of glomeruli in the mouse OB is ~50-120μm (Royet et al. 1988), we considered the average diameter of a glomerulus to be 85μm in our analysis. Hence the total number of glomeruli counted was divided by a factor of 4.25 (85μm average/20μm per section counted).

*Innate olfactory avoidance test*

This test was performed as previously described (Cho et al., 2011). Three month old adult control and *slit-1*$^{-/-}$ littermate mice were used only once for testing. The test cage was

visually divided into two compartments (1:3) using masking tape on the outside of the cage to discern the two areas during analysis. Mice were habituated to the experimental environment for 30 min and then to the test cage for 10 min. After habituation, a filter paper (2 X 2 cm) scented with water was introduced in the part of the cage containing the smaller partition and the duration of time spent by the mouse in the larger part of the cage measured over a 3-minute test period. The filter paper was taken out, replaced with a filter paper scented with test odorant and the duration of time spent by the mouse in the large compartment of the cage was measured. The time spent in the large compartment with the water control was subtracted from the value obtained with odorants to give the recorded avoidance time. Statistical analyses were performed using unpaired t-tests. Odorants used for the avoidance test was TMT (7.65M).

## RESULTS

*Expression of Robo-2 and Slits in OSNs*

During development of olfactory projections, Robo-2 expression in OSNs is graded across the olfactory epithelium with high levels of Robo-2 in OSNs located in the dorsomedial region and low levels in OSNs from the ventrolateral region of the OE (Cho et al., 2007, Fig. 1A). We examined whether Robo-2 is expressed in three specific populations of OSNs expressing the ORs MOR174-9, P2, or MOR28, which innervate different regions along the dorso-ventral axis of the OB (Fig. 1E). While MOR174-9-expressing axons innervate the dorsal region, P2 and MOR28-expressing axons project to two ventral regions of the OB. *In situ* hybridization analyses demonstrated that both MOR174-9 and P2 positive OSNs co-express *robo-2*, while MOR28-expressing OSNs do

not express robo-2 (Figs. 1A, C, D). In addition, immunostaining of coronal sections of OB from mice expressing tau-GFP or tau-lacZ under the control of the MOR174-9, P2, or MOR28 promoters revealed that Robo-2 protein is expressed on MOR174-9 and P2-positive axons (Figs. 1F-I) but absent from MOR28-positive axons (Figs. 1J-K). Expression of Robo-2 in MOR174-9-positive axons is essential for their accurate coalescence in the dorsal region of the OB (Cho et al. 2011). The expression of Robo-2 in P2-expressing OSNs suggest that, in addition to controlling coalescence of axons in the dorsal OB, Robo-2 may also contribute to the targeting of subsets of axons within the ventral OB.

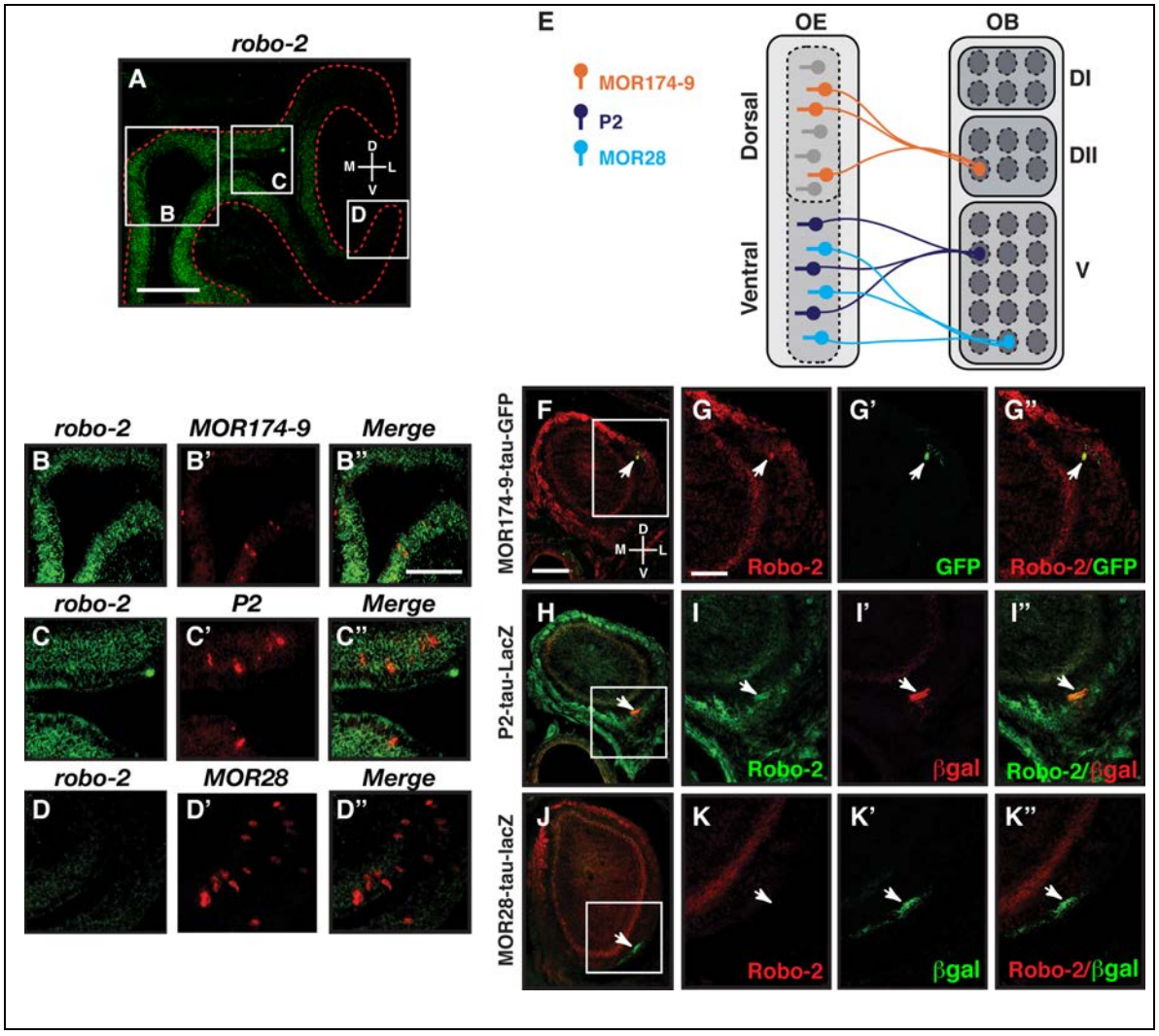

**Figure 1. Robo-2 expression in OSNs.**

A-D". Fluorescent *in situ* hybridization of adjacent coronal sections of olfactory epithelium isolated from E18 embryos with a cRNA probe specific for *robo-2* (A-D, B", C'', D"), *MOR174-9* (B', B"), *P2* (C', C") and *MOR28* (D', D"). High magnification views of regions of the OE corresponding to insets in panel A from different sections are shown in B, C, and D. *robo-2* is expressed in a gradient in the OE with highest levels of expression detected in the dorsomedial regions of the OE and lowest levels of expression in the lateral region as we have previously reported (A) (Cho et al., 2007). *Robo-2* is expressed in *MOR174-9*- and *P2*-expressing OSNs but not in *MOR28*-positive OSNs (B", C", D"). D, dorsal; V, ventral; L, lateral; M, medial. Scale bar: 250μm; inset 100μm.

E. Schematic representation of the glomerular targeting of MOR174-9, P2, and MOR28-expressing axons along the dorsoventral axis of the OB.

F-K". Coronal sections of OBs isolated from P0 pups expressing *MOR174-9-tau-GFP* (F-G"), *P2-tau-LacZ* (H-I"), or *MOR28-tau-GFP* (J-K") were stained with Robo-2 (F, G, G", H, I, I", J, K, K") and GFP (F, G', G") or β-galactosidase antibodies (H, I', I", J, K', K"). High magnification views of the insets in panels F, H, and J are shown in G-K". Robo-2 is expressed on axons innervating MOR174-9 and P2-positive glomeruli but not on axons in MOR28-positive glomeruli. D, dorsal; V, ventral; L, lateral; M, medial. Scale bar: 250μm; inset 50μm.

We have previously shown that Robo-2 ligands, the Slits, are expressed in the developing OB and contribute to preventing dorsally projecting axons from innervating the ventral region of the OB (Cho et al. 2007). The expression of Slits in the developing OB along with the defects observed in the targeting of OSN axons in *slit-1*$^{-/-}$ suggest that Robo-2-expressing axons respond to Slits secreted within the OB (Cho et al., 2007). However, it remains possible that expression of Slits in OSNs and in their axons could contribute to the guidance of Robo-2-expressing axons innervating the OB. In keeping with this possibility, another secreted repellent, Sema3F, is expressed by axons

innervating the dorsal part of the OB which prevents Npn-2 expressing OSN axons that innervate the ventral OB from projecting to the dorsal region (Takeuchi et al. 2010).

We therefore examined the pattern of expression of Slit-1 and Slit-2 in OSNs by taking advantage of the fact that the specific gene-targeting strategy employed to create *slit-1* and *slit-2* mutant alleles results in expression of GFP under the control of their respective promoters and in the transport of GFP along OSN axons (Nguyen-Ba-Charvet et al, 2008). Our immunostaining analyses revealed that GFP expression is mostly restricted to OCAM-positive OSN axons that project to the ventral region of the OB in *slit-1*$^{+/GFP}$ and *slit-2*$^{+/GFP}$ mice (Figs. 2A-O). In contrast, OSN axons expressing the highest levels of Robo-2 and that project to the dorsal OB, do not express significant levels of GFP (Figs. 2A-C). The segregated expression of Slit-1 and Slit-2 in OSNs that innervate the ventral region of the OB raises the possibility that secretion of Slits by OSN axons, in addition to Slits secreted by the OB, may contribute to the targeting of these axons in the OB.

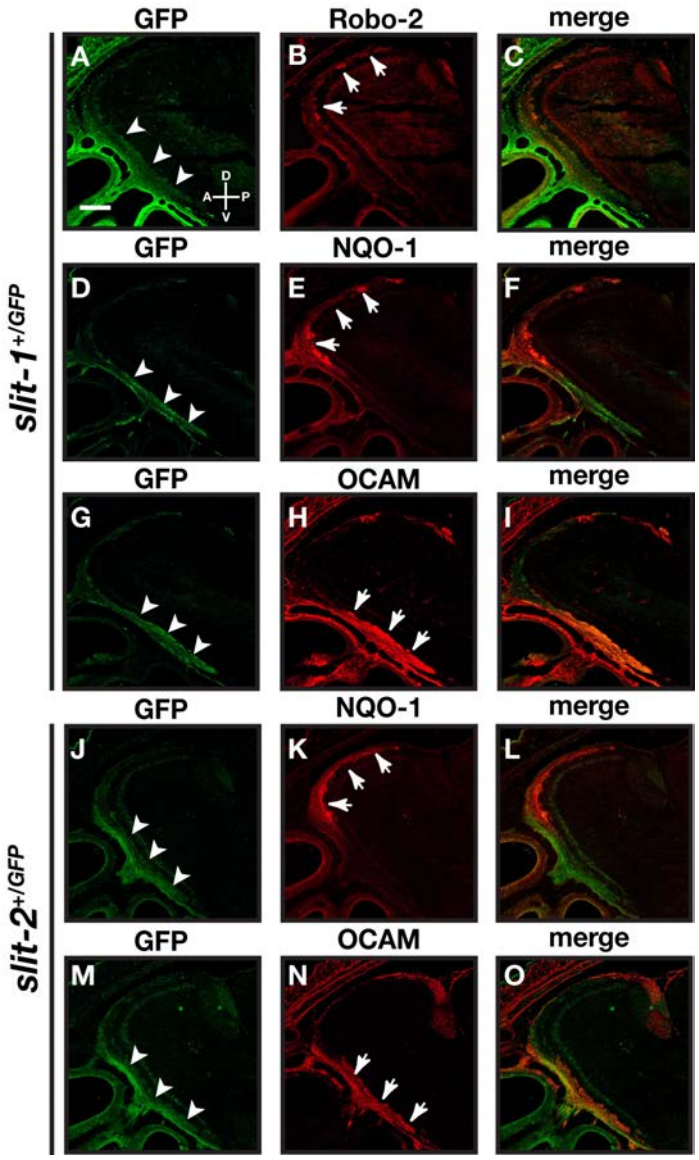


**Figure 2. Slit-1 and Slit-2 are expressed in OSNs projecting axons to the ventral region of the OB.**

Parasagital sections of olfactory bulbs from post-natal day P0 *slit-1*$^{+/GFP}$ (A-I) and *slit-2*$^{+/GFP}$ (J-O) mice stained with either anti-GFP (A, C, D, F, G, I, J, L, M, O) anti-Robo-2 (B, C), anti-OCAM (H, I, N, O), or anti-NQO-1 (E, F, K, L). In *slit-1*$^{+/GFP}$ mice, GFP-expressing axons (arrowheads) are restricted to the ventral region of the OB (A, C, D, F, G, I) while Robo-2 expressing axons (arrows) target to the rostrodorsal region of the OB

(B, C). Ventrally-projecting OCAM-expressing axons (arrows) are positive for GFP (G-I) while dorsally projecting NQO1-expressing axons (arrows) are not (D-F). As observed in *slit-1*$^{+/GFP}$ mice, GFP expressing axons (arrowheads) are restricted to the ventral region of the OB and express OCAM (arrows) in *slit-2*$^{+/GFP}$ mice (J, L, M, N, O). D, dorsal; V, ventral; A, anterior; P, posterior. Scale bars: 250μm.

*Slit-1 is not required for the coalescence of MOR174-9-expressing axons*

We have previously shown that Robo-2 expression is required for the glomerular targeting of MOR174-9 axons in the dorsal region of the OB and that changes in the glomerular map in this region leads to reduced avoidance behavior to the predator odorant TMT (Cho et al., 2011). To examine whether Slit-1 contributes to the Robo-2-mediated coalescence of this population of axons, we examined these projections in *slit-1* mutant mice. *Slit-1* mice were crossed with mice expressing the marker protein tau-GFP in OSNs expressing the OR MOR174-9. We quantified the location of MOR174-9-positive glomeruli in the OBs of control and *slit-1*$^{-/-}$ mice by immunostaining consecutive coronal sections of the OB with GFP antibodies. In controls and *slit-1*$^{-/-}$*; MOR174-9-GFP* mice, one or two glomeruli were detected on both the medial and lateral sides of the OB (Figs. 3A-J). Examination of the location of MOR174-9 glomeruli did not reveal any significant change between the controls and *slit-1*$^{-/-}$ mice (Figs. 3A-J). Furthermore, in contrast to Robo-2 mutant mice, *slit-1*$^{-/-}$ mice showed normal avoidance behavior in response to TMT (Fig. 3O, Cho et al, 2011). These findings suggest that other Slit ligands may contribute to the Robo-2 dependent coalescence of MOR174-9 axons in the OB. Unfortunately, the early lethality of compound Slit-1;Slit-2 and of most Slit-1;Slit-3

mutants prevent us from examining the role of other Slit ligand in mediating accurate coalescence of axons in the dorsal OB.

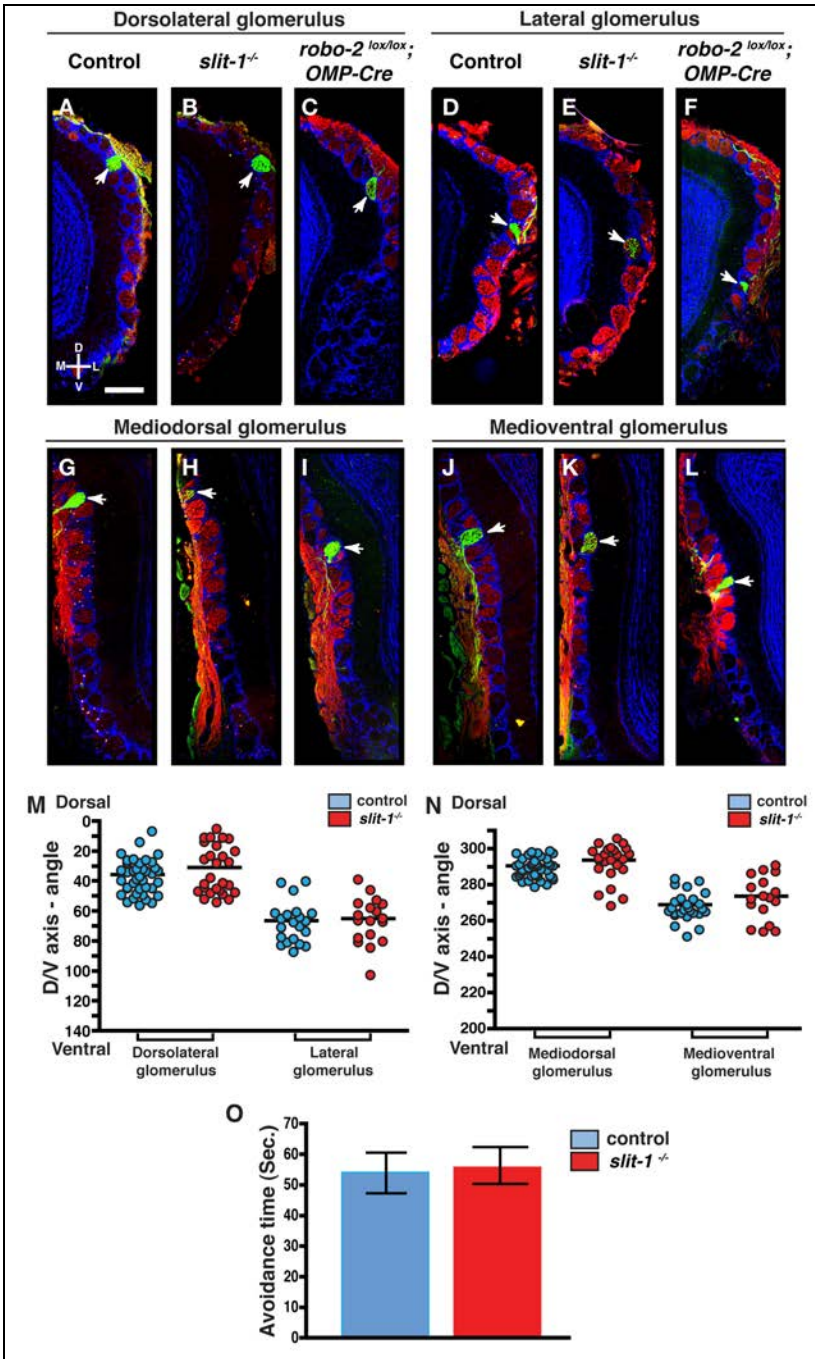


**Figure 3. Slit-1 is not required for the targeting of MOR174-9-expressing OSN axons to the dorsal OB.**

Coronal sections of OBs isolated from control (A, D, G, J), *slit-1*$^{-/-}$*; MOR174-9-tau-GFP* (B, E, H, K), and *robo-2*$^{lox/lox}$*;OMP-Cre; MOR174-9-tau-GFP* (C, F, I, L) mice were stained with NQO-1 and GFP antibodies (A-L). NQO-1 antibodies stain axons of OSNs innervating the dorsal region of the OB. On the lateral side of the OB, a GFP-positive glomerulus is consistently observed in the dorsal region of the OB (A-C) and a second GFP-positive glomerulus is observed in approximately half of the OBs analyzed (21/38 controls and 18/24 Slit-1$^{-/-}$) (D-F). On the medial side of the OB, all OBs analyzed contained at least one GFP-positive glomerulus (G-I) and the majority of OBs analyzed (26/37 for controls and 17/24 for Slit-1$^{-/-}$) contained an additional GFP-positive glomerulus (J-L). Sections from *robo-2*$^{lox/lox}$*;OMP-Cre; MOR174-9-tau-GFP* mice (C, F, I, L) are shown as a reference to compare the location of MOR174-9-positive glomeruli in these mice to *slit-1*$^{-/-}$ mice. A detailed analysis of these projections in *robo-2*$^{lox/lox}$*;OMP-Cre; MOR174-9-tau-GFP* has previously been reported (Cho et al., 2011). The relative positions of GFP-positive glomeruli in the dorsoventral axis of the OB on the lateral and medial sides of the OB in control and *slit-1*$^{-/-}$ mice are represented on scatter plots (M, N). Parameters are shown as mean ± SEM. No significant change was observed in the mean location of MOR174-9 expressing axons on both the lateral and medial sides of the OB in *slit-1*$^{-/-}$mice. D, dorsal; V, ventral; L, lateral; M, medial. Scale bar: 250μm.

O. Innate olfactory avoidance test. A test cage was divided into two regions (1:3) using a tape marker on the side of the cage. A scented filter paper was placed in the smaller partition and the duration of time spent by each animal in the larger partition of the cage was measured over a period of three minutes. The mean avoidance times (sec +/- SEM)

for TMT is shown relative to the mean avoidance time for water for control (blue) and *slit-1*$^{-/-}$ (red) mice. n=13 control and 15 *slit-1*$^{-/-}$ mice.

*Robo-2 and Slit-1 control the coalescence of P2-expressing axons in the ventral OB*

To address whether Robo-2 directs the coalescence of axons in the ventral region of the OB, we examined the targeting accuracy of P2-expressing OSN axons in mice carrying a *robo-2* deletion in OSNs. A mouse containing a *robo-2* floxed allele was crossed with mice expressing the Cre recombinase under the control of the olfactory marker protein (OMP) promoter and a marker protein (tau-lacZ) in P2-expressing OSNs. We have previously shown that Robo-2 expression is efficiently ablated in OSNs in *robo-2*$^{lox/lox}$*;OMP-Cre* (Cho et al., 2011). In control animals, one or two P2-positive glomeruli were observed on both the medial and lateral side of the OB (Figs. 4A, C, F). In both control and *robo-2*$^{lox/lox}$*; OMP-Cre* mice, one subset of P2 positive glomeruli on the lateral part of the OB appear to coalesce accurately in the same region of the OB (Figs. 4A-D, H). In contrast, a second subset of P2 glomeruli that are located slightly more ventrally in the OB of control animals showed a significant shift towards the ventral region in *robo-2*$^{lox/lox}$*; OMP-Cre* mice (Figs. 4C, D, E, H). Additionally, P2-positive glomeruli located on the medial part of the OB show an overall ventral shift in their location in *robo-2*$^{lox/lox}$*; OMP-Cre* mice when compared to controls (Figs. 4F, G, I). Interestingly, we observed a significant increase in the total number of P2-positive glomeruli present on each side of the OB in *robo-2*$^{lox/lox}$*; OMP-Cre* mice (Table 1).

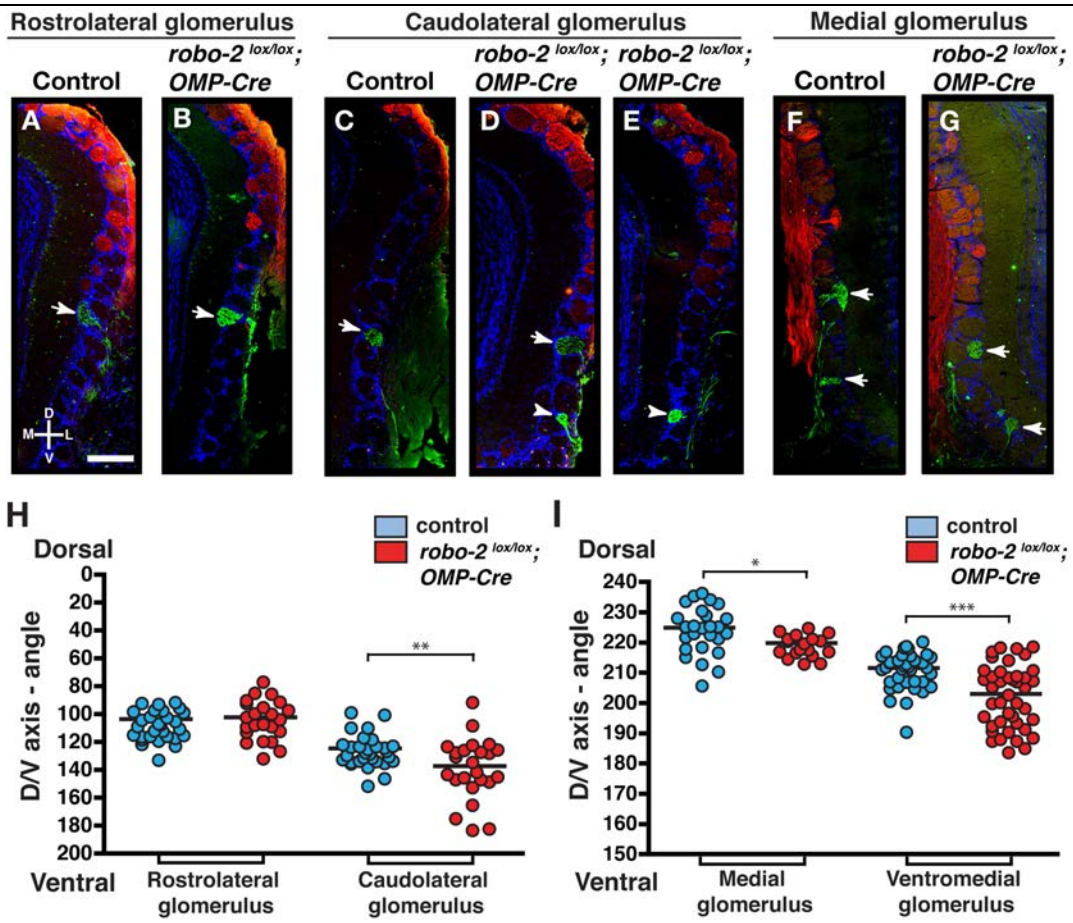


**Figure 4. Robo-2 controls the targeting of P2-expressing OSN axons in the OB.**

Coronal sections of OBs isolated from control (A, C, F) and *robo-2$^{lox/lox}$;OMP-Cre; P2-tau-lacZ* (B, D, E, G) mice were stained with NQO-1 and β-galactosidase antibodies (A-G). A β-galactosidase positive glomerulus (arrows) is consistently observed on the lateral side of the OB in all mice analyzed (A, B). In addition, a second β-galactosidase positive glomerulus is observed more caudally on the lateral side (arrows) of the OB (20/35 controls and 17/20 *robo-2$^{lox/lox}$;OMP-Cre; P2-tau-lacZ*) (C, D, E) in the majority of mice analyzed. Additional glomeruli are also observed more ventrally (arrowhead) in a subset of OB analyzed from *robo-2$^{lox/lox}$;OMP-Cre; P2-tau-lacZ* mice (8/20). On the medial side of the OB, all OBs analyzed contained at least one β-galactosidase-positive glomerulus

and the majority of OBs analyzed (21/35 for controls and 18/20 for *robo-2$^{lox/lox}$;OMP-Cre; P2-tau-lacZ* mice) contained two β-galactosidase-positive glomeruli (F, G). Additional glomeruli could also be observed in the ventrolateral region of the OB in the majority of OB analyzed from *robo-2$^{lox/lox}$;OMP-Cre; P2-tau-lacZ* mice (16/20).

The relative positions of β-galactosidase-positive glomeruli in the dorsoventral axis of the OB on the lateral and medial sides are represented on scatter plots (H, I). Parameters are shown as mean ± SEM. The mean location of caudolateral, medial, and ventromedial P2 glomeruli is shifted ventrally in *robo-2$^{lox/lox}$;OMP-Cre; P2-tau-lacZ* mice. Note that in panels A, B, C, D, F, and G, sections with glomeruli located approximately at the mean angle are shown. Triple asterisk: P<0.001. Double asterisk: P<0.01. Single asterisk: P<0.02. D, dorsal; V, ventral; L, lateral; M, medial. Scale bar: 250μm.

| | Control | | | *robo-2$^{lox/lox}$; OMP-Cre* | | | *slit-1$^{-/-}$* | | |
|---|---|---|---|---|---|---|---|---|---|
| | # of glomeruli | N (# of OB) | P | # of glomeruli | N (# of OB) | P | # of glomeruli | N (# of OB) | P |
| Total # of glomeruli/OB | 1725 ± 27.25 | 16 | | 1672 ± 27.94 | 14 | | 1714 ± 65.28 | 14 | |
| P2-positive/Lateral | 1.71 ± 0.127 | 35 | P =0.0063 | 2.35 ± 0.196 | 20 | P =0.0063 | 1.96 ± 0.165 | 24 | |
| P2-positive/Medial | 1.76 ± 0.125 | 37 | P <0.0001 | 3.15 ± 0.233 | 20 | P <0.0001 | 1.89 ± 0.115 | 26 | |
| Sp1-positive/Lateral | 1.72 ± 0.109 | 29 | | 1.67 ± 0.114 | 18 | | 1.55 ± 0.127 | 22 | |
| Sp1-positive/Medial | 1.92 ± 0.123 | 26 | P =0.0027 | 1.37 ± 0.114 | 19 | P =0.0027 | 1.79 ± 0.120 | 24 | |

**Table 1: Number of P2 and MOR28 glomeruli in control, *robo-2$^{lox/lox}$;OMP-Cre*, and *slit-1$^{-/-}$* mice.**

Values are presented as mean +/- SEM; Data was analyzed for statistical significance using unpaired t-tests. P values are shown for statistically significant differences.

To determine whether Slits direct the Robo-2-dependent coalescence of P2-expressing axons, we examined the location of P2 glomeruli in *slit-1$^{-/-}$* mice. As observed in *robo-2$^{lox/lox}$; OMP-Cre* mice, the location of P2-positive glomeruli in the dorsolateral

region of the OB is unchanged in *slit-1*$^{-/-}$ mice (Figs. 5A, B, E), while the location of P2-positive glomeruli in the ventrolateral region of the OB is shifted ventrally (Figs. 5C, D, E). Examination of the location of P2 glomeruli on the medial side of the OB also revealed an overall ventral shift in *slit-1*$^{-/-}$ mice (Figs. 5F-J). However, in contrast to *robo-2*$^{lox/lox}$*; OMP-Cre* mice, we did not observe an increase in the number of P2-positive glomeruli in the OBs of *slit-1*$^{-/-}$ mice. Hence, both Robo-2 and Slit-1 are necessary for the accurate coalescence of subsets of P2-expressing axons along the dorsoventral axis of the OB, and Robo-2 is also required to prevent formation of ectopic P2 glomeruli in the OB.

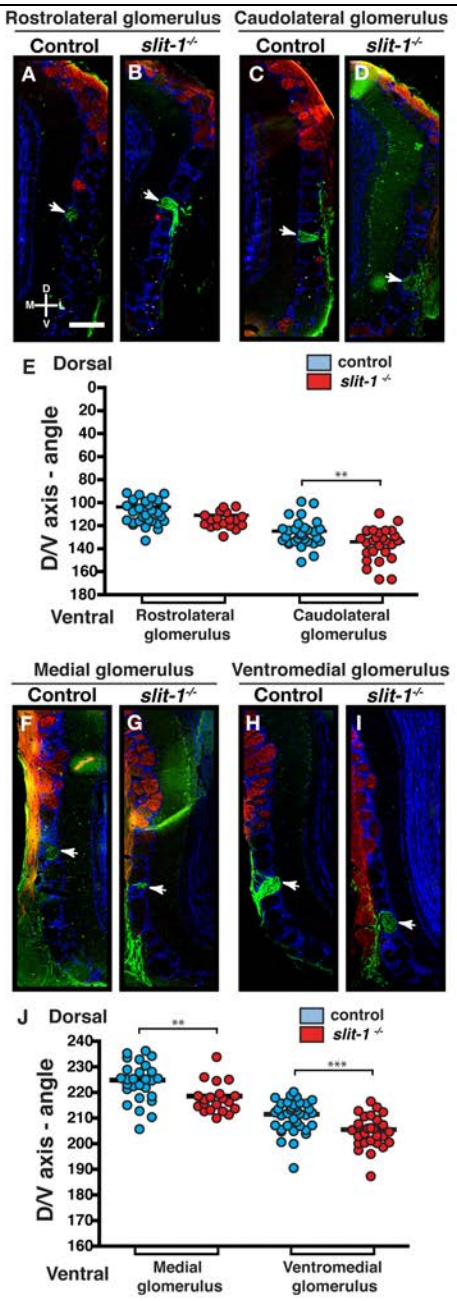


**Figure 5. Slit-1 is required for the targeting of P2-expressing OSN axons in the OB.**

Coronal sections of OBs isolated from control (A, C, F, H) and *slit-1*$^{-/-}$*; P2-tau-lacZ* (B, D, G I) mice stained with NQO-1 and β-galactosidase antibodies (A-D, F-I). A β-galactosidase positive glomerulus is consistently observed in the lateral part of the OB in all mice analyzed (A, B). In addition, a second β-galactosidase positive glomerulus is

observed more caudally on the lateral part of the OB in most OBs analyzed (21/38 controls and 17/24 *slit-1*$^{-/-}$) (C, D). Additional glomeruli were also observed in the ventral part of the OB in a few OBs from control and *slit-1*$^{-/-}$ mice (4/38 controls and 5/24 *slit-1*$^{-/-}$) (data not shown). On the medial side of the OB, all OBs analyzed contained at least one β-galactosidase positive glomerulus and the majority of OBs contained two β-galactosidase positive glomeruli (21/38 for controls and 21/26 for *slit-1*$^{-/-}$ mice). In addition, a third glomerulus was observed in some OBs analyzed (4/38 controls and 3/24 *slit-1*$^{-/-}$) (data not shown). The relative positions of β-galactosidase-positive glomeruli along the dorsoventral axis of the OB on the lateral and medial sides are represented on scatter plots (E, J). Parameters are shown as mean ± SEM. The mean location of the caudolateral and medial P2 glomeruli is shifted ventrally in *slit-1*$^{-/-}$ mice. Note that in panels A-D and F-I sections with glomeruli located approximately at the mean angle are shown. Triple asterisk: $P<0.001$. Double asterisk: $P<0.01$. D, dorsal; V, ventral; L, lateral; M, medial. Scale bar: 250μm.

*A non-cell autonomous role for Robo-2 in the innervation of the ventral OB*

Although Robo-2 is not expressed in OSNs that innervate the most ventral region of the OB, our observation that P2-expressing axons coalesce into glomeruli more ventrally in *robo-2*$^{lox/lox}$*; OMP-Cre* and *slit-1*$^{-/-}$ raises the possibility that the targeting of axons innervating the most ventral region may also be indirectly affected. We therefore examined the targeting accuracy of a population of axons that do not endogenously express Robo-2 in *robo-2*$^{lox/lox}$*; OMP-Cre* mice. We assessed the location of MOR28-positive glomeruli in controls, *robo-2*$^{lox/lox}$*; OMP-Cre,* and *slit-1*$^{-/-}$ mice that were crossed

with *MOR28-tau-lacZ* mice by immunostaining consecutive coronal sections of OBs with β-gal antibodies. One or two MOR28-positive glomeruli were observed on each side of the OB in most mice analyzed. While the overall location of MOR28-positive glomeruli was not significantly affected in *robo-2$^{lox/lox}$; OMP-Cre* mice (Fig. 6), a small but statistically significant dorsal shift in the location of an MOR28-positive glomerulus was observed on the medial side of the OB in *slit-1$^{-/-}$* mice (Figs. 7H-J). Although the location of MOR28-positive glomeruli was unaffected in *robo-2$^{lox/lox}$; OMP-Cre*, we observed a significant decrease in the number of MOR28 glomeruli on the medial side of the OB in these mice (Table 1). In contrast, the overall number of glomeruli in the OBs of *robo-2$^{lox/lox}$; OMP$^{Cre/+}$* mice is not significantly changed when compared to control mice (Table 1). These observations would suggest that the formation of ectopic glomeruli, such as P2, in the ventral region of the OB observed in these mice may contribute to the elimination of other subsets of glomeruli in the most ventral region of the OB, although the exact cause for this elimination remains to be determined. Taken together, our results demonstrate that both Robo-2 and Slit-1 contribute to the accurate innervation of glomeruli in the ventral region of the OB.

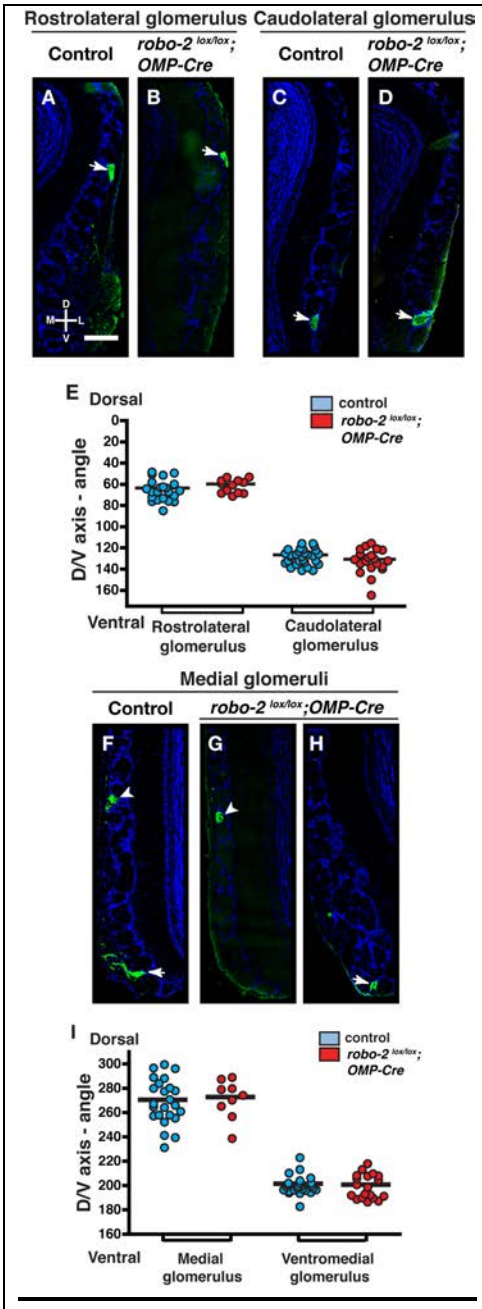


**Figure 6. MOR28-expressing axons coalesce accurately in *robo-2$^{lox/lox}$;OMP-Cre* mice.**

Coronal sections of OBs isolated from control (A, C, F) and *robo-2$^{lox/lox}$;OMP-Cre; MOR28-tau-lacZ* (B, D, G, H) mice stained with NQO-1 and β-galactosidase antibodies (A-D, F-H). A β-galactosidase positive glomerulus is consistently observed in the lateral region of the OB in all mice analyzed (A, B). In addition, a second β-galactosidase

positive glomerulus is observed more caudally on the lateral side of the OB in the majority of mice analyzed (19/29 controls and 13/19 robo-$2^{lox/lox}$; OMP-Cre) (C, D). All OBs analyzed contained at least one β-galactosidase positive glomerulus (G) and the majority of OBs analyzed from control mice (20/26) contained two β-galactosidase positive glomeruli on the medial side (F). In contrast a significant number of *robo-$2^{lox/lox}$;OMP-Cre; MOR28-tau-lacZ* mice are missing the MOR28 glomerulus located more dorsally on the medial side shown by an arrowhead in panels F and G (11/20; see Table 1). The relative positions of β-galactosidase positive glomeruli on the lateral and medial sides of the OB are represented on scatter plots (E, I). Parameters are shown as mean ± SEM. No significant change was observed in the mean location of MOR28 glomeruli on both the lateral and medial sides of the OB in *robo-$2^{lox/lox}$; OMP-Cre; MOR28-tau-lacZ* mice. Note that in panels A-D and F-H sections with glomeruli located approximately at the mean angle are shown. D, dorsal; V, ventral; L, lateral; M, medial. Scale bar: 250μm.

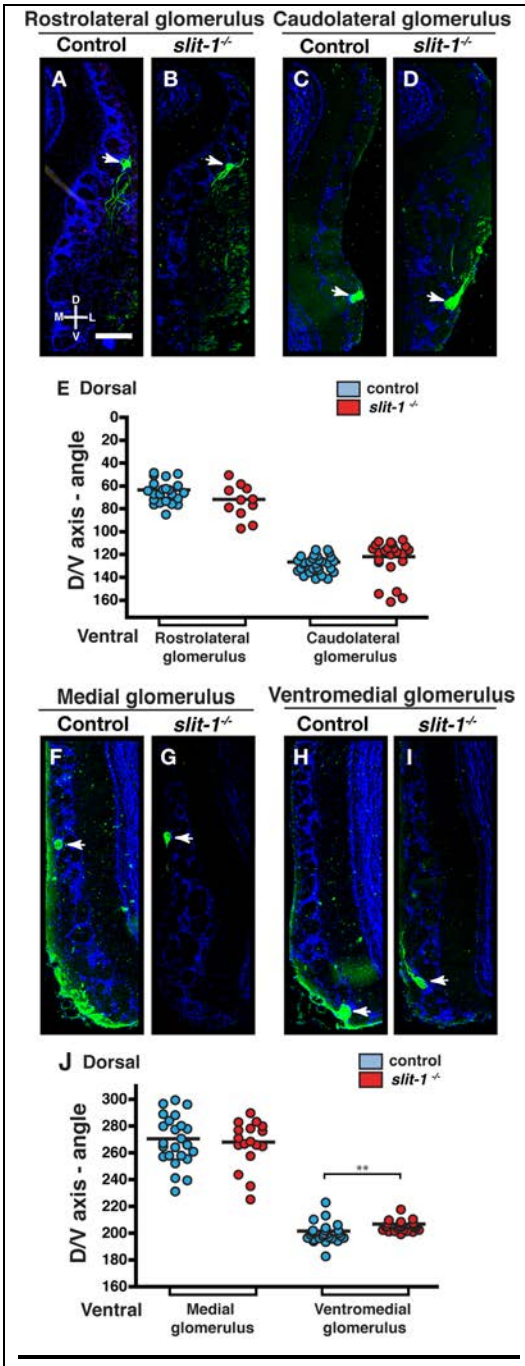


**Figure 7. Slit-1 regulates the coalescence of a subset of MOR28-expressing axons in the OB.**

Coronal sections of OBs isolated from control (A, C, F, H) and *slit-1*$^{-/-}$*; MOR28-tau-lacZ* (B, D, G, I) mice stained with NQO-1 and β-galactosidase antibodies (A-D, F-I). A β-

galactosidase positive glomerulus is consistently observed on the lateral side of the OB in all mice analyzed (A, B). In addition, a second β-galactosidase-positive glomerulus is observed more caudally in the lateral region of the OB (19/29 controls and 11/22 *slit-1*$^{-/-}$) (C, D). On the medial side of the OB, all OBs analyzed contained at least one β-galactosidase positive glomerulus (H, I) and the majority of OBs analyzed (20/26 for controls and 17/24 for *slit-1*$^{-/-}$ mice) contained a second β-galactosidase positive glomerulus (F, G). The relative positions of β-galactosidase positive glomeruli along the dorsoventral axis of the OB on the lateral and medial sides are represented on scatter plots (E, J). Parameters are shown as mean ± SEM. While the location of the majority of MOR28 glomeruli appear unaffected in *slit-1*$^{-/-}$ mice, the mean location of the MOR28 glomerulus located in the ventromedial region of the OB is shifted dorsally in these mice. Note that in panels A-D and F-I sections with glomeruli located approximately at the mean angle are shown. Double asterisk: $P<0.01$. D, dorsal; V, ventral; L, lateral; M, medial. Scale bar: 250μm.

**DISCUSSION**

The detection and processing of odour information requires the formation of stereotypic connections between OSNs in the periphery and second-order neurons located in the OB. A spatial correlation exists between the location of OSNs within the OE and their target glomeruli within the OB such that OSNs located in the dorso-medial aspect of the OE project dorsally to the OB while OSNs present in the ventro-lateral region of the OE send their axons to more ventral targets in the OB (Astic and Saucier, 1986; Saucier and Astic, 1986; Miyamichi et al., 2005). The axon guidance receptor Robo-2 is essential

for the formation of an accurate glomerular map in the dorsal region of the OB and this map is crucial for proper processing of aversive odorant information in mice (Cho et al., 2011). The present study examined the role of Robo-2 and of one of its ligands, Slit-1, in the formation of the glomerular map in the ventral region of the OB. We demonstrate that Robo-2 is expressed on subsets of OSN axons that innervate the ventral OB. Robo-2 expression is essential for accurate coalescence of OSN axons expressing the P2 OR along the dorso-ventral axis of the OB and to prevent formation of ectopic glomeruli. In addition, *robo-2* ablation leads to a decrease in the number of MOR28-positive glomeruli in the OB. Furthermore, we show that Slit-1 and Slit-2 are expressed in OSNs that project their axons to the ventral region of the OB raising the possibility that axonally-derived Slits may contribute to the targeting of OSN axons.

*Slit-1 and Robo-2 regulate the formation of the glomerular map in the ventral region of the OB*

OSNs expressing a specific OR are scattered within four spatially distinct but partially overlapping zones of the OE where OR expression domains form a continuous gradient in the OE (Strotmann et al., 1992; Ressler et al., 1993; Vassar et al., 1993; Strotmann et al., 1994; Mombaerts et al., 1996; Sullivan et al., 1996; Tsuboi et al., 1999; Miyamichi et al., 2005). Consistent with this notion, we have previously shown that Robo-2 is expressed in a gradient across the OE where Robo-2 is highly expressed in the dorso-medial region and lower levels are observed in more ventral regions of the OE (Cho et al., 2007). Moreover, Robo-2 is required for the accurate targeting of MOR174-9-expressing OSN axons within the dorsal region of the OB (Cho et al., 2011). We have examined whether Robo-2 also controls the coalescence of OSN axons in more ventral

regions of the OB. Our analyses revealed a ventral shift in the targeting of P2-expressing axons and the formation of additional P2-positive glomeruli upon *robo-2* deletion (Figure 3). In contrast, the location of MOR28-positive glomeruli was unaffected in *robo-2$^{lox/lox}$; OMP-Cre* mice but we observed a decreased number of these glomeruli. The decrease in the number of MOR28 glomeruli in *robo-2$^{lox/lox}$; OMP-Cre* mice suggest that the formation of ectopic glomeruli in the ventral region by other populations of axons, such as the P2-expressing axons, may fill the space available for glomerulus formation, which could prevent later arriving axons from forming the appropriate number of glomeruli.

We have examined the contribution of Slit-1 to Robo-2-mediated targeting of axons in the OB. While Slit-1 is not required for the targeting of MOR174-9-expressing axons, it is necessary for the accurate coalescence of P2-expressing axons in the dorso-ventral axis of the OB. Interestingly, Slit-1 is also not essential to prevent the formation of ectopic P2 glomeruli in the most ventral region of the OB. Taken together, these results strongly suggest that other Slit family members also contribute to the formation of the glomerular map. Unfortunately, the quantitative analysis of glomerular location must be performed in adult mice, which has made examination of compound *slit* mutant impossible as all *slit-2$^{-/-}$* and the majority of *slit-1$^{-/-}$; slit-3$^{-/-}$* mice die at birth. It is nonetheless interesting to note that an increased number of MOR256-17-positive glomeruli has been reported in *slit-1$^{-/-}$;slit-2$^{-/-}$* embryos as well as in *slit-1$^{-/-}$;slit-2$^{+/-}$* adult mice, suggesting that Slit-2 can also regulate the targeting of OSN axons (Nguyen-Ba-Charvet et al., 2008). Alternatively, Robo-2 may control coalescence of some populations of axons in a Slit-independent manner by regulating axonal fasciculation as previously shown in the visual system (Plachez et al., 2008). An analysis of axonal projections in

compound *slit* conditional mutant mice will be necessary to fully address their roles in glomerular map formation.

Slit-1 may also regulate axonal targeting independently of Robo-mediated repulsion. We observed a small but significant dorsal shift in the location of a specific MOR28 glomerulus in *slit-1*$^{-/-}$ mice that is not observed in *robo-2*$^{lox/lox}$*; OMP-Cre*. Since Robo-1 and -3 are not expressed in OSNs, this defect is unlikely to result from a change in Slit-mediated axonal repulsion (Cho et al., 2007; Nguyen-Ba-Charvet et al., 2008). It is possible that ablation of Slit expression results in defects in the development of the OB that indirectly affects the guidance of MOR28 OSN axons in the OB. Indeed, Slit-1 influences the migration of precursor cells in the rostral migratory stream to the OB, although we could not observe morphological changes in the OB of *slit-1*$^{-/-}$ mice (data not shown) (Nguyen-Ba-Charvet et al., 2004). Slit-1 could also control the guidance of this population of axons through an as yet unidentified receptor. A recent report has proposed that additional Slit receptors may also be involved in axonal repulsion in the spinal cord (Jaworski et al., 2010). Alternatively, Slit may regulate expression of additional guidance molecules that can control the dorsoventral targeting of axons within the OB.

*Is there an axonal Slit contribution to the targeting of OSN axons?*

Npn-2 and Sema3F are crucial for the targeting of OSN axons along the dorsoventral axis of the OB (Takeuchi et al., 2010). Sema3F is highly expressed in OSN axons that innervate the dorsal region of the OB. These axons express high levels of Robo-2 and project early during development of the olfactory system. Expression of Slits in the ventral region of the developing OB may repel early-arriving axons to the dorsal

region of the OB. OSNs that target to the ventral region of the OB express Npn-2 and are prevented from projecting in the dorsal region of the OB by Sema3F secreted from axons in the dorsal OB (Takeuchi et al., 2010). It is therefore possible that in addition to OB-derived Slits, expression of Slits in OSN axons may also regulate the coalescence of axons in glomeruli of the OB. Our analyses revealed that both Slit-1 and Slit-2 are expressed in OSNs that project their axons to the ventral part of the OB. Since these axons project to the OB at a later time than axons that innervate the dorsal region of the bulb (Takeuchi et al., 2010), it is unlikely that secreted Slits from these axons would serve to repel Robo-2-expressing axons to the dorsal OB. Nonetheless the graded expression of Robo-2 in ventrally-targeting axons and secretion of Slits by these axons may fine-tune their dorsoventral positioning within the ventral region of the OB. Furthermore, since OSNs continually regenerate and send axons to the OB, axonally-derived Slit may also regulate the targeting of regenerating axons in the adult OB. Ablation of Slits in specific populations of OSNs will be necessary to address these possibilities.

*An accurate glomerular map in the ventral OB is not required for avoidance of aversive odorants*

The detection of aversive odorants and the innate avoidance behavior they trigger in mice is crucial for their survival. The relative contribution of odor information processing in the dorsal and ventral regions of the OB for avoidance behavior remains to be fully characterized. For example, TMT, a component of fox feces, can activate glomeruli present in both the dorsal and ventral regions of the OB (Kobayakawa et al.,

2007). We have previously shown that changes in the glomerular map within the dorsal region of the OB in *robo-2*$^{lox/lox}$*; OMP-Cre* mice are associated with reduced avoidance of TMT by these mice (Cho et al., 2011). Our observation that subsets of ventrally-projecting axons, such as P2, are mistargeted in *robo-2*$^{lox/lox}$*; OMP-Cre* mice raises the possibility that defects in the formation of the ventral glomerular map may also contribute to the reduced avoidance observed in these mice. However, while *slit-1*$^{-/-}$ mice have a disrupted glomerular map in the ventral OB, they display robust avoidance behavior in response to TMT suggesting that formation of an accurate glomerular map in the ventral OB is not essential for responses to aversive odorants. Nonetheless, we cannot exclude the possibility that the location of TMT-activated glomeruli in the ventral OB may be unaffected in *slit-1*$^{-/-}$ mice. Interestingly, *slit-1*$^{-/-}$ mice do not display the changes observed in the dorsal glomerular map of *robo-2*$^{lox/lox}$*; OMP-Cre* further supporting an important role for this map in regulating avoidance behavior to aversive odorants.

Taken together, our results demonstrate that glomerular map formation in the ventral region of the OB is dependent on Slit-1 and Robo-2, and suggest that Slits expressed by OSN axons may also play a role in the formation and refinement of the glomerular map along the dorsoventral axis of the OB.

# CHAPTER 5

## GENERAL DISCUSSION

### SUMMARY

The major aim of this thesis was to study the molecular mechanisms that regulate the formation of stereotypic connections in the mouse main olfactory system. I was interested in the role of the Slit and Robo axon guidance molecules in the accurate segregation of different OSN axons to the OB. The results presented herein address the importance of Robo-2 and its ligands, the Slits, in the formation of this stereotypic sensory map in the main olfactory system (MOS). The results also reveal the importance of this stereotypic map for the processing of aversive odorants by the animals.

Chapter 2 of this thesis described the expression pattern of Robo-2 by OSNs located in the OE and of Slit-1 in the ventral part of the OB. I provided direct evidence for the involvement of Slit-1-Robo-2 signaling in the accurate segregation of zone 1 OSN axons to the dorsal region of the OB.

In chapter 3 of this thesis, I looked more closely at the role of Robo-2 in the segregation of DI and DII OSN axons to the dorsal region of the OB. These two subdomains are part of zone 1 and are shown to be crucial for processing of aversive odorants by the animals (Kobayakawa et al. 2007). My results showed that Robo-2 is essential for the innervation of DII OSN axons along the dorsal to ventral axis of the OB. In addition, my observations demonstrate that this accurate targeting of DII domain axons is critical for eliciting proper avoidance behavior in mice in response to a predator odorant.

In chapter 4 of this thesis, we examined the role of Slit-1 and Robo-2 in the targeting of different subpopulations of OSN axons to the OB, more specifically zones 2 and 4. Our results uncover a non cell-autonomous role for Robo-2 in the innervation of zone 4 OSN axons to the OB. In addition, our results show that Slit-1 and Slit-2 are expressed by the OSN axons and these ligands might also be important for the targeting of zone 1 OSN axons to the dorsal region of the OB.

This thesis provides insights into the molecular mechanisms that regulate the formation of stereotypic connections in the main olfactory system and reveals the importance of the accurate arrangement of this sensory map for the processing of aversive odorants by the animals.

**AXON GUIDANCE MOLECULES**

In all sensory systems, accurate connections between sensory neurons in the periphery and second-order neurons in the CNS are primordial to correctly represent outside stimuli to our brain. Such stereotyped connections are essential for the specific detection and perception of a variety of odorants by the olfactory system. OSNs are distributed within four spatially distinct yet partially overlapping zones of the OE and these ONS axons project to four specific regions of the OB (Strotmann et al. 1992; Ressler et al. 1993; Vassar et al. 1993; Strotmann et al. 1994; Vassar et al. 1994; Mombaerts et al. 1996; Sullivan et al. 1996; Tsuboi et al. 1999; Norlin et al. 2001; Iwema et al. 2004; Miyamichi et al. 2005). Additionally, there is a strong correlation between the location of the OSN cell bodies within the OE and their targeting area along the dorsal to ventral axis of the OB where OSNs located in zone 1 (dorso-medial in the OE)

target their axons to the most dorsal region of the OB while OSNs located in zone 4 (dorso-lateral in the OE) target their axons to the most ventral region of the OB (Astic and Saucier 1986; Saucier and Astic 1986; Miyamichi et al. 2005). However, the molecular mechanisms that regulate the segregation of OSN axons along the dorsal to ventral axis of the OB were not known.

*Robo and Slit axon guidance molecules*

What molecular mechanisms could regulate the innervation of this complex target field? One of the potential candidates was the Slit family of axon guidance molecules. Not only are they implicated in the segregation of OSN axons in the *Drosophila* and zebrafish olfactory system but they were also shown to regulate the innervation of another complex target field, the accessory olfactory bulb in mouse (Cloutier et al. 2004; Jhaveri et al. 2004; Miyasaka et al. 2005). Another clue pointing to a role for Robos in the segregation of different subpopulations of OSN axons came from observations in *Drosophila* where a combinatorial code of Robo expression was proposed to regulate the segregation of post-crossing commissural neurons. The combinatorial Robo code theory was first proposed based on the observation that specific Robos are expressed by axon bundles in the three lateral positions when longitudinal axons project in the *Drosophila* ventral nerve cord (Rajagopalan et al. 2000; Simpson et al. 2000). Axons that occupy the most medial pathway, adjacent to the midline, express only Robo-1 (Rajagopalan et al. 2000). Intermediate tract axons express Robo-1 and Robo-3 while axons belonging to the lateral pathway express all three Robos (Rajagopalan et al. 2000; Simpson et al. 2000). Therefore, it was believed that this combinatorial expression of the three Robo receptors

regulated the segregation of axons into these three lateral pathways. Initially, we thought that a combinatorial Robo expression could be present in OSNs to regulate the innervation of OSN axons originating from 4 different zones along the dorsal to ventral axis of the OB. Instead of finding a 'combinatorial Robo code' of expression, we discovered that only Robo-2 is expressed by OSNs in the OE. Interestingly, the Robo-2 expression pattern is graded in such a way that OSNs located in zone 1 (dorso-medial) strongly expressed Robo-2 while OSNs present in zone 4 (dorso-lateral) did not express Robo-2. The expression patterns of Robo-2 observed in the OE were also reflected by the distribution of Robo-2 protein on axons targeting to the OB where OSN axons expressing high levels of Robo-2 targeted the dorsal region of the OB while OSN axons not expressing any Robo-2 targeted the ventral region of the OB. These observations indicated to us that Slits, the Robo-2 repulsive ligands, could be present in the ventral region of the OB to repel Robo-2-positive OSN axons toward the dorsal part of the OB. Indeed, by *in situ* hybridization, *slit-1* and *slit-3* are expressed at the ventral region of the OB around the time when OSN axons are targeting the OB (around E15-E18) (Chapter 2). Furthermore, using *slit-1*$^{+/-}$ and *slit-2*$^{+/-}$ mice which have a reporter gene GFP knock into their coding sequences, immunohistochemistry experiments reveal that Slit-1 and Slit-2 are expressed by the OSN axons targeting the ventral region of the OB (Chapter 4). Although, these observations revealed that *slit-1* and *slit-3* are also expressed in the OB and Slit-1 and Slit-2 by the OSN axons, they do not reveal how the Slit proteins are present in the OB since Slits are secreted proteins. In order to find out how the Slits secreted in the OB, we tried to generate antibodies against Slit-1 and Slit-3. Although, the antibodies could recognize their appropriate proteins by western blot, they did not

specifically recognize the Slits by immunohistochemistry on tissue sections. In addition to these antibodies, we also tried using a Robo-1-Fc construct to determine the Slits protein location in the OB using a section binding assay. I could not detect Slit proteins using this assay possibly due to their low expression in the OB. Therefore, even though we know where and when the Slits are expressed in the olfactory system, we still do not know how far or how much Slits proteins are secreted in the OB. It would be interesting to find whether Slits diffuse through the OB. Other secreted molecules, such as Netrin-1, which was thought to diffuse readily was later shown to stick to membranes (Manitt et al. 2001). Hence, insight into how the Slits are diffusing in the OB could tell us if Slits act as long-range repellent or act as contact-mediated repellents in our system.

*Role of Slits in the OSN axons*

Recently, two studies have shown that Npn-2 and its ligand Sema3F are involved in the targeting of OSN axons along the dorso-ventral axis of the OB (Takahashi et al. 2010; Takeuchi et al. 2010). One of the most interesting points from these studies was that expression of the chemorepellent Sema3F by the OSN axons in the dorsal part of the OB repels the OSN axons expressing Npn-2 into the ventral region of the OB (Takeuchi et al. 2010). Therefore, these observations led to the possibility that Slits could also be expressed by the OSN axons to repel OSN axons expressing Robo-2 to the dorsal region of the OB. Indeed, in chapter 4, we found that Slit-1 and Slit-2 are expressed by the OSN axons. Furthermore, Slit-1 and Slit-2 expressing OSN axons targeted the ventral region of the OB which is devoid of Robo-2 expressing OSN axons (Chapter 4, Figure 2). Hence, these observations lead to the notion that both Slits in the OB and in the OSN axons could be essential for the accurate innervation of OSN axons expressing Robo-2

along the dorsal-ventral axis of the OB. However, which one is more important, Slits in the OB or Slits in the OSN axons?

Temporal analysis of OSN axons targeting the OB tells us that OSNs located in zone 1 send their axons to the OB first (before E14.5) and subsequently, OSNs located in zone 4 send their axons to the OB last (later than E14.5) (Takeuchi et al. 2010). Therefore, the Slit-1 expressing OSN axons are arriving much later to the OB than Robo-2 expressing OSN axons. The earliest time point that we have examined for the expression of Slits in the OB is E15 and at this time, *slit-1* and *slit-3* are already expressed at the ventral part of the OB. These observations show that *slit-1* and *slit-3* expressed in the OB should first mediate the initial segregation of Robo-2 expressing OSN axons to the dorsal region of the OB. Then Slits in OSN axons could mediate the segregation of later arriving OSN axons to the OB since OSN axons constantly target the OB throughout life. One solution that could allow us to distinguish between the role of Slits in the OB or in OSN axons is to use any conditional Slits knock out mice in which we could ablate the expression of Slits in OSN axons. By ablating the Slits only in the OSN axons and not in the OB, we could easily determine how all the Slits in the OB and in the OSN axons are involved in the innervations of the OSN axons to the OB.

Another role of Slits present in OSN axons could be to prevent the formation of ectopic glomeruli in the OB. The first evidence of this role was noticed from our results where the formation of multiple P2 glomeruli was present in our conditional Robo-2 mutant animals and not in Slit-1 deficient mice (Chapter 4, figures 4 and 5). These results indicated that other Slits could be involved in the prevention of ectopic glomeruli. Slit-2 is not expressed in the OB but is expressed by OSN axons. *slit-3* is expressed in

the ventral part of the OB but we do not know if it is also expressed in OSN axons. The more likely candidate in the prevention of ectopic glomeruli is Slit-2 in OSN axons because in a previous study, both Slit-1 and Slit-2 can prevent the formation of ectopic MOR256-17 glomeruli (Nguyen-Ba-Charvet et al. 2008). Therefore, Slit-1 and Slit-2 present in the OSN axons could not only prevent the mistargeting of Robo-2 expressing OSN axons along the dorsal to ventral axis of the OB, but could also be essential in the segregation of these axons to form the appropriate number of glomeruli. However, we cannot rule out a role for Slit-3 since it is expressed in the OB. To determine the role of Slit-3, we could compare the number of P2 glomeruli in different combinations of Slits mutant animals: Slit-1/Slit-2 or Slit-1/Slit-3 double mutant mice. These proposed experiments could shed light on the role of different Slits in the proper segregation of glomeruli in the OB.

Taken together, our observations indicate that Slit-Robo-2 signaling is important for the accurate formation of a sensory map in the OB. It remains to be determined how much the Slits in OSN axons play a role in the accurate innervation of OSN axons along the dorsal-ventral axis of the OB. Furthermore, it will be interesting to know which Slits are implicated in the prevention of ectopic glomeruli in the OB.

*Other axon guidance molecules*

Although a subset of zone 1 OSN axons are mistargeted in either Slit or Robo-2 deficient mice, many zone 1 OSN axons are still properly targeted to the dorsal region of the OB. These observations indicated that long-range attractant cues may also promote their segregation to the dorsal region of the OB. During this thesis work, we looked at

additional axon guidance molecules that could be involved in the segregation of OSN axons along the dorsal to ventral axis of the OB. One of the first candidates for long-range attractant cue was Netrin-1. Netrin-1 and its receptor DCC (deleted in colorectal caner) are expressed in the rat olfactory system. DCC is expressed on the pioneer olfactory axons around E13 and its expression is decreased after E16 (Astic et al. 2002). Netrin-1 is expressed within the mesenchyme surrounding the region including the pioneering olfactory axons and the presumptive olfactory nerve layer. Therefore, these observations indicated that Netrin-1 may attract pioneer olfactory axons expressing DCC toward the presumptive OB. Hence, we obtained DCC and Netrin-1 deficient mouse from Dr. Timothy Kennedy's lab to look at the targeting of zone 1 (NQO-1 positive) OSN axons to the OB. However, our results did not show any targeting defects or decrease of NQO-1 positive OSN axons innervating the OB (Unpublished data).

Another candidate that could mediate attraction is Sonic hedgehog (Shh). Shh is a secreted morphogen which can also function as a chemoattractive axon guidance molecule for commissural axons (Charron et al. 2003; Okada et al. 2006). Shh can attract migrating neuroblasts originating from the SVZ to the OB (Angot et al. 2008). In recent study, Shh is expressed in the glomeruli of the rat OB and can promote OSN axon branching and outgrowth (Gong et al. 2009). These observations prompted us to look at the expression pattern of the Shh receptors, Boc (bioregional Cdon-binding protein) and Cdon (cell-adhesion-molecule-related/downregulated by oncogenes) that have been shown to regulate Shh-mediated attraction. We obtained *in situ* hybridization probes for Boc and Cdon from Dr Frédéric Charron. *In situ* hybridization experiments demonstrated that *Cdon* is expressed only by OSNs located in the zone 4 of the OE and *Boc* is

expressed in the mesenchyme surrounding the OE at E18 (Unpublished data). Furthermore, their ligand, *Shh* is also expressed in the mitral cell layer of the OB. These results suggest that Shh might promote the outgrowth of OSNs located in zone 4 which express *Cdon*. It will be very interesting to determine whether OSN axon targeting defects are observed in either Shh or Cdon-deficient mice.

Another candidate of axon guidance molecule that I was interested in was Sema5A. Sema5A can act as a bifunctional (can act as both attractant or repelling cues) axon guidance cue for mammalian midbrain neurons and for vertebrate motor axons (Kantor et al. 2004; Hilario et al. 2009). The bifunctional effect of Sema5A is mediated by two clusters of type-1 thrombospondin repeats which promote axon outgrowth and a sema domain which acts as an inhibitory cue (Kantor et al. 2004; Hilario et al. 2009). These observations suggest a very interesting possibility that Sema5A could attract one subpopulation of OSN axons while repelling another population of OSN axons. Therefore, I performed Sema5A *in situ* hybridization experiments to analyze the expression pattern of Sema5A in the olfactory system. During the embryonic development period when OSN axons are targeting the OB (E15-18), *sema5A* is strongly expressed in the ventral part of the OB which strongly resembled the expression of *slit-1* and *slit-3* (unpublished data). Next, we tried to determine the expression pattern of a receptor for Sema5A, Plexin B3, however, I did not detect any expression in OSNs (unpublished data). Nevertheless, it is possible that Sema5A could act through an unidentified receptor. Sema5A is also essential for vascular patterning during development although Plexin B3 is not expressed in the vascular system during embryogenesis, suggesting the presence of other Sema5A functional receptors (Fiore et

al. 2005). Therefore, it will be very interesting to define the role of Sema5A in the innervations of OSN axons to the OB.

In summary, although further investigation is needed to determine if Shh or Sema5A are involved in the segregation of OSN axons to the OB, tantalizing evidence suggests that these axon guidance molecules might have a role in innervation of OSN axons.

## CONTROL OF BEHAVIOR IN THE OLFACTORY SYSTEM

Until recently, the functional role of axonal zonal segregation in the main olfactory system (MOS) was not known. Recent observations demonstrated that the dorsal OB which is further subdivided into two different zones: DI and DII is essential for eliciting innate behavior responses in mice in the presence of aversive odorants (Kobayakawa et al. 2007). Even though the dorsal region is important for the processing of aversive odorants, the requirement for precise innervations by OSN axons to this zone of the OB remained to be elucidated. Our results in chapter 3 examined the role of accurate segregation of DI and DII OSN axons to the OB for the proper processing of different aversive odorant information by the animals. Indeed, our results indicate that the proper innervation of OSN axons to the DII region of the OB are crucial for the animal to display avoidance behavior in the presence of the predator odorant (TMT) (Chapter 3, Figure 5). These observations suggest that the MOS must possess hard-wired circuits to elicit appropriate innate behavior responses in the presence of aversive odorants.

*Dorsal domain glomeruli vs. ventral domain glomeruli*

In the Kobayakawa et al. (2007) study, the odorant TMT used to elicit avoidance behavior activates glomeruli in the DII region but also glomeruli located in the ventral region of the OB. This activation pattern of glomeruli by TMT raises an important question. Is the formation of the glomerular map in the ventral region of the OB also important for innate behaviors? In Chapter 3, using the robo-$2^{lox/lox}$; $OMP^{Cre/+}$ mice, we illustrated that the accurate segregation of DII region is crucial for the proper behavioral response by the animals in the presence of TMT. However, in our subsequent study (Chapter 4), the OSN axons located in the zone 2 and zone 4 are also mistargeted in the robo-$2^{lox/lox}$; $OMP^{Cre/+}$ mice. This raised the possibilities that the ventral gluomeruli activated by TMT could have affected our behavior experiments in Chapter 3. To answer this question of which domain is more important, we used Slit-1-deficient mice because in these mice, the targeting to DII region is unaffected, while innervation in the ventral region is affected (Chapter 4). Therefore, we assessed the innate avoidance behavior of Slit-$1^{-/-}$ mice to TMT. The Slit-$1^{-/-}$ mice showed no selective decrease in avoidance behavior in response to TMT (Chapter 4, Figure 3) unlike the robo-$2^{lox/lox}$; $OMP^{Cre/+}$ mice (Chapter 3). Our results illustrate that the proper innervation of DII glomeruli is more important than the accurate targeting of ventral glomeruli for the processing of the predator odorant TMT.

It was once thought that both dorsal and ventral domain glomeruli contribute equally to the processing of odor information in the glomerular map. However, our observations and also observations from Kobayakawa et al. (2007) suggest that the mouse MOS might be composed of at least two functional modalities: dorsal domain glomeruli

for innate odor responses which is hard-wired and ventral domain glomeruli for learned responses based on memory which can rely on a more plastic sensory map (Chapters 3 and 4; (Kobayakawa et al. 2007). Indeed, although OSNs in the dorsal region (zone 1) is ablated from the OB, these mutant mice could still learn to discriminate structurally related odorants (Kobayakawa et al. 2007). Furthermore, this notion is reinforced by new results showing how second order neurons (Mitral/tufted cells) send their axons to the cortex (Miyamichi et al. 2010). In a recent study, although mitral/tufted cells from the same glomeruli send their axons to different parts of the olfactory cortex such as the piriform cortex, mitral cells in the dorsal region of the OB send their axons preferentially to the cortical amygdala (Miyamichi et al. 2010). These observations are very interesting because the amygdala is the central structure within a brain circuitry processing fear and the piriform cortex acts as an association cortex (Davis and Shi 1999; Fendt and Fanselow 1999; Stettler and Axel 2009). It seems very plausible that the dorsal region of the OB is required for the processing of innate odorant information while the ventral region of the OB functions in learned odorant information.

*Accessory olfactory system vs. main olfactory system*

Mice, unlike humans, possess another olfactory system called accessory olfactory system (AOS). The AOS detects pheromones which regulate specific innate behaviors such as sexual behavior, aggression and pups rearing (reviewed in Stowers and Marton 2005). The AOS is also organized in a very similar manner as the MOS where first order neurons termed vomeronasal sensory neuron (VSN) located in the vomeronasal organ send their axons to the accessory olfactory bulb (AOB). In addition to eliciting social

behaviors, the AOS can also elicit innate fear responses to predator odorants (Papes et al. 2010). This observation also raises interesting questions. Which system is important for innate fear responses? Many observations suggest that depending on the source of odorants, either the MOS or AOS could be activated to mediate the innate fear responses. Odorants such as TMT present in fox feces or leopard urine activate the innate avoidance behavior through the dorsal region of the OB and not through the AOS (Kobayakawa et al. 2007). In contrast, cat, rat and snake odors require a functional AOS to initiate avoidance behavior in mice (Papes et al. 2010). How can one odorant activate one system and not the other? This might depend on the type of odorant eliciting the innate fear responses. For the MOS, odorants are small chemicals. For the AOS, odorants are pheromones. Although the identity of the mammalian pheromones is poorly understood, some compounds with pheromonal activity have been purified from complex mixtures and these compounds are found to be both proteins and small molecules (Dulac and Torello 2003; Chamero et al. 2007). Therefore, odorants present in cat, rat and snake that elicit fear responses might be proteins and will not be detected by OR in the MOS.

## CONCLUSION

Robo-2 is expressed by OSNs in a graded manner in the OE and the ligands, Slit-1 and Slit-3 are expressed in the OB. In response to different Slits, Robo-2 expressing OSN axons are repelled to target the dorsal region of the OB. Evidence provided in this thesis reveals that Slit-Robo-2 signaling regulates the accurate innervation of different subpopulations of OSN axons along the dorsal to ventral axis of the OB.

These studies are not only important for our fundamental understanding of axon guidance in the development of stereotypic connections in a sensory system, but will also contribute to our understanding of how one group of axon guidance molecules can regulate the proper segregation of axons in a complex target field. In addition, the thesis provides insight into how the development of the glomerular map in the olfactory bulb contributes to the regulation of innate behavior in mice.

# APENDIX I

## ANIMAL USE PROTOCOLS AND PERMIT TO USE BIOHAZARDOUS MATERIALS

RECEIVED JUN 0 1 2010

www.mcgill.ca/researchoffice/compliance/animal/forms

**McGill University**
**Animal Use Protocol – Research**

For Office Use Only:
Protocol #: 4877
Approval End Date: 31 MAY 2011
Facility Committee: MNI

**Title:** Molecular Mechanisms of Sensory Systems Development and Axon Guidance Mechanisms governing the formation of Topographic Maps.
*(must match the title of the funding source application)*

☐ New Application ☒ Renewal of Protocol # 4877 ☐ Pilot **Category** *(see section 11)*: C

**1. Investigator Data:**

**Principal Investigator:** Jean-François Cloutier **Phone #:** 514-398-6351
**Unit/Department:** Montreal Neurological Institute **Fax#:** 514-398-1319
**Address:** 3801 University, Room MP105 **Email:** jf.cloutier@mcgill.ca

**2. Emergency Contacts:** Two people must be designated to handle emergencies.

**Name:** Jean-François Cloutier **Work #:** 6351 **Emergency #:** (514) 482-8766
**Name:** Emilie Dumontier **Work #:** 3176 **Emergency #:** (450) 536-8595

**3. Funding Source:**

**External** ☒
**Source (s):** CIHR
**Peer Reviewed for the project proposed in this Animal Use Protocol:** ☒YES ☐ NO**
**Status :** ☒ Awarded ☐ Pending
**Funding period:** 10/2008-10/2013

**Internal** ☒
**Source (s):** MNI start-up
**Peer Reviewed:** ☒ YES ☐ NO**
**Status:** ☒ Awarded ☐ Pending
**Funding period:** 04/2004-04/2014

For Office Use Only: TC=OK

| ACTION | ✓ | DATE |
|---|---|---|
| COs | ✓ | 4 |
| DB | ✓ | 29 JUN 2010 |
| APPROVED | | |

** For projects that have not been reviewed for scientific merit by the funding source, the Dean/Director of the Principal Investigator's Faculty/Institution will obtain peer reviews and communicate the outcome to the facility animal care committee. Only those protocols receiving a positive assessment of scientific merit can be approved.

**Proposed Start Date of Animal Use (d/m/y):** ____ **or ongoing** ☒
**Expected Date of Completion of Animal Use (d/m/y):** ____ **or ongoing** ☒

**Investigator's Statement:** The information in this application is exact and complete. I assure that all care and use of animals in this proposal will be in accordance with the guidelines and policies of the Canadian Council on Animal Care and those of McGill University. I shall request the Animal Care Committee's approval prior to any deviations from this protocol as approved. I understand that this approval is valid for one year and must be approved on an annual basis. I will ensure that all collaborators and staff are aware of all changes to this protocol.

**Principal Investigator's signature:** [signature] **Date:** June 1, 2010

*Approved by:*

| | | |
|---|---|---|
| **Chair, Facility Animal Care Committee:** | Ken Hastings | **Date:** June 3, 2010 |
| **Animal Compliance Office:** | [signature] | **Date:** 2010, 6, 29 |
| **Chair, Ethics Subcommittee** (as per UACC policy): | — | **Date:** — |
| **Approved Animal Use** | **Beginning:** 01 JUN 2010 | **Ending:** 31 MAY 2011 |

☐ This protocol has been approved with the modifications noted in Section 13.

January 2010

RECEIVED JUN 15 2010

## 4. Research Personnel and Qualifications

**List the names of the Principal Investigator and of all individuals who will be in contact with animals in this study and their employment classification (investigator, technician, research assistant, undergraduate/ graduate student, fellow). Indicate if Principal Investigator is not handling animals. If an undergraduate student is involved, the role of the student and the supervision received must be described. Training is mandatory for all personnel listed here. Refer to *www.animalcare.mcgill.ca* for details. Each person listed in this section must sign to indicate that s/he has read this protocol and related applicable SOPs.** ***(Space will expand as needed)***

| Name | Classification | Animal Related Training Information | | Species Handled | Signature |
|---|---|---|---|---|---|
| | | UACC on-line Theory course | Workshops + others | | |
| Jean-François Cloutier | Principal Investigator | Theory course+rat and mouse workshop; mouse | | | |
| Jin Hyung Cho | Graduate student | Theory course+rat and mouse workshop; mouse,rat | | | |
| Joseph Kam | Graduate student | Theory course+rat and mouse workshop; mouse,rat | | | |
| Émilie Dumontier | Research assistant | Theory course+rat and mouse workshop;mouse | | | |
| François Beaubien | Graduate student | Theory course+rat and mouse workshop; mouse,rat | | | |
| Janet Prince | Graduate Student | Theory course+rat and mouse workshop;mouse.rat | | | |
| Pavel Gris | Post-doctoral fellow | Theory coourse+mouse workshop;mouse | | | |
| Vesselina Deleva | Research Assistant | Theory course – mouse workshop; mouse | | | |

**Occupational Health Program information:** *http://www.mcgill.ca/ehs/ohs/*

## 5. Summary

**5 a) AIMS AND BENEFITS: Describe in language that will be understood by members of the general public, in a short paragraph, the overall aim of the study and its potential benefit to human/animal health or to the advancement of scientific knowledge.** (no acronyms (eg. PDRFR1), scientific terms (eg use liver cancer not hepatoma) or jargon )

During development, nerve cells form an intricate array of precise connections required to obtain a functioning nervous system. Over the past ten years, molecules capable of influencing the formation of these connections have been identified. These molecules are expressed in the cellular environment during development and bind to receptors at the surface of the growing axons inducing signals inside the cell telling the axons to either grow more, stop growing, or turn in a specific directions. Our studies are aimed at defining the molecular mechanisms through which these molecules can shape neuronal connections. Understanding the mechanisms involved in the formation of accurate connections will be important in the future elaboration and use of regenerative therapies to treat brain disorders.

**5 b) SPECIFIC OBJECTIVES OF THE STUDY: Summarize in point form the primary objectives of this study.**

-Examine the role of Slit-Roundabout signaling in the development of the olfactory systems
-Examine the role of Repulsive guidance molecule-Neogenin signaling in the development of the hippocampus, olfactory and somatosensory systems
-Examine the role of RET in the development of the olfactory system
-Examine the role of nephrin-like proteins (Kirrels) in the development of the olfactory system
-Identify new molecules that guide axons during development of the nervous system.
-Examine the role of CAM-related, down-regulated by oncogenes (Cdo), brother of Cdo (Boc,) and Amigo-1 in the development of the olfactory systems.

**5 c) Indicate if and how the current goals differ from those in last year's application.**

Same as last year.

**5 d) List the section / subsection numbers where significant changes have been made**

Through expression pattern analyses, we have identified three new potential regulators of axon guidance in the olfactory system. We have therefore added a new specific objective to examine the role of Boc, Cdo, and Amigo-1 in axon guidance in the olfactory system.
Section 7D: Generation of new knock-out mice (Sp/Strain 24, 25, 26).

**5 e) KEYWORDS: Using keywords only, list the procedures used on animals (e.g. anaesthesia, breeding colony, injection IP, gavage, drug administration, major survival surgery, euthanasia by exsanguination, behavioural studies). For a more complete list of suggested keywords refer to Appendix I of the Guidelines (www.mcgill.ca/researchoffice/compliance/animal/forms ).**

anaesthesia, breeding colony, injection IP, euthanasia, tissue collection

## 6. Animals Use data for CCAC

**6 a) Purpose of Animal Use (Check most appropriate one):**
1. ☒ **Studies of a fundamental nature/basic research**
2. ☐ **Studies for medical purposes relating to human/animal diseases/disorders**
3. ☐ **Regulatory testing**
4. ☐ **Development of products/appliances for human/veterinary medicine**
5. **If for Teaching, use the Animal Use Protocol form for Teaching (www.mcgill.ca/researchoffice/compliance/animal/forms )**

**6 b) Will field studies be conducted?** NO ☒ YES ☐ If yes, complete "Field Study Form"
**Will the project involve genetically altering animals?** NO ☐ YES ☒ If yes, supply details in section 10c
**Will the project involve breeding animals?** NO ☐ YES ☒

## 7. Animal Data

**7 a) Please justify the need for live animals versus alternate methods (e.g. tissue culture, computer simulation)**

It is essential that we define the mechanism of action of guidance cues such as the RGMs and slits in their native cellular context and environment. It is well established that the cellular effects axon guidance cues trigger in neurons can be regulated by extracellular components in the environment. We must therefore determine the effect of these molecules on specific populations of primary neurons in culture (ie directly derived from embryos) and in situ (within transgenic and knock-out animals).

**7 b) Describe the characteristics of the animal species selected that justifies its use in the proposed study ( consider characteristics such as body size, species, strain, data from previous studies or unique anatomic/physiological features)**

Mouse is the model species for the generation of transgenic and knock-out animals based on the technology availability, our knowledge of their genetic information, and their high-breeding capacity. Rats will be used to derive primary neurons since neurons from rat tend to survive better in culture than neurons isolated from other species.

**7 c) Description of animals**

Quality Control Assurance: To prevent introduction of infectious diseases into animal facilities, a health status report or veterinary inspection certificate may be required prior to receiving animals from all non-commercial sources or from commercial sources whose animal health status is unknown or questionable. Quarantine and further testing may be required for these animals.

*If more than 6 columns are needed, please attach another page*

| | Sp/strain 1 | Sp/strain 2 | Sp/strain 3 | Sp/strain 4 | Sp/strain 5 | Sp/strain 6 |
|---|---|---|---|---|---|---|
| Species | rat | mouse | mouse | mouse | mouse | mouse |
| Supplier/Source | Charles River | Charles River | in house breeding | in house breeding | in house breeding | in house breeding |
| Strain | Sprague-Dawley | CD1 | C57Bl6-Neogenin-1 (Knock-out) | C57Bl6-Slit-1 (Knockout) | C57Bl6-Slit-2 (Knockout) | C57Bl6-Slit-3 (Knock-out) |
| Sex | F | F | M/F | M/F | M/F | M/F |

January 2010

# MCGILL UNIVERSITY PERMIT TO USE BIOHAZARDOUS MATERIALS

## McGill University

### APPLICATION TO USE BIOHAZARDOUS MATERIALS*

Projects involving potentially biohazardous materials should not be commenced without approval from the Environmental Safety Office. Submit applications before 1) starting new projects, 2) renewing existing projects, or 3) changing the nature of the biohazardous materials within existing projects.

1. PRINCIPAL INVESTIGATOR: Jean-François Cloutier PHONE: 514-398-6351
DEPARTMENT: Neurology and Neurosurgery/Montreal Neurological Institute FAX: 514-398-1319
ADDRESS: 3801 University Room F105 E-MAIL: jf.cloutier@mcgill.ca

PROJECT TITLE: Molecular mechanisms of sensory systems development

2. EMERGENCY: Person(s) designated to handle emergencies
Name: Jean-François Cloutier Phone No: work: 514-398-6351 home: 514-482-8766
Name: Manon Lépine Phone No: work: 6351 home: 450-439-6898

3. FUNDING SOURCE OR AGENCY (specify): CIHR
Grant No.: MOP-77571 Beginning date: 01/10/2008 End date: 30/09/2013

4. Indicate if this is
☒ Renewal: procedures previously approved without alterations.
Approval End Date: 31/08/08
☐ New funding source: project previously reviewed and approved under an application to another agency.
Agency: _____ Approval End Date: _____
☐ New project: project not previously reviewed.
☐ Approved project: change in biohazardous materials or procedures.
☐ Work/project involving biohazardous materials in teaching/diagnostics.

CERTIFICATION STATEMENT: The Environmental Safety Office approves the experimental procedures proposed and certifies with the applicant that the experiment will be in accordance with the principles outlined in Health Canada's "Laboratory Biosafety Guidelines" and in the "McGill Laboratory Biosafety Manual".

Containment Level (select one): ☐ 1 ☒ 2 ☐ 2 with additional precautions ☐ 3

Principal Investigator or course director: _____ (SIGNATURE) date: 19 (day) 08 (month) 2008 (year)

*Approved by:* Environmental Safety Office: _____ (SIGNATURE) date: 04 (day) 09 (month) 2008 (year)

Expiry: 30 (day) 09 (month) 2013 (year)

*as defined in the "McGill Laboratory Biosafety Manual"

5. RESEARCH PERSONNEL: (attach additional sheets if preferred)

| Name | Department | Job Title/Classification | Attended *Safe Use of Biological Safety Cabinets* seminar? If yes, indicate date of attendance |
|---|---|---|---|
| Jin Hyung Cho | Neurology and Neurosurgery | Graduate student | yes, May 11, 2005 |
| David da Silva | Neurology and Neurosurgery | Graduate student | yes, May 11, 2005 |
| Manon Lépine | Neurology and Neurosurgery | Research Assistant | Yes, 2004 |
| François Beaubien | Neurology and Neurosurgery | Graduate Student | Yes, September 2006 |
| Janet Prince | Neurology and Neurosurgery | Graduate Student | Yes, September 2006 |
| | | | |

6. Briefly describe:

i) the biohazardous material involved (e.g. bacteria, viruses, human tissues, toxins of biological origin) & designated biosafety risk group

- Tissue culture waste
- Non-pathogenic bacterial waste
- Broken glass, sharps
- Organic solvents

ii) the procedures involving biohazards

- Cell lines will be used to express recombinant DNA fragments produced in vitro by standard molcular biology techniques. The constructs tested represent known proteins that show no ability to transform cells.

- Tissue culture will be performed in an approved laminar flow hood located in a room dedicated for this purpose. Personel working in this area will be suitably trained in sterile technique.

- Biohazardous waste will be disposed of separately from regular garbage. Cell and bacterial culture waste is placed in biohazard autoclave bags and autoclaved prior to disposal. Liquid waste will be neutralized with 0.1% Roccal or sodium hypochlorite solution (5.25% bleach diluted 1:10).

- Containers/equipment leaving the lab will be decontaminated with 1% bleach or 70% ethanol.

- Working areas will be regularly wiped with 70% ethanol

- Chloroform and phenol will be disposed of as toxic waste

- Sharps will be disposed of in impermeable sealed plastic containers; glass in sealed cardboard boxes.

- Organic/caustic chemicals will be stored in a reinforced cabinet and used in a fume hood.

iii) the protocol for decontaminating spills

Spills will be decontaminated by first allowing aerosols to settle. We will then cover the spill with paper towel and then apply 70% ethanol from the periphery inwards. After a 30 minute incubation period in the applied bleach, the paper towel will be disposed of in a biohazard bin.

7. Does the protocol present conditions (e.g. handling of large volumes or high concentrations of pathogens) that could increase the hazards?

NO

8. Do the specific procedures to be employed involving genetically engineered organisms have a history of safe use?

YES

9. What precautions will be taken to reduce production of infectious droplets and aerosols?

Biosafety cabinets are used.

10. Will the biohazardous materials in this project expose members of the research team to any risks that might require special training, vaccination or other protective measures? If yes, please explain.

NO

11. Will this project produce combined hazardous waste – i.e. radioactive biohazardous waste, biohazardous animal carcasses contaminated with toxic chemicals, etc.? If yes, please explain how disposal will be handled.

NO

12. List the biological safety cabinets to be used.

| Building | Room No. | Manufacturer | Model No. | Serial No. | Date Certified |
|---|---|---|---|---|---|
| MNI Fieldhouse | F104 | Forma | | 16069-1477 | June 2, 2008 |
| MNI Fieldhouse | F104 | Forma | | 14517-327 | June 2, 2008 |

# REFERENCE


Alenius, M. and S. Bohm (1997). Identification of a novel neural cell adhesion molecule-related gene with a potential role in selective axonal projection. J Biol Chem. **272:** 26083-26086.

Angot, E., K. Loulier, et al. (2008). Chemoattractive Activity of Sonic Hedgehog in the Adult Subventricular Zone Modulates the Number of Neural Precursors Reaching the Olfactory Bulb. Stem Cells. **26:** 2311-2320.

Astic, L., V. Pellier-Monnin, et al. (2002). Expression of netrin-1 and netrin-1 receptor, DCC, in the rat olfactory nerve pathway during development and axonal regeneration. Neuroscience. **109:** 643-656.

Astic, L. and D. Saucier (1986). Anatomical mapping of the neuroepithelial projection to the olfactory bulb in the rat. Brain Res Bull. **16:** 445-454.

Barnea, G., S. O'Donnell, et al. (2004). Odorant receptors on axon termini in the brain. Science. **304**(5676): 1468.

Barth, A. L., N. J. Justice, et al. (1996). Asynchronous onset of odorant receptor expression in the developing zebrafish olfactory system. Neuron. **16**(1): 23-34.

Bedell, V. M., S.-Y. Yeo, et al. (2005). roundabout4 is essential for angiogenesis in vivo. Proc Natl Acad Sci USA. **102:** 6373-6378.

Belluscio, L., G. H. Gold, et al. (1998). Mice deficient in G(olf) are anosmic. Neuron. **20**(1): 69-81.

Bozza, T., A. Vassalli, et al. (2009). Mapping of class I and class II odorant receptors to glomerular domains by two distinct types of olfactory sensory neurons in the mouse. Neuron. **61:** 220-233.

Brose, K., K. S. Bland, et al. (1999). Slit proteins bind Robo receptors and have an evolutionarily conserved role in repulsive axon guidance. Cell. **96:** 795-806.

Buck, L. and R. Axel (1991). A novel multigene family may encode odorant receptors: a molecular basis for odor recognition. Cell. **65:** 175-187.

Bulfone, A., F. Wang, et al. (1998). An olfactory sensory map develops in the absence of normal projection neurons or GABAergic interneurons. Neuron. **21:** 1273-1282.

Bunting, M., K. E. Bernstein, et al. (1999). Targeting genes for self-excision in the germ line. Genes Dev. **13**(12): 1524-1528.

Caiazzo, M., L. Colucci-D'amato, et al. (2010). Krüppel-like factor 7 is required for olfactory bulb dopaminergic neuron development. Experimental Cell Research.

Cajal, R. (1892). La rétine des vertèbres. Cellule. 9:119-258.

Cau, E., G. Gradwohl, et al. (2000). Hes genes regulate sequential stages of neurogenesis in the olfactory epithelium. Development. **127:** 2323-2332.

Chamero, P., T. F. Marton, et al. (2007). Identification of protein pheromones that promote aggressive behaviour. Nature. **450:** 899-902.

Charron, F., E. Stein, et al. (2003). The morphogen sonic hedgehog is an axonal chemoattractant that collaborates with netrin-1 in midline axon guidance. Cell. **113:** 11-23.

Chen, Z., B. B. Gore, et al. (2008). Alternative splicing of the Robo3 axon guidance receptor governs the midline switch from attraction to repulsion. Neuron. **58:** 325-332.

Cheng, L. E. and R. R. Reed (2007). Zfp423/OAZ participates in a developmental switch during olfactory neurogenesis. Neuron. **54:** 547-557.
Chesler, A. T., D. J. Zou, et al. (2007). A G protein/cAMP signal cascade is required for axonal convergence into olfactory glomeruli. Proc Natl Acad Sci USA. **104**(3): 1039-1044.
Chess, A., I. Simon, et al. (1994). Allelic inactivation regulates olfactory receptor gene expression. Cell. **78**(5): 823-834.
Cho, J. H., M. Lépine, et al. (2007). Requirement for Slit-1 and Robo-2 in zonal segregation of olfactory sensory neuron axons in the main olfactory bulb. J Neurosci. **27:** 9094-9104.
Cho, J. H., J. E. Prince, et al. (2009). Axon guidance events in the wiring of the mammalian olfactory system. Mol Neurobiol. **39**(1): 1-9.
Cho, J. H., J. E. Prince, et al. (2011). The pattern of glomerular map formation defines the responsiveness to aversive odorants in mice. J Neurosci. **31**: 7920-7926.
Cloutier, J.-F., A. Sahay, et al. (2004). Differential requirements for semaphorin 3F and Slit-1 in axonal targeting, fasciculation, and segregation of olfactory sensory neuron projections. J Neurosci. **24:** 9087-9096.
Cloutier, J. F., R. J. Giger, et al. (2002). Neuropilin-2 mediates axonal fasciculation, zonal segregation, but not axonal convergence, of primary accessory olfactory neurons. Neuron. **33**(6): 877-892.
Col, J. A. D., T. Matsuo, et al. (2007). Adenylyl cyclase-dependent axonal targeting in the olfactory system. Development. **134:** 2481-2489.
Coryell, M. W., A. M. Wunsch, et al. (2008). Restoring Acid-sensing ion channel-1a in the amygdala of knock-out mice rescues fear memory but not unconditioned fear responses. J Neurosci. **28:** 13738-13741.
Crandall, J. E., C. Dibble, et al. (2000). Patterning of olfactory sensory connections is mediated by extracellular matrix proteins in the nerve layer of the olfactory bulb. J Neurobiol. **45**(4): 195-206.
Cutforth, T., L. Moring, et al. (2003). Axonal ephrin-As and odorant receptors: coordinate determination of the olfactory sensory map. Cell. **114:** 311-322.
Davis, M. and C. Shi (1999). The extended amygdala: are the central nucleus of the amygdala and the bed nucleus of the stria terminalis differentially involved in fear versus anxiety? Ann N Y Acad Sci. **877:** 281-291.
Day HE, Masini CV, Campeau S (2004) The pattern of brain c-fos mRNA induced by a component of fox odor, 2,5-dihydro-2,4,5-trimethylthiazoline (TMT), in rats, suggests both systemic and processive stress characteristics. Brain Res **1025**:139-151.
de Castro, F., L. Hu, et al. (1999). Chemoattraction and Chemorepulsion of olfactory bulb axons by different secreted semaphorins. J. Neurosci. **19**: 4428-4436.
Dickson, B. J. (2002). Molecular mechanisms of axon guidance. Science. **298:** 1959-1964.
Dickson, B. J. and G. F. Gilestro (2006). Regulation of commissural axon pathfinding by slit and its Robo receptors. Annu Rev Cell Dev Biol. **22:** 651-675.
Duggan, C. D., S. DeMaria, et al. (2008). Foxg1 is required for development of the vertebrate olfactory system. J Neurosci. **28**(20): 5229-5239.

Dulac, C. and A. T. Torello (2003). Molecular detection of pheromone signals in mammals: from genes to behaviour. Nature Publishing Group. **4:** 551-562.
Eggan, K., K. Baldwin, et al. (2004). Mice cloned from olfactory sensory neurons. Nature. **428**(6978): 44-49.
Eichenbaum, H., T. H. Morton, et al. (1983). Selective olfactory deficits in case H.M. Brain. **106 (Pt 2):** 459-472.
Feinstein, P., T. Bozza, et al. (2004). Axon guidance of mouse olfactory sensory neurons by odorant receptors and the beta2 adrenergic receptor. Cell. **117**(6): 833-846.
Feinstein, P. and P. Mombaerts (2004). A contextual model for axonal sorting into glomeruli in the mouse olfactory system. Cell. **117**(6): 817-831.
Fendt, M., T. Endres, et al. (2003). Temporary inactivation of the bed nucleus of the stria terminalis but not of the amygdala blocks freezing induced by trimethylthiazoline, a component of fox feces. J Neurosci. **23:** 23-28.
Fendt, M. and M. S. Fanselow (1999). The neuroanatomical and neurochemical basis of conditioned fear. Neurosci Biobehav Rev. **23:** 743-760.
Fiore, R., B. Rahim, et al. (2005). Inactivation of the Sema5a gene results in embryonic lethality and defective remodeling of the cranial vascular system. Mol Cell Biol. **25:** 2310-2319.
Fleischmann, A., B. M. Shykind, et al. (2008). Mice with a "monoclonal nose": perturbations in an olfactory map impair odor discrimination. Neuron. **60**(6): 1068-1081.
Fouquet, C., T. Di Meglio, et al. (2007). Robo1 and robo2 control the development of the lateral olfactory tract. J Neurosci. **27:** 3037-3045.
Fujisawa, K., J. L. Wrana, et al. (2007). The slit receptor EVA-1 coactivates a SAX-3/Robo mediated guidance signal in C. elegans. Science. **317**(5846): 1934-1938.
Gong, Q., H. Chen, et al. (2009). Olfactory sensory axon growth and branching is influenced by sonic hedgehog. Dev. Dyn. **238:** 1768-1776.
Grieshammer, U., L. Ma, et al. (2004). SLIT2-mediated ROBO2 signaling restricts kidney induction to a single site. Dev Cell. **6:** 709-717.
Guillemot, F., L. C. Lo, et al. (1993). Mammalian achaete-scute homolog 1 is required for the early development of olfactory and autonomic neurons. Cell. **75:** 463-476.
Gussing, F. and S. Bohm (2004). NQO1 activity in the main and the accessory olfactory systems correlates with the zonal topography of projection maps. Eur J Neurosci. **19**(9): 2511-2518.
Haberly, L. B. and J. L. Price (1977). The axonal projection patterns of the mitral and tufted cells of the olfactory bulb in the rat. Brain Res. **129:** 152-157.
Hao, J. C., T. W. Yu, et al. (2001). C. elegans slit acts in midline, dorsal-ventral, and anterior-posterior guidance via the SAX-3/Robo receptor. Neuron. **32:** 25-38.
Hasegawa, S., S. Hamada, et al. (2008). The protocadherin-alpha family is involved in axonal coalescence of olfactory sensory neurons into glomeruli of the olfactory bulb in mouse. Mol Cell Neurosci. **38**(1): 66-79.
Hasselmo, M. E. and E. Barkai (1995). Cholinergic modulation of activity-dependent synaptic plasticity in the piriform cortex and associative memory function in a network biophysical simulation. J Neurosci. **15:** 6592-6604.

Henion, T. R., D. Raitcheva, et al. (2005). Beta1,3-N-acetylglucosaminyltransferase 1 glycosylation is required for axon pathfinding by olfactory sensory neurons. J Neurosci. **25**(8): 1894-1903.
Hilario, J. D., L. R. Rodino-Klapac, et al. (2009). Semaphorin 5A is a bifunctional axon guidance cue for axial motoneurons in vivo. Devel Biol. 1-11.
Hirata, T., M. Nakazawa, et al. (2006). Zinc-finger gene Fez in the olfactory sensory neurons regulates development of the olfactory bulb non-cell-autonomously. Development. **133:** 1433-1443.
Hirota, J. and P. Mombaerts (2004). The LIM-homeodomain protein Lhx2 is required for complete development of mouse olfactory sensory neurons. Proc Natl Acad Sci USA. **101**(23): 8751-8755.
Hivert, B., Z. Liu, et al. (2002). Robo1 and Robo2 are homophilic binding molecules that promote axonal growth. Mol Cell Neurosci. **21**(4): 534-545.
Holmes, G. P., K. Negus, et al. (1998). Distinct but overlapping expression patterns of two vertebrate slit homologs implies functional roles in CNS development and organogenesis. Mech Dev. **79:** 57-72.
Hu, H. (1999). Chemorepulsion of neuronal migration by Slit2 in the developing mammalian forebrain. Neuron. **23:** 703-711.
Huber, A. B., A. L. Kolodkin, et al. (2003). Signaling at the growth cone: ligand-receptor complexes and the control of axon growth and guidance. Annu Rev Neurosci. **26:** 509-563.
Hummel, T., K. Schimmelpfeng, et al. (1999). Commissure formation in the embryonic CNS of Drosophila. Dev Biol. **209:** 381-398.
Illig, K. R. and L. B. Haberly (2003). Odor-evoked activity is spatially distributed in piriform cortex. J Comp Neurol. **457:** 361-373.
Imai, T. and H. Sakano (2008). Odorant receptor-mediated signaling in the mouse. Curr Opin Neurobiol.
Imai, T., M. Suzuki, et al. (2006). Odorant receptor-derived cAMP signals direct axonal targeting. Science. **314:** 657-661.
Imai, T., T. Yamazaki, et al. (2009). Pre-Target Axon Sorting Establishes the Neural Map Topography. Science. **325:** 585-590.
Ishii, T., M. Omura, et al. (2004). Protocols for two- and three-color fluorescent RNA in situ hybridization of the main and accessory olfactory epithelia in mouse. J Neurocytol. **33:** 657-669.
Ishii, T., S. Serizawa, et al. (2001). Monoallelic expression of the odourant receptor gene and axonal projection of olfactory sensory neurones. Genes Cells. **6**(1): 71-78.
Itoh, A., T. Miyabayashi, et al. (1998). Cloning and expressions of three mammalian homologues of Drosophila slit suggest possible roles for Slit in the formation and maintenance of the nervous system. Brain Res Mol Brain Res. **62:** 175-186.
Iwema, C. L., H. Fang, et al. (2004). Odorant receptor expression patterns are restored in lesion-recovered rat olfactory epithelium. J Neurosci. **24:** 356-369.
Jaworski, A., H., Long, et al. (2010). Collaborative and specialized functions of Robo1 and Robo2 in spinal commissural axon guidance. J Neurosci. **30**: 9445-9453.
Jefferis, G. S. X. E., C. J. Potter, et al. (2007). Comprehensive maps of Drosophila higher olfactory centers: spatially segregated fruit and pheromone representation. Cell. **128:** 1187-1203.

JJhaveri, D., S. Saharan, et al. (2004). Positioning sensory terminals in the olfactory lobe of Drosophila by Robo signaling. Development. **131:** 1903-1912.
Johnson, B. A. and M. Leon (2007). Chemotopic odorant coding in a mammalian olfactory system. J Comp Neurol. **503**(1): 1-34.
Jortner, R. A., S. S. Farivar, et al. (2007). A simple connectivity scheme for sparse coding in an olfactory system. J Neurosci. **27:** 1659-1669.
Kaneko-Goto, T., S.-i. Yoshihara, et al. (2008). BIG-2 mediates olfactory axon convergence to target glomeruli. Neuron. **57:** 834-846.
Kantor, D. B., O. Chivatakarn, et al. (2004). Semaphorin 5A is a bifunctional axon guidance cue regulated by heparan and chondroitin sulfate proteoglycans. Neuron. **44:** 961-975.
Kawauchi, S., J. Kim, et al. (2009). Foxg1 promotes olfactory neurogenesis by antagonizing Gdf11. Development. **136:** 1453-1464.
Keleman, K., S. Rajagopalan, et al. (2002). Comm sorts robo to control axon guidance at the Drosophila midline. Cell. **110:** 415-427.
Keleman, K., C. Ribeiro, et al. (2005). Comm function in commissural axon guidance: cell-autonomous sorting of Robo in vivo. Nat Neurosci. **8:** 156-163.
Kerr, M. A. and L. Belluscio (2006). Olfactory experience accelerates glomerular refinement in the mammalian olfactory bulb. Nat Neurosci **9**(4): 484-486.
Kidd, T., K. S. Bland, et al. (1999). Slit is the midline repellent for the robo receptor in Drosophila. Cell. **96:** 785-794.
Kidd, T., K. Brose, et al. (1998). Roundabout controls axon crossing of the CNS midline and defines a novel subfamily of evolutionarily conserved guidance receptors. Cell. **92:** 205-215.
Knöll, B., H. Schmidt, et al. (2003). On the topographic targeting of basal vomeronasal axons through Slit-mediated chemorepulsion. Development. **130:** 5073-5082.
Kobayakawa, K., R. Kobayakawa, et al. (2007). Innate versus learned odour processing in the mouse olfactory bulb. Nature. **450:** 503-508.
Kolterud, A., M. Alenius, et al. (2004). The Lim homeobox gene Lhx2 is required for olfactory sensory neuron identity. Development. **131:** 5319-5326.
Kratz, E., J. C. Dugas, et al. (2002). Odorant receptor gene regulation: implications from genomic organization. Trends Genet. **18**(1): 29-34.
LaMantia, A. S., N. Bhasin, et al. (2000). Mesenchymal/epithelial induction mediates olfactory pathway formation. Neuron. **28:** 411-425.
Laub, F., C. Dragomir, et al. (2006). Mice without transcription factor KLF7 provide new insight into olfactory bulb development. Brain Res. **1103:** 108-113.
Ledoux, J. E. (2000). Emotion circuits in the brain. Annu Rev Neurosci. **23:** 155-184.
Lee, J. S., R. Ray, et al. (2001). Cloning and expression of three zebrafish roundabout homologs suggest roles in axon guidance and cell migration. Dev Dyn. **221:** 216-230.
Levai, O., H. Breer, et al. (2003). Subzonal organization of olfactory sensory neurons projecting to distinct glomeruli within the mouse olfactory bulb. J Comp Neurol. **458**(3): 209-220.
Levi, G., A. C. Puche, et al. (2003). The Dlx5 homeodomain gene is essential for olfactory development and connectivity in the mouse. Mol Cell Neurosci. **22:** 530-543.

Lewcock, J. W. and R. R. Reed (2004). A feedback mechanism regulates monoallelic odorant receptor expression. Proc Natl Acad Sci USA. **101**(4): 1069-1074.
Li, H. S., J. H. Chen, et al. (1999). Vertebrate slit, a secreted ligand for the transmembrane protein roundabout, is a repellent for olfactory bulb axons. Cell. **96:** 807-818.
Lin, D. M., F. Wang, et al. (2000). Formation of precise connections in the olfactory bulb occurs in the absence of odorant-evoked neuronal activity. Neuron. **26:** 69-80.
Lin, D. Y., S. D. Shea, et al. (2006). Representation of natural stimuli in the rodent main olfactory bulb. Neuron. **50:** 937-949.
Lin, H.-H., J. S.-Y. Lai, et al. (2007). A map of olfactory representation in the Drosophila mushroom body. Cell. **128:** 1205-1217.
Liu, J., L. Zhang, et al. (2003). Congenital diaphragmatic hernia, kidney agenesis and cardiac defects associated with Slit3-deficiency in mice. Mech Dev. **120:** 1059-1070.
Long, H., C. Sabatier, et al. (2004). Conserved roles for Slit and Robo proteins in midline commissural axon guidance. Neuron. **42:** 213-223.
López-Mascaraque, L., J. A. De Carlos, et al. (1996). Early onset of the rat olfactory bulb projections. Neuroscience. **70:** 255-266.
Lu, W., A. M. van Eerde, et al. (2007). Disruption of ROBO2 is associated with urinary tract anomalies and confers risk of vesicoureteral reflux. Amer J of hum genetics. **80**(4): 616-632.
Luskin, M. B. (1998). Neuroblasts of the postnatal mammalian forebrain: their phenotype and fate. J Neurobiol. **36**(2): 221-233.
Mahanthappa, N. K., D. N. Cooper, et al. (1994). Rat olfactory neurons can utilize the endogenous lectin, L-14, in a novel adhesion mechanism. Development. **120**(6): 1373-1384.
Malnic, B., J. Hirono, et al. (1999). Combinatorial receptor codes for odors. Cell. **96:** 713-723.
Manitt, C., M. A. Colicos, et al. (2001). Widespread expression of netrin-1 by neurons and oligodendrocytes in the adult mammalian spinal cord. J Neurosci. **21:** 3911-3922.
Marillat, V., O. Cases, et al. (2002). Spatiotemporal expression patterns of slit and robo genes in the rat brain. J Comp Neurol. **442:** 130-155.
Matsumoto, H., K. Kobayakawa, et al. (2010). Spatial Arrangement of Glomerular Molecular-Feature Clusters in the Odorant-Receptor Class Domains of the Mouse Olfactory Bulb. J Neurophysiol. **103:** 3490-3500.
Miyamichi, K., F. Amat, et al. (2010). Cortical representations of olfactory input by trans-synaptic tracing. Nature.
Miyamichi, K., S. Serizawa, et al. (2005). Continuous and overlapping expression domains of odorant receptor genes in the olfactory epithelium determine the dorsal/ventral positioning of glomeruli in the olfactory bulb. J Neurosci. **25:** 3586-3592.
Miyasaka, N., K. Morimoto, et al. (2009). From the olfactory bulb to higher brain centers: genetic visualization of secondary olfactory pathways in zebrafish. J Neurosci. **29:** 4756-4767.

Miyasaka, N., Y. Sato, et al. (2005). Robo2 is required for establishment of a precise glomerular map in the zebrafish olfactory system. Development. **132:** 1283-1293.
Mombaerts, P. (2006). Axonal wiring in the mouse olfactory system. Annu Rev Cell Dev Biol. **22**: 713-737.
Mombaerts, P., F. Wang, et al. (1996). Visualizing an olfactory sensory map. Cell. **87:** 675-686.
Mori, K., Y. K. Takahashi, et al. (2006). Maps of odorant molecular features in the Mammalian olfactory bulb. Physiol Rev. **86**(2): 409-433.
Muller M, Fendt M (2006) Temporary inactivation of the medial and basolateral amygdala differentially affects TMT-induced fear behavior in rats. Behav Brain Res **167**:57-62.
Murthy, M., I. Fiete, et al. (2008). Testing odor response stereotypy in the Drosophila mushroom body. Neuron. **59:** 1009-1023.
Nakatani, H., S. Serizawa, et al. (2003). Developmental elimination of ectopic projection sites for the transgenic OR gene that has lost zone specificity in the olfactory epithelium. Eur J Neurosci **18**(9): 2425-2432.
Nguyen, M. Q., Z. Zhou, et al. (2007). Prominent roles for odorant receptor coding sequences in allelic exclusion. Cell. **131**(5): 1009-1017.
Nguyen-Ba-Charvet, K. T., T. Di Meglio, et al. (2008). Robos and slits control the pathfinding and targeting of mouse olfactory sensory axons. J Neurosci. **28:** 4244-4249.
Nguyen-Ba-Charvet, K. T., N. Picard-Riera, et al. (2004). Multiple roles for slits in the control of cell migration in the rostral migratory stream. J Neurosci. **24:** 1497-1506.
Nguyen-Ba-Charvet, K. T., A. S. Plump, et al. (2002). Slit1 and slit2 proteins control the development of the lateral olfactory tract. J Neurosci. **22:** 5473-5480.
Niimura, Y. and M. Nei (2005). Evolutionary dynamics of olfactory receptor genes in fishes and tetrapods. Proc Natl Acad Sci USA. **102:** 6039-6044.
Nishizumi, H., K. Kumasaka, et al. (2007). Deletion of the core-H region in mice abolishes the expression of three proximal odorant receptor genes in cis. Proc Natl Acad Sci USA. **104**(50): 20067-20072.
Norlin, E. M., M. Alenius, et al. (2001). Evidence for gradients of gene expression correlating with zonal topography of the olfactory sensory map. Mol Cell Neurosci. **18:** 283-295.
Norlin, E. M. and A. Berghard (2001). Spatially restricted expression of regulators of G-protein signaling in primary olfactory neurons. Mol Cell Neurosci. **17**(5): 872-882.
Novotny, M., S. Harvey, et al. (1985). Synthetic pheromones that promote inter-male aggression in mice. Proc Natl Acad Sci USA. **82:** 2059-2061.
Oka, Y., S. Katada, et al. (2006). Odorant receptor map in the mouse olfactory bulb: in vivo sensitivity and specificity of receptor-defined glomeruli. Neuron. **52:** 857-869.
Okada, A., F. Charron, et al. (2006). Boc is a receptor for sonic hedgehog in the guidance of commissural axons. Nature. **444:** 369-373.

Papes, F., D. W. Logan, et al. (2010). The vomeronasal organ mediates interspecies defensive behaviors through detection of protein pheromone homologs. Cell. **141:** 692-703.
Park, K. W., C. M. Morrison, et al. (2003). Robo4 is a vascular-specific receptor that inhibits endothelial migration. Dev Biol. **261:** 251-267.
Pasterkamp, R. J., R. J. Giger, et al. (1998). Regulation of semaphorin III/collapsin-1 gene expression during peripheral nerve regeneration. Exp Neurol. **153**(2): 313-327.
Pasterkamp, R. J., M. J. Ruitenberg, et al. (1999). Semaphorins and their receptors in olfactory axon guidance. Cell Mol Biol (Noisy-le-grand). **45**(6): 763-779.
Philpot, B. D., T. C. Foster, et al. (1997). Mitral/tufted cell activity is attenuated and becomes uncoupled from respiration following naris closure. J Neurobiol. **33**(4): 374-386.
Pini, A. (1993). Chemorepulsion of axons in the developing mammalian central nervous system. Science. **261:** 95-98.
Plachez, C., W. Andrews, et al. (2008). Robos are required for the correct targeting of retinal ganglion cell axons in the visual pathway of the brain. Mol Cell Neurosci. **37:** 719-730.
Plump, A. S., L. Erskine, et al. (2002). Slit1 and Slit2 cooperate to prevent premature midline crossing of retinal axons in the mouse visual system. Neuron. **33**(2): 219-232.
Poo, C. and J. S. Isaacson (2009). Odor representations in olfactory cortex: "sparse" coding, global inhibition, and oscillations. Neuron. **62:** 850-861.
Prince, J. E. A., J. H. Cho, et al. (2009). Robo-2 controls the segregation of a portion of basal vomeronasal sensory neuron axons to the posterior region of the accessory olfactory bulb. J Neurosci. **29:** 14211-14222.
Rajagopalan, S., V. Vivancos, et al. (2000). Selecting a longitudinal pathway: Robo receptors specify the lateral position of axons in the Drosophila CNS. Cell. **103:** 1033-1045.
Rennaker, R. L., C.-F. F. Chen, et al. (2007). Spatial and temporal distribution of odorant-evoked activity in the piriform cortex. J Neurosci. **27:** 1534-1542.
Renzi, M. J., T. L. Wexler, et al. (2000). Olfactory sensory axons expressing a dominant-negative semaphorin receptor enter the CNS early and overshoot their target. Neuron. **28**(2): 437-447.
Ressler, K. J., S. L. Sullivan, et al. (1993). A zonal organization of odorant receptor gene expression in the olfactory epithelium. Cell. **73:** 597-609.
Ressler, K. J., S. L. Sullivan, et al. (1994). Information coding in the olfactory system: evidence for a stereotyped and highly organized epitope map in the olfactory bulb. Cell. **79**(7): 1245-1255.
Rink, E. and M. F. Wullimann (2004). Connections of the ventral telencephalon (subpallium) in the zebrafish (Danio rerio). Brain Res. **1011:** 206-220.
Rodriguez-Gil, D. J., H. B. Treloar, et al. (2010). Chromosomal location-dependent nonstochastic onset of odor receptor expression. J Neurosci. **30**(30): 10067-10075.

Rothberg, J. M., J. R. Jacobs, et al. (1990). slit: an extracellular protein necessary for development of midline glia and commissural axon pathways contains both EGF and LRR domains. Genes Dev. **4:** 2169-2187.
Royet, J. P., C. Souchier, et al. (1988). Morphometric study of the glomerular population in the mouse olfactory bulb: numerical density and size distribution along the rostrocaudal axis. J Comp Neurol. **270:** 559-568.
Saar, D., Y. Grossman, et al. (2001). Long-lasting cholinergic modulation underlies rule learning in rats. J Neurosci. **21:** 1385-1392.
Sabatier, C., A. S. Plump, et al. (2004). The divergent Robo family protein rig-1/Robo3 is a negative regulator of slit responsiveness required for midline crossing by commissural axons. Cell. **117:** 157-169.
Saucier, D. and L. Astic (1986). Analysis of the topographical organization of olfactory epithelium projections in the rat. Brain Res Bull. **16:** 455-462.
Sawamoto, K., H. Wichterle, et al. (2006). New neurons follow the flow of cerebrospinal fluid in the adult brain. Science. **311:** 629-632.
Schaefer, M. L., T. E. Finger, et al. (2001). Variability of position of the P2 glomerulus within a map of the mouse olfactory bulb. J Comp Neurol. **436**(3): 351-362.
Schoenfeld, T. A. and F. Macrides (1984). Topographic organization of connections between the main olfactory bulb and pars externa of the anterior olfactory nucleus in the hamster. J Comp Neurol. **227:** 121-135.
Schwarting, G. A. and J. E. Crandall (1991). Subsets of olfactory and vomeronasal sensory epithelial cells and axons revealed by monoclonal antibodies to carbohydrate antigens. Brain Res. **547**(2): 239-248.
Schwarting, G. A., G. Deutsch, et al. (1992). Glycoconjugates are stage- and position-specific cell surface molecules in the developing olfactory system, 1: The CC1 immunoreactive glycolipid defines a rostrocaudal gradient in the rat vomeronasal system. J Neurobiol. **23**(2): 120-129.
Schwarting, G. A. and T. R. Henion (2007). Lactosamine differentially affects olfactory sensory neuron projections to the olfactory bulb. Develop neurobiol. **67**(12): 1627-1640.
Schwarting, G. A., C. Kostek, et al. (2000). Semaphorin 3A is required for guidance of olfactory axons in mice. J Neurosci. **20:** 7691-7697.
Schwarting, G. A., D. Raitcheva, et al. (2004). Semaphorin 3A-mediated axon guidance regulates convergence and targeting of P2 odorant receptor axons. Eur J Neurosci. **19:** 1800-1810.
Schwob, J. E. and J. L. Price (1984). The development of axonal connections in the central olfactory system of rats. J Comp Neurol. **223:** 177-202.
Scolnick, J. A., K. Cui, et al. (2008). Role of IGF signaling in olfactory sensory map formation and axon guidance. Neuron. **57**(6): 847-857.
Scott, J. W. (1981). Electrophysiological identification of mitral and tufted cells and distributions of their axons in olfactory system of the rat. J Neurophysiol. **46:** 918-931.
Seeger, M., G. Tear, et al. (1993). Mutations affecting growth cone guidance in Drosophila: genes necessary for guidance toward or away from the midline. Neuron. **10:** 409-426.

Serizawa, S., T. Ishii, et al. (2000). Mutually exclusive expression of odorant receptor transgenes. Nat Neurosci. **3**(7): 687-693.
Serizawa, S., K. Miyamichi, et al. (2003). Negative feedback regulation ensures the one receptor-one olfactory neuron rule in mouse. Science. **302**(5653): 2088-2094.
Serizawa, S., K. Miyamichi, et al. (2006). A neuronal identity code for the odorant receptor-specific and activity-dependent axon sorting. Cell. **127:** 1057-1069.
Shykind, B. M., S. C. Rohani, et al. (2004). Gene switching and the stability of odorant receptor gene choice. Cell. **117**(6): 801-815.
Simpson, J. H., K. S. Bland, et al. (2000). Short-range and long-range guidance by Slit and its Robo receptors: a combinatorial code of Robo receptors controls lateral position. Cell. **103:** 1019-1032.
Simpson, J. H., T. Kidd, et al. (2000). Short-range and long-range guidance by slit and its Robo receptors. Robo and Robo2 play distinct roles in midline guidance. Neuron. **28:** 753-766.
Sosulski DL, Bloom ML, Cutforth T, Axel R, Datta SR, 2011, Distinct representations of olfactory information in different cortical centres. Nature **472**, 213-216.
Soucy, E. R., D. F. Albeanu, et al. (2009). Precision and diversity in an odor map on the olfactory bulb. Nat Neurosci. **12:** 210-220.
Sperry, R. (1943). Effect of 180 degree rotation of the retinal field on visuomotor coordination. J Exp Zool. 92:263-279.
Spitzweck, B., M. Brankatschk, et al. (2010). Distinct protein domains and expression patterns confer divergent axon guidance functions for Drosophila Robo receptors. Cell. **140:** 409-420.
Spors, H. and A. Grinvald (2002). Spatio-temporal dynamics of odor representations in the mammalian olfactory bulb. Neuron. **34:** 301-315.
Stettler, D. D. and R. Axel (2009). Representations of Odor in the Piriform Cortex. Neuron. **63:** 854-864.
Stockinger, P., D. Kvitsiani, et al. (2005). Neural circuitry that governs Drosophila male courtship behavior. Cell. **121:** 795-807.
Storan, M. J., T. Magnaldo, et al. (2004). Expression and putative role of lactoseries carbohydrates present on NCAM in the rat primary olfactory pathway. J Comp Neurol. **475**(3): 289-302.
Stowers, L. and T. F. Marton (2005). What is a pheromone? Mammalian pheromones reconsidered. Neuron. **46:** 699-702.
Strotmann, J., O. Levai, et al. (2004). Olfactory receptor proteins in axonal processes of chemosensory neurons. J Neurosci. **24**(35): 7754-7761.
Strotmann, J., I. Wanner, et al. (1994). Rostro-caudal patterning of receptor-expressing olfactory neurones in the rat nasal cavity. Cell Tissue Res. **278**(1): 11-20.
Strotmann, J., I. Wanner, et al. (1994). Olfactory neurones expressing distinct odorant receptor subtypes are spatially segregated in the nasal neuroepithelium. Cell Tissue Res. **276:** 429-438.
Strotmann, J., I. Wanner, et al. (1992). Expression of odorant receptors in spatially restricted subsets of chemosensory neurones. Neuroreport. **3:** 1053-1056.
Suh, G. S. B., A. M. Wong, et al. (2004). A single population of olfactory sensory neurons mediates an innate avoidance behaviour in Drosophila. Nature. **431:** 854-859.

Sullivan, S. L., M. C. Adamson, et al. (1996). The chromosomal distribution of mouse odorant receptor genes. Proc Natl Acad Sci USA. **93:** 884-888.
Sullivan, S. L., S. Bohm, et al. (1995). Target-independent pattern specification in the olfactory epithelium. Neuron. **15:** 779-789.
Takahashi, H., S. I. Yoshihara, et al. Neuropilin-2 is required for the proper targeting of ventral glomeruli in the mouse olfactory bulb. Mol Cell Neurosci.
Takeuchi, H., K. Inokuchi, et al. (2010). Sequential Arrival and Graded Secretion of Sema3F by Olfactory Neuron Axons Specify Map Topography at the Bulb. Cell. **141:** 1056-1067.
Taniguchi, M., H. Nagao, et al. (2003). Distorted odor maps in the olfactory bulb of semaphorin 3A-deficient mice. J Neurosci. **23:** 1390-1397.
Tenne-Brown, J., A. C. Puche, et al. (1998). Expression of galectin-1 in the mouse olfactory system. The Interna J of devel bio. **42**(6): 791-799.
Tessier-Lavigne, M. and C. S. Goodman (1996). The molecular biology of axon guidance. Science. **274:** 1123-1133.
Theriault, F. M., H. N. Nuthall, et al. (2005). Role for Runx1 in the proliferation and neuronal differentiation of selected progenitor cells in the mammalian nervous system. J Neurosci. **25:** 2050-2061.
Tietjen, I., J. M. Rihel, et al. (2003). Single-cell transcriptional analysis of neuronal progenitors. Neuron. **38:** 161-175.
Treloar HB, Purcell AL, Greer CA (1999) Glomerular formation in the developing rat olfactory bulb. J Comp Neurol **413**:289-304.
Treloar HB, Miller AM, et al. (2009) Development of the olfactory system. In: The Neurobiology of Olfaction. Edited by Menini A. New York: CRC Press; 131-156.
Tsuboi, A., T. Miyazaki, et al. (2006). Olfactory sensory neurons expressing class I odorant receptors converge their axons on an antero-dorsal domain of the olfactory bulb in the mouse. Eur J Neurosci. **23**(6): 1436-1444.
Tsuboi, A., Y. Takafuji, et al. (2009). Response properties of trigeminal ganglion mechanosensitive neurons innervating the temporomandibular joint of the rabbit. Exp Brain Res. **199**(2): 107-116.
Tsuboi, A., S. Yoshihara, et al. (1999). Olfactory neurons expressing closely linked and homologous odorant receptor genes tend to project their axons to neighboring glomeruli on the olfactory bulb. J Neurosci. **19:** 8409-8418.
Uchida, N., Y. K. Takahashi, et al. (2000). Odor maps in the mammalian olfactory bulb: domain organization and odorant structural features. Nat Neurosci. **3:** 1035-1043.
Vargesson, N., V. Luria, et al. (2001). Expression patterns of Slit and Robo family members during vertebrate limb development. Mech Dev. **106:** 175-180.
Vassar, R., S. K. Chao, et al. (1994). Topographic organization of sensory projections to the olfactory bulb. Cell. **79**(6): 981-991.
Vassar, R., J. Ngai, et al. (1993). Spatial segregation of odorant receptor expression in the mammalian olfactory epithelium. Cell. **74:** 309-318.
Vernet-Maury, E., E. Polak, et al. (1984). Structure-activity relationship of stress-inducing odorants in the rat. J Chem Ecol. **10**(7): 1007-1018.
Walker, D. L. and M. Davis (2002). The role of amygdala glutamate receptors in fear learning, fear-potentiated startle, and extinction. Pharmacol Biochem Behav. **71:** 379-392.

Walz, A., I. Rodriguez, et al. (2002). Aberrant sensory innervation of the olfactory bulb in neuropilin-2 mutant mice. J Neurosci. **22:** 4025-4035.
Wang, S. S., J. W. Lewcock, et al. (2004). Genetic disruptions of O/E2 and O/E3 genes reveal involvement in olfactory receptor neuron projection. Development. **131**(6): 1377-1388.
Watanabe, Y., K. Inoue, et al. (2009). Fezf1 is required for penetration of the basal lamina by olfactory axons to promote olfactory development. J Comp Neurol. **515:** 565-584.
Weiss, P.A. (1934). In vitro experiments on the factors determining the course of the outgrowing nerve fiber. J Exp Zool. 68:393-448.

Weiss, P.A. (1941). Self-differentiation of the basic patterns of coordination. Comp Psych Monographs. 17:1-96.
Wilson, D. A. (2001). Scopolamine enhances generalization between odor representations in rat olfactory cortex. Learn Mem. **8:** 279-285.
Wilson, D. A. and R. J. Stevenson (2003). The fundamental role of memory in olfactory perception. Trends Neurosci. **26:** 243-247.
Wong, C. J. (1997). Connections of the basal forebrain of the weakly electric fish, Eigenmannia virescens. J Comp Neurol. **389:** 49-64.
Wu, W., K. Wong, et al. (1999). Directional guidance of neuronal migration in the olfactory system by the protein Slit. Nature. **400:** 331-336.
Xian, J., K. J. Clark, et al. (2001). Inadequate lung development and bronchial hyperplasia in mice with a targeted deletion in the Dutt1/Robo1 gene. Proc Natl Acad Sci USA. **98:** 15062-15066.
Xu, F., N. Liu, et al. (2003). Odor maps of aldehydes and esters revealed by functional MRI in the glomerular layer of the mouse olfactory bulb. Proc Natl Acad Sci USA. **100:** 11029-11034.
Xuan, S., C. A. Baptista, et al. (1995). Winged helix transcription factor BF-1 is essential for the development of the cerebral hemispheres. Neuron. **14:** 1141-1152.
Yaksi, E., F. von Saint Paul, et al. (2009). Transformation of odor representations in target areas of the olfactory bulb. Nat Neurosci. **12:** 474-482.
Yeo, S. Y., M. H. Little, et al. (2001). Overexpression of a slit homologue impairs convergent extension of the mesoderm and causes cyclopia in embryonic zebrafish. Dev Biol. **230:** 1-17.
Yoshihara, S.-i., K. Omichi, et al. (2005). Arx homeobox gene is essential for development of mouse olfactory system. Development. **132:** 751-762.
Yoshihara, Y., M. Kawasaki, et al. (1997). OCAM: A new member of the neural cell adhesion molecule family related to zone-to-zone projection of olfactory and vomeronasal axons. J Neurosci. **17:** 5830-5842.
Young, W. W., Jr., J. Portoukalian, et al. (1981). Two monoclonal anticarbohydrate antibodies directed to glycosphingolipids with a lacto-N-glycosyl type II chain. J Biol Chem. **256**(21): 10967-10972.
Yu, C. R., J. Power, et al. (2004). Spontaneous neural activity is required for the establishment and maintenance of the olfactory sensory map. Neuron. **42**(4): 553-566.

Yuan, W., Y. Rao, et al. (2003). A genetic model for a central (septum transversum) congenital diaphragmatic hernia in mice lacking Slit3. Proc Natl Acad Sci USA. **100:** 5217-5222.

Yuan, W., L. Zhou, et al. (1999). The mouse SLIT family: secreted ligands for ROBO expressed in patterns that suggest a role in morphogenesis and axon guidance. Dev Biol. **212**(2): 290-306.

Zhang, B., U. M. Dietrich, et al. (2009). Repulsive axon guidance molecule Slit3 is a novel angiogenic factor. Blood. **114:** 4300-4309.

Zhang, X. and S. Firestein (2002). The olfactory receptor gene superfamily of the mouse. Nat Neurosci. **5:** 124-133.

Zhang, X., M. Rogers, et al. (2004). High-throughput microarray detection of olfactory receptor gene expression in the mouse. Proc Natl Acad Sci USA. **101:** 14168-14173.

Zhao, H., L. Ivic, et al. (1998). Functional expression of a mammalian odorant receptor. Science. **279:** 237-242.

Zhao, H. and R. R. Reed (2001). X inactivation of the OCNC1 channel gene reveals a role for activity-dependent competition in the olfactory system. Cell. **104**(5): 651-660.

Zheng, C., P. Feinstein, et al. (2000). Peripheral olfactory projections are differentially affected in mice deficient in a cyclic nucleotide-gated channel subunit. Neuron. **26**(1): 81-91.

Zhou, D., A. Dinter, et al. (1999). A beta-1,3-N-acetylglucosaminyltransferase with poly-N-acetyllactosamine synthase activity is structurally related to beta-1,3-galactosyltransferases. Proc Natl Acad Sci USA. **96**(2): 406-411.

Ziemann, A. E., J. E. Allen, et al. (2009). The amygdala is a chemosensor that detects carbon dioxide and acidosis to elicit fear behavior. Cell. **139:** 1012-1021.

Zou, D.-J., A. T. Chesler, et al. (2007). Absence of adenylyl cyclase 3 perturbs peripheral olfactory projections in mice. J Neurosci. **27:** 6675-6683.

Zou, D. J., P. Feinstein, et al. (2004). Postnatal refinement of peripheral olfactory projections. Science. **304**(5679): 1976-1979.

Zou, Z., L. F. Horowitz, et al. (2001). Genetic tracing reveals a stereotyped sensory map in the olfactory cortex. Nature. **414**(6860): 173-179.